UNIVERSIDADE FEDERAL DE GOIÁS
PROGRAMA DE PÓS-GRADUAÇÃO EM CIÊNCIAS FARMACÊUTICAS

RAYANE SANTA CRUZ MARTINS DE QUEIROZ ANTONINO

Alternativas tecnológicas para aumentar a biodisponibilidade de anti-inflamatórios: gel mucoadesivo termorreversível e aplicação de sílica mesoporosa para amorfização

GOIÂNIA
2020

sistema de bibliotecas ufg

PRPG
PRÓ-REITORIA DE PÓS-GRADUAÇÃO

UFG

TERMO DE CIÊNCIA E DE AUTORIZAÇÃO PARA DISPONIBILIZAR VERSÕES ELETRÔNICAS DE TESES E DISSERTAÇÕES NA BIBLIOTECA DIGITAL DA UFG

Na qualidade de titular dos direitos de autor, autorizo a Universidade Federal de Goiás (UFG) a disponibilizar, gratuitamente, por meio da Biblioteca Digital de Teses e Dissertações (BDTD/UFG), regulamentada pela Resolução CEPEC nº 832/2007, sem ressarcimento dos direitos autorais, de acordo com a Lei nº 9610/98, o documento conforme permissões assinaladas abaixo, para fins de leitura, impressão e/ou *download*, a título de divulgação da produção científica brasileira, a partir desta data.

O conteúdo das dissertações e teses disponibilizados são de responsabilidade exclusiva dos autores. Ao encaminhar(em) o produto final, o autor e o orientador firmam o compromisso de que ele não contém nenhuma violação de quaisquer direitos autorais ou outro direito de terceiros.

1. Identificação do material bibliográfico: [ ] Dissertação [X] Tese

2. Identificação da Tese ou Dissertação:

Nome completo do autor: Rayane Santa Cruz Martins de Queiroz Antonino

Título do trabalho: Alternativas tecnológicas para aumentar a biodisponibilidade de anti-inflamatórios: gel mucoadesivo bucal associado à captação de sílica mesoporosa para ornalização

3. Informações de acesso ao documento:

Concorda com a liberação total do documento [X] SIM [ ] NÃO[1]

Independente da concordância com a disponibilização eletrônica, é imprescindível o envio do(s) arquivo(s) em formato digital PDF da tese ou dissertação.

Rayane Santa Cruz Martins de Queiroz Antonino
Assinatura do(a) autor(a)[2]

Ciente e de acordo:

Assinatura do(a) orientador(a)[2]

Data: 20 / 03 / 2020

[1] Neste caso o documento será embargado por até um ano a partir da data de defesa. O documento não será disponibilizado durante o período de embargo.
Casos de embargo:
- Solicitação de registro de patente;
- Submissão de artigo em revista científica;
- Publicação como capítulo de livro;
- Publicação da dissertação/tese em livro.

[2] As assinaturas devem ser originais sendo assinadas no próprio documento, imagens coladas não serão aceitas.

RAYANE SANTA CRUZ MARTINS DE QUEIROZ ANTONINO

Alternativas tecnológicas para aumentar a biodisponibilidade de anti-inflamatórios: gel mucoadesivo termorreversível e aplicação de sílica mesoporosa para amorfização

Tese de Doutorado apresentada ao Programa de Pós-Graduação em Ciências Farmacêuticas da Universidade Federal de Goiás para obtenção do Título de Doutor em Ciências Farmacêuticas

Orientadora: Prof. Drª. Eliana Martins Lima
Coorientadora: Drª. Thais Leite Nascimento

Goiânia
2020

Ficha de identificação da obra elaborada pelo autor, através do
Programa de Geração Automática do Sistema de Bibliotecas da UFG.

Antonino, Rayane Santa Cruz Martins de Queiroz
Alternativas tecnológicas para aumentar a biodisponibilidade de anti inflamatórios: gel mucoadesivo termorreversível e aplicação de sílica mesoporosa para amorfização [manuscrito] / Rayane Santa Cruz Martins de Queiroz Antonino. - 2020.
xv, 153 f.: il.

Orientador: Profa. Dra. Eliana Martins Lima; co-orientadora Dra. Thais Leite Nascimento.
Tese (Doutorado) - Universidade Federal de Goiás, Faculdade Farmácia (FF), Programa de Pós-Graduação em Ciências Farmacêuticas, Goiânia, 2020.
Bibliografia. Anexos.
Inclui gráfico, tabelas, lista de figuras, lista de tabelas.

1. Mucoadesão. 2. Gel termorreversível. 3. Biodisponibilidade. 4. Anti-inflamatórios. 5. Sílica mesoporosa. I. Lima, Eliana Martins, orient. II. Título.

CDU 615.1

UNIVERSIDADE FEDERAL DE GOIÁS

FACULDADE DE FARMÁCIA

ATA DE DEFESA DE TESE

Ata Nº **13** da sessão de Defesa de Tese de **Rayane Santa Cruz Martins de Queiroz Antonino** que confere o título de Doutora em **Ciências Farmacêuticas**, na área de concentração em **Fármacos e Medicamentos.**

Aos **vinte dias do mês de março de dois mil e vinte**, a partir das **14:00 horas** , na **sala da pós-graduação/anexo II da Faculdade de Farmácia**, realizou-se a sessão pública de Defesa de Tese intitulada **"Alternativas tecnológicas para aumentar a biodisponibilidade de anti-inflamatórios: gel mucoadesivo termoreversível e aplicação de sílica mesoporosa para amorfização**". Os trabalhos foram instalados pela Orientadora, Professora Doutora **Eliana Martins Lima (FF/UFG)** com a participação dos demais membros da Banca Examinadora: Professor Doutor **Eric de Souza Gil (FF/UFG)**, membro titular interno; Professor Doutor **Christian Gonçalves Alonso (IQ/UFG)**, membro titular externo, Professor Doutor **Wesley de Almeida Brito (UEG)**, membro titular externo; Professor Doutor **Luís Antônio Dantas Silva (Uni-Anhanguera)**, membro titular externo. Durante a argüição os membros da banca **não fizeram** sugestão de alteração do título do **trabalho**. A Banca Examinadora reuniu-se em sessão secreta a fim de concluir o julgamento da Tese tendo sido a candidata **aprovada** pelos seus membros. Proclamados os resultados pela Professora Doutora **Eliana Martins Lima (FF/UFG)**, Presidente da Banca Examinadora, foram encerrados os trabalhos e, para constar, lavrou-se a presente ata que é assinada pelos Membros da Banca Examinadora, aos **vinte dias do mês de março de dois mil e vinte**.

TÍTULO SUGERIDO PELA BANCA

Documento assinado eletronicamente por **Eliana Martins Lima**, **Professora do Magistério Superior**, em 20/03/2020, às 16:05, conforme horário oficial de Brasília, com fundamento no art. 6º, § 1º, do Decreto nº 8.539, de 8 de outubro de 2015.

Documento assinado eletronicamente por **Eric De Souza Gil**, **Professor do Magistério Superior**, em 20/03/2020, às 16:06, conforme horário oficial de Brasília, com fundamento no art. 6º, § 1º, do Decreto nº 8.539, de 8 de outubro de 2015.

Documento assinado eletronicamente por **Luís Antônio Dantas Silva**, **Usuário Externo**, em 20/03/2020, às 16:08, conforme horário oficial de Brasília, com fundamento no art. 6º, § 1º, do Decreto nº 8.539, de 8 de outubro de 2015.

Documento assinado eletronicamente por **Christian Gonçalves Alonso**, **Professor do Magistério Superior**, em 25/03/2020, às 17:03, conforme horário oficial de Brasília, com fundamento no art. 6º, § 1º, do Decreto nº 8.539, de 8 de outubro de 2015.

Documento assinado eletronicamente por **WESLEY DE ALMEIDA BRITO**, **Usuário Externo**, em 01/04/2020, às 20:46, conforme horário oficial de Brasília, com fundamento no art. 6º, § 1º, do Decreto nº 8.539, de 8 de outubro de 2015.

A autenticidade deste documento pode ser conferida no site https://sei.ufg.br/sei/controlador_externo.php?acao=documento_conferir&id_orgao_acesso_externo=0, informando o código verificador **1236220** e o código CRC **D31C6FAE**.

Referência: Processo nº 23070.012960/2020-46 SEI nº 1236220

UFG

UNIVERSIDADE FEDERAL DE GOIÁS
PROGRAMA DE PÓS-GRADUAÇÃO EM CIÊNCIAS FARMACÊUTICAS

Coordenador do Programa de Pós-Graduação

Prof. Dr. Eric de Souza Gil

Vice-Coordenador do Programa de Pós-Graduação

Prof. Dr. Matheus Lavorenti Rocha

Goiânia-GO
2020

UFG

UNIVERSIDADE FEDERAL DE GOIÁS
PROGRAMA DE PÓS-GRADUAÇÃO EM CIÊNCIAS FARMACÊUTICAS

BANCA EXAMINADORA

Aluna: Rayane Santa Cruz Martins de Queiroz Antonino

Orientadora: Prof. Drª Eliana Martins Lima

Coorientadora: Drª Thais Leite Nascimento

Prof. Drª Eliana Martins Lima / Presidente
Professor Titular da Faculdade de Farmácia da Universidade Federal de Goiás, FF/UFG.

Prof. Dr Christian Gonçalves Alonso / Membro Titular
Professor do Instituto de Química da Universidade Federal de Goiás, IQ/UFG.

Prof. Dr Eric de Souza Gil/ Membro Titular
Professor da Faculdade de Farmácia da Universidade Federal de Goiás, FF/UFG.

Prof. Dr Luís Antônio Dantas Silva / Membro Titular
Professor da Faculdade de Farmácia da Universidade Anhaguera, FF/Uni-Anhaguera.

Prof. Dr Wesley de Almeida Brito / Membro Titular
Professor da Faculdade de Farmácia da Universidade Estadual de Goiás, FF/UEG.

Prof. Dr Korbinian Löbmann / Membro Suplente
Professor da Faculdade de Farmácia da Universidade de Copenhague, FF/UC.

Drª Thais Leite Nascimento / Membro Suplente
Pesquisadora da Faculdade de Farmácia da Universidade Federal de Goiás, FF/UFG.

Data:20/03/2020

DEDICATÓRIA

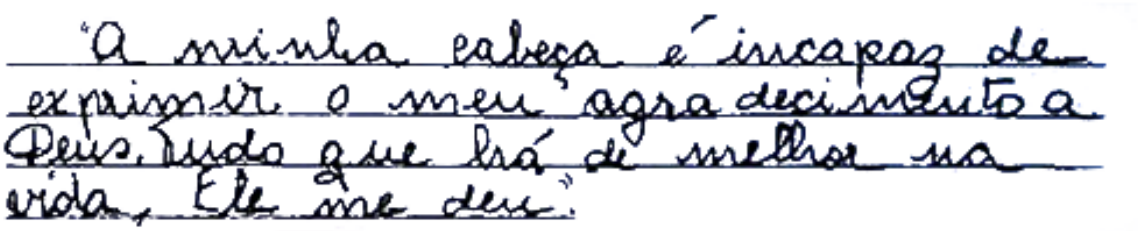

Nilza Maria Santa Cruz Martins
(*in memorian*)

AGRADECIMENTOS/ACKNOWLEDGMENT

A Profª. Drª. Eliana Martins Lima, minha orientadora durante os anos de doutoramento, minha gratidão pela confiança desde o início ao me receber em seu laboratório, como também pelas oportunidades de trabalho e aprendizado no laboratório. Por ser exemplo de que é possível fazer ciência de alta qualidade no Brasil, inspirando jovens com sua vasta experiência.

A Drª. Thais Leite Nascimento, minha coorientadora, meu agradecimento pela oportunidade de trabalhar com uma pesquisadora jovem, dedicada, profissional e competente, com a qual muito aprendi sobre pesquisa científica.

Professor Korbinian Löbmann PhD, my sincere thanks for the dedication and guidance to my work during my time at the University of Copenhagen. My thanks also to the researcher Adam Bohr PhD for his availability, attention and guidance during his time at the University of Copenhagen. My thanks for the opportunity to work with internationally recognized researchers.

Professor Heloisa Bordallo PhD, my gratitude for the support when I was in Copenhagen, for the professional guidance and for being an example of competence and professionalism. Thank you for being an example and the inspiration of a female researcher.

A coordenação de aperfeiçoamento de pessoal de nível superior (CAPES), ao Conselho Nacional de Desenvolvimento Científico e Tecnológico (CNPq), a fundação de amparo à pesquisa do estado de Goiás (FAPEG) pelo apoio financeiro.

A Deus pelo dom da vida e por tudo que me deu e me dá todos os dias.

Aos meus pais, João e Ceiça, que são o meu exemplo de força, determinação, respeito, responsabilidade e família.

Aos meus irmãos, Thâmisa, Ibysson e Raysse pelo apoio durante toda esta caminhada, como também aos meus cunhados, meu muito obrigada.

Ao meu amor, Rodrigo, que cuidadosamente me ajudou em cada etapa desta pesquisa, sabendo diferenciar o pessoal do profissional.

A minha família amada, tios e primos, que estão comigo sempre. Dos momentos mais leves até a grandes dificuldades, meu muito obrigada.

A Fernada Bellato que sempre mostrou cooperação e vontade de ajudar para a concretização deste trabalho, meu sincero agradecimento.

A todos do FARMATEC, que ajudaram direta e indiretamente para realização deste trabalho.

SUMÁRIO

LISTA DE FIGURAS

CAPÍTULO 01

CAPÍTULO 02

CAPÍTULO 03

LISTA DE QUADROS

CAPÍTULO 01

LISTA DE TABELAS

CAPÍTULO 03

INTRODUÇÃO

Melhorar a resposta terapêutica dos fármacos é um dos grandes objetivos da tecnologia farmacêutica. Esta grande área de pesquisa e desenvolvimento, utiliza-se de tecnologias e conhecimentos multidisciplinares voltados à otimização dos sistemas de liberação de fármacos. Busca-se, por exemplo diminuir os efeitos colaterais com aplicação de sistemas nanoparticulados (Chung *et al.*, 2019), melhorar o alcance de fármacos no sistema nervoso central (SNC) através de novos sistemas de liberação e administração (Qureshi *et al.*, 2019), aumentar a entrega e ação terapêutica de fármacos ao promover o maior tempo de contato do fármaco no local de ação, como o desenvolvimento de formulações mucoadesivas para tratamento de mucosas inflamadas (Léber *et al.*, 2019). Busca-se ainda aumentar a biodisponibilidade de fármacos com baixa solubilidade aquosa obtendo a forma amorfa do fármaco seja por sistemas porosos adsorventes, como as sílicas mesoporosas, como também aumentar a estabilidade da forma amorfa em relação ao tempo de armazenamento (Zůza *et al.*, 2019).

A busca por melhor eficácia terapêutica de fármacos foi a grande motivação dessa pesquisa, empregando distintas tecnologias para desenvolvimento de formulações com diferentes objetivos e alvos terapêuticos. A primeira parte desta pesquisa teve como objetivo desenvolver um gel termorreversível *in situ* mucoadesivo, capturando um corticosteroide para o tratamento de regiões mucosas com um quadro de inflamação. Desta primeira parte foram produzidas três publicações científicas que estão organizadas como os dois primeiros capítulos desse documento e um anexo. Já a segunda parte da pesquisa teve como objetivo investigar o papel adsorvente da sílica mesoporosa em dois fármacos distintos quanto à tendência à cristalização, visando além da biodisponibilidade o aumento da estabilidade física dos sistemas e o impacto dos fármacos no armazenamento dos sistemas. Através do desenvolvimento deste estudo foi produzido um artigo científico apresentado no terceiro e último capítulo deste documento. Em síntese a pesquisa desenvolvida durante o período do doutorado está organizada em duas partes, nas quais:

Capítulo 01 - Este capítulo tem como tema central a mucoadesão, e constitui uma revisão da literatura publicada como capítulo no livro “Ciências aplicadas a produtos para a saúde”, pela editora da Universidade Estadual de Goiás em 2019, ISBN 978-85-5582-060-1 (anexo 3). Estratégias de desenvolvimento de novas formas farmacêuticas mucoadesivas, o muco e sua função no corpo humano, as teorias que analisam a

mucoadesão, as formulações mucoadesivas já disponíveis e as técnicas e ensaios utilizados para quantificar a mucoadesão foram abordados neste capítulo.

Capítulo 02 – Neste capítulo descrevemos o desenvolvimento e a caracterização *in vitro* / *in vivo* de uma formulação gelificante *in situ* mucoadesiva usando poloxamer 407 (Pluronic® F 127), um polímero termorreversível, capturando budesonida (BUD)[1], um potente corticosteróide usado para o tratamento de uma ampla gama de doenças inflamatórias, incluindo aqueles que afetam mucosas, como no trato gastrointestinal. Este capítulo foi publicado em 2019 como artigo original no periódico *Journal of Controlled Release*, intitulado *Thermoreversible mucoadhesive polymer-drug dispersion for sustained local delivery of budesonide to treat inflammatory disorders of the GI tract* (anexo 4). O termo com a aprovação pelo comitê de ética para uso de animais está anexo (anexo 1). Outra publicação, referente a composições farmacêuticas orais de corticosteroides que gelificam *in situ*, foi a produção de uma patente (anexo 2). Patente depositada e publicada no *United States Patent and Trademark Office*, com aplicação internacional sob *Patent Cooperation Treaty (PCT)*, WO 2018/193423 A1, 2018. Esta patente é resultado de uma parceria entre a Universidade e uma indústria farmacêutica, *Ferring Pharmaceuticals*, estabelecida para o desenvolvimento de formulações farmacêuticas mucoadesivas.

Por sua vez, consoante a segunda parte, que trata de tecnologias voltadas à otimização da biodisponibilidade e promover maior estabilidade utilizando sistemas porosos adsorventes, tem-se o capítulo 3.

Capítulo 03 - Neste capítulo, foi descrito um método para determinar a capacidade de carga em monocamada (MLC) do naproxeno[2], fármaco fraco para amorfizar, em sílica mesoporosa (MS). MS pode ser usada como portador para estabilizar a forma amorfa de um fármaco. Além disso, o impacto da monocamada, preenchimento dos poros e excesso, na estabilidade física desse sistema foi estudado e comparado ao ibuprofeno[3], fármaco forte para amorfizar. Por fim, investigou-se o impacto da carga do fármaco no armazenamento abaixo e acima da temperatura de transição vítrea (T_g), em particular com foco na (in) estabilidade amorfa do fármaco confinado, para ambos os fármacos. Usando a Teoria do Densidade Funcional Teórica (DFT) e a Dinâmica Molecular *ab initio* (AIMD), as energias de ligação para a monocamada sugerem que a monocamada é termodinamicamente mais favorável do que a forma cristalina, enquanto que a forma amorfa confinada é termodinamicamente menos favorável. Este capítulo foi publicado na

[1] Estrutura da budesonida (anexo 6).

[2] Difratograma do naproxeno puro (anexo 7).

[3] Difratograma do ibuprofeno puro (anexo 8).

forma de artigo original na revista *International Journal of Pharmaceutics: X*, em 2019 (anexo 5).

PARTE I

1. GEL TERMORREVERSÍVEL

Os géis são sistemas semissólidos que consistem em dispersões de pequenas ou grandes moléculas em um veículo líquido aquoso que adquire consistência semelhante às geleias pela adição de um agente gelificante (Allen Jr *et al.*, 2013). Os agentes gelificantes são polímeros sintéticos, como as macromoléculas de carbômeros ou semissintéticos, como os derivados de celulose, carboximetilcelulose (CMC), hidroxipropilmetilcelulose (HPMC), além dos naturais como, a goma xantana.

Géis poliméricos geralmente exibem viscosidade muito alta por causa da interação das cadeias poliméricas em nível tridimensional com o sistema solvente. Os géis podem ser classificados em dois tipos, i) dependentes da natureza das ligações entre as cadeias da rede, ou seja, sistemas irreversíveis com uma rede tridimensional formada por ligações covalentes entre as macromoléculas e, ii) sistemas reversíveis pela variação de temperatura ou pH, mantendo suas ligações intermoleculares entre as macromoléculas (Storpirtis et al., 2009).

Os sistemas reversíveis são potencialmente aplicáveis no desenvolvimento farmacotécnico pela habilidade de modificar as características de um gel seja pela variação de temperatura, variação do pH, adição de sais e outros, resultando em um produto com perfil de liberação diferente. Os copolímeros tem papel importante na área farmacêutica, pois podem produzir cadeias de macromoléculas com segmentos que possuem solubilidades diferentes em um determinado solvente (Eshel-Green e Bianco-Peled, 2016).

Os copolímeros de polioxietileno (POE ou PEO) e polioxipropileno (POP ou PPO), comercialmente conhecidos como poloxamers ou Pluronics, são bastante empregados como agentes dispersores, solubilizadores e estabilizadores para sistemas emulsivos. O Pluronic® F-127 (PF127) ou poloxamer 407 é um copolímero não iônico formado por unidades tribloco de PEO-PPO-PEO (Akkari *et al.*, 2016). As propriedades de termorreversibilidade e atoxicidade tem tornado esse copolímero bastante atrativo para o desenvolvimento de géis para administração na mucosa oral, na mucosa vaginal, na mucosa ocular, na pele e outras (Caramella *et al.*, 2015; Ban *et al.*, 2017).

O PF127 em solução aquosa a partir de 15% (m/m) e com a variação de temperatura modifica a organização micelar, agregando-as e formando uma rede interconectada, e, consequentemente, um gel firme (Bhowmik *et al.*, 2013; Akash e Rehman, 2015). As

micelas apresentam uma estrutura esférica, em que a cadeia central de PPO localiza-se no seu interior, devido ao caráter hidrofóbico, e as duas cadeias de PEO localizam-se no exterior, devido ao caráter hidrofílico (Bruschi *et al.*, 2007). As forças intermoleculares, como as ligações de hidrogênio estabelecidas entre o polímero e a água, direcionam o processo de geleificação, sendo a viscosidade do gel dependente da temperatura e da concentração do polímero em solução (Escobar-Chávez *et al.*, 2006). Sabe-se que a temperatura de geleificação pode ser influenciada por muitos fatores, dentre eles, a concentração do polímero, a massa molecular do polímero, a adição de fármaco, a adição de solventes, sais e outros (Attwood *et al.*, 1985; Lenaerts *et al.*, 1987).

O entendimento das propriedades reológicas destes géis é necessário para o desenvolvimento de um sistema de liberação eficaz, uma vez que o processo de geleificação térmica *in situ* aumenta o tempo de contato e permanência do fármaco no local de ação (Boateng *et al.*, 2015). O aumento na viscosidade do gel promove a adesão às superfícies mucosas, mucoadesão. Ou seja, a geleificação *in situ* aumenta a vicosidade do gel e, consequentemente adesão à mucosa. Os géis termorreversíveis constituem sistemas de liberação promissores, pois a localização do fármaco mais próxima do local de ação pode levar a redução da dose administrada pelo paciente, redução dos efeitos colaterais e o aumento da eficácia terapêutica (Bashir *et al.*, 2019).

CAPÍTULO 01

ESTRATÉGIAS PARA FORMULAÇÃO DE PRODUTOS FARMACÊUTICOS MUCOADESIVOS

*Revisão da literatura publicada como capítulo no livro "Ciências aplicadas a produtos para a saúde", pela editora da Universidade Estadual de Goiás, Anápolis, em 2019, ISBN 978-*85-5582-060-1.

Autores: Rayane Santa Cruz Martins de Queiroz Antonino[1]; Eliana Martins Lima[1]; Thais Leite Nascimento[1,2]

[1]Centro de Pesquisa, Desenvolvimento e Inovação Tecnológica em Fármacos, Medicamentos e Cosméticos, Faculdade de Farmácia, UFG, Goiânia, GO, Brasil.
[2]Programa de Pós-Graduação em Ciências Aplicadas a Produtos para Saúde, Universidade Estadual de Goiás, Anápolis, GO, Brasil.

RESUMO

Formulações mucoadesivas são uma estratégia de desenvolvimento de novas formas farmacêuticas, que tem como objetivo aumentar o tempo de contato do fármaco com a superfície mucosa, melhorando sua eficiência terapêutica. Para o desenvolvimento de formulações mucoadesivas faz-se necessário compreender a função e localização do muco no corpo humano, como também as teorias que explicam o processo de mucoadesão. Este capítulo introduz as definições sobre muco e o processo de interação de formulações com as mucosas. Como também as formas farmacêuticas mucoadesivas já disponíveis, assim como as técnicas e ensaios utilizados para quantificarem a mucoadesão deste tipo de formulação.

Palavras-Chave: Muco; mucina; mucoadesão; formulações mucoadesivas.

ABSTRACT

Mucosadhesive formulations are a strategy of development of new pharmaceutical forms, which aims to increase the time of contact of the drug with the mucosal surface, improving its therapeutic efficiency. For the development of mucoadhesive formulations it is necessary to understand the function and location of the mucus in the human body, as well as the theories that explain the process of mucoadhesion. This chapter introduces the definitions on mucus and the process of interaction of formulations with mucous membranes. As well as the mucoadhesive dosage forms already available, as well as the techniques and assays used to quantify the mucoadhesion of this type of formulation.

Keywords: Mucus; mucin; mucoadhesion; mucoadhesive formulations.

ESTRATÉGIAS PARA FORMULAÇÃO DE PRODUTOS FARMACÊUTICOS MUCOADESIVOS

Rayane Santa Cruz Martins de Queiroz Antonino[1]; Eliana Martins Lima[1]; Thais Leite Nascimento[1,2]

[1]Centro de Pesquisa, Desenvolvimento e Inovação Tecnológica em Fármacos, Medicamentos e Cosméticos, Faculdade de Farmácia, UFG, Goiânia, GO, Brasil.
[2]Programa de Pós-Graduação em Ciências Aplicadas a Produtos para Saúde, Universidade Estadual de Goiás, Anápolis, GO, Brasil.

INTRODUÇÃO

O avanço em tecnologias que buscam melhorias e inovações na área da saúde inclui o desenvolvimento de novos produtos e materiais. Os frutos dessas pesquisas visam atender as necessidades de terapias com objetivos cada vez mais específicos e refinados (Latheeshjal et al., 2011; Camblin et al., 2016).

Na área de tecnologia farmacêutica, a pesquisa em medicamentos busca maior eficácia, segurança e melhoria do bem-estar do paciente em tratamento (Patil et al., 2016). Essa busca movimenta três setores importantes da sociedade: pesquisa, indústria e clínica. Dentro das inúmeras estratégias de desenvolvimento de novas formas farmacêuticas, estão as formulações mucoadesivas, que têm como objetivo aumentar o tempo de contato do fármaco com a superfície mucosa, aumentando sua absorção e eficiência terapêutica (Laffleur, 2016; Rajaram e Laxman, 2017).

Neste capítulo, o leitor será introduzido às definições sobre muco e o processo de interação de formulações com as mucosas. As formas farmacêuticas mucoadesivas e os materiais que as compõem, assim como as técnicas e ensaios utilizados para quantificarem a mucoadesão de formulações, serão abordados.

MUCO E MUCOADESÃO

Para o desenvolvimento de formulações mucoadesivas faz-se necessário compreender as bases fisiológicas, composição, função e localização do muco no corpo humano. A mucosa representa a superfície úmida que recobre algumas regiões do corpo como a cavidade oral, trato respiratório, trato gastrointestinal (TGI), região vaginal e conjuntiva ocular (Laffleur, 2016).

Além de desempenharem um papel importante na proteção do epitélio celular contra danos químicos e mecânicos, as membranas mucosas também proporcionam lubrificação e molhabilidade do epitélio da célula e regulam o seu teor de umidade (Khutoryanskiy, 2011). A mucosa é composta por proteínas livres, lipídios, glicoproteínas, sais minerais e

água (Quadro 1), sendo esta composição variável de acordo com a localização do muco no organismo.

Quadro 1– Representação geral da composição química do muco.

Constituintes	Proporções
Proteínas livres	0,5 - 1%
Lipídios e glicoproteínas	1 - 5%
Sais minerais	0,5 - 5%
Água	95%

Adaptado de (Kharenko et al., 2009; Laffleur, 2016)

A mucina é principal glicoproteína do muco, responsável por formar uma camada de gel viscoelástico quando hidratada, que confere ao muco sua viscosidade característica. Esta biomacromolécula tem elevado peso molecular (0,5 – 40 MDa), com subunidades de 500 KDa unidas por ligações peptídicas e pontes dissulfeto de cisteína – cisteína intramoleculares (Peppas e Sahlin, 1996; Khutoryanskiy, 2011), e pode estar estruturada de forma linear ou não linear.

Cada unidade de mucina é composta por cadeias de oligossacarídeos associadas a agregados proteicos. A região proteica representa 12 a 17% do peso total da mucina, e é 70% composta pelos aminoácidos prolina, treonina e serina. Já as cadeias de oligossacarídeos são feitas de N-acetilglucosamina, N-acetilgalactosamina, galactose, fucose e ácido N-acetilneuramico (ácido siálico) (Yang e Robinson, 1998). As cadeias de oligossacarídeos recobrem mais de 60% da fração proteica, sendo o restante não glicosilado (Kharenko et al., 2009). A cobertura dos oligossacarídeos confere carga negativa à mucina, devido à presença dos grupamentos carboxilatos do ácido siálico e dos ésteres sulfatados em algumas unidades de açúcar (Figura 1). O pKa aproximado destes grupos ácidos está entre 1,0 a 2,6 resultando na sua ionização sob condições fisiológicas (Laffleur, 2016).

Figura 1 – Imagem esquemática da subunidade de mucina.

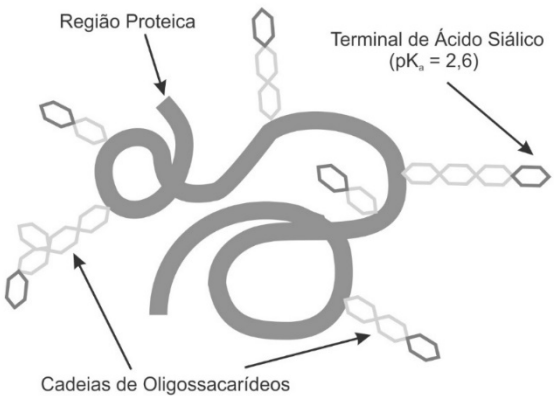

Adaptado com autorização de Macromolecular Bioscience (Khutoryanskiy, 2011)

Em 1986, Longer e Robinson definiram o termo bioadesão como a "ligação de uma macromolécula sintética ou natural a uma superfície biológica" (Longer e Robinson, 1986; Salamat-Miller et al., 2005). Já a mucoadesão é definida como a interação entre duas superfícies, sendo uma delas material natural ou sintético e a outra o muco (humano ou animal) e/ou uma superfície epitelial (Smart, 2005; Rajaram e Laxman, 2017).

O processo de mucoadesão acontece em dois estágios, o estágio de contato e o de consolidação. O primeiro é caracterizado pelo umedecimento, expansão e inchaço da formulação adesiva, aumentando o contato com a mucosa (Camblin et al., 2016; Rajaram e Laxman, 2017). No estágio de consolidação, a umidade facilita o movimento das moléculas poliméricas mucoadesivas. Essas moléculas se separam umas das outras e começam a interagir com o muco/epitélio através de forças de van der Waals, atrações eletrostáticas, ligações de hidrogênio e interações hidrofóbicas (Smart, 2005). Evidentemente, para que a adesão das duas superfícies seja consolidada, é necessário que as forças atrativas sejam mais dominantes que as forças repulsivas (Reineke et al., 2013)(Figura 2).

Figura 2 – Esquema ilustrativo dos estágios de mucoadesão.

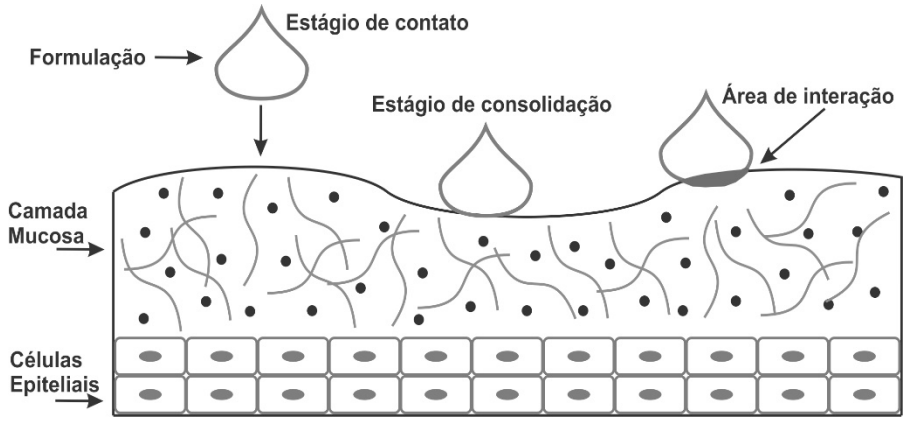

Adaptado com autorização de Elsevier (Patil et al., 2016)

As teorias que baseiam os mecanismos pelos quais acontece o processo de mucoadesão serão abordadas no próximo tópico deste capítulo.

MECANISMOS DE MUCOADESÃO

O processo de mucoadesão é extensamente detalhado na literatura por algumas teorias. Alguns autores consideram cinco teorias (Kharenko et al., 2009; Laffleur, 2016) e outros seis (Smart, 2005; Khutoryanskiy, 2011). Abordaremos aqui as seis teorias que explicam os mecanismos de mucoadesão, sendo elas:

i. Teoria eletrônica – Aplica-se quando o material mucoadesivo e o muco tem diferentes características eletrônicas, gerando uma atração eletrostática devido às cargas opostas (Ahuja et al., 1997; Khutoryanskiy, 2011);

ii. Teoria da adsorção – Considera-se que atração entre o muco e os polímeros mucoadesivos é conseguida através de interações específicas como ligação de hidrogênio e forças de van der Waals, como também as interações hidrofóbicas quando o material mucoadesivo tem características anfifílicas. Considera ainda, a possibilidade de formar fortes ligações covalentes entre a mucina e o material mucoadesivo (Smart, 2005; Ugwoke et al., 2005);

iii. Teoria da molhabilidade – Aplicável principalmente a sistemas líquidos considera a energia superficial e interfacial. Correlaciona a tensão superficial do muco e do material mucoadesivo com a sua capacidade de se espalhar sobre a camada de muco. A afinidade de um líquido para uma superfície pode ser determinada considerando o ângulo de contato do líquido na superfície. Sendo a regra geral que quanto menor o ângulo de contato, maior a afinidade do líquido na superfície (Shankar et al., 2010; Rajaram e Laxman, 2017);

iv. Teoria da difusão – Descreve a interdifusão de macromoléculas mucoadesivas no gel de muco. Este processo é conduzido pelo gradiente de concentração e sofre influência do peso molecular do material adesivo e da sua mobilidade de cadeia. A profundidade de interpenetração depende do coeficiente de difusão e do tempo de contato (Garti, 2008; Laffleur, 2016);

v. Teoria da fratura - Relaciona a dificuldade de separação de duas superfícies após a adesão. Esta teoria é bastante aceita e descreve que a força de fratura (ou tensão de tração) é a força necessária para separar as duas superfícies após a adesão. A força de fratura pode ser calculada pela seguinte equação (Rajaram e Laxman, 2017):

$$\mathrm{Sm} = {}^{\mathrm{Fm}}/_{\mathrm{Ao}}$$

Em que;
Sm – Força de fratura
Fm – Força máxima de desprendimento
Ao – Área de superfície

vi. Teoria mecânica – Esta teoria considera o efeito da rugosidade superficial, favorecendo a adesão devido à maior área de contato. A contribuição dos efeitos da teoria mecânica na mucoadesão torna-se mais importante para os materiais ásperos e porosos (Batchelor, 2004a).

Cada teoria aqui apresentada é igualmente importante para descrever o processo de mucoadesão. Nenhuma delas isoladamente explica a mucoadesão das variadas formulações farmacêuticas já desenvolvidas, pois esta resulta da combinação de vários mecanismos (Rajaram e Laxman, 2017).

Alguns autores explicam o processo de mucoadesão em fases sequenciais, estando cada uma das fases associadas a um mecanismo diferente. Primeiramente, o material mucoadesivo molha e dilata (teoria de molhagem), sequencialmente são criadas interações (físicas), não covalentes, dentro da interface muco/polímero (teorias eletrônicas e de adsorção). Em seguida, as cadeias de polímero e mucina interpenetram-se (teoria da difusão) e se entrelaçam juntas, formando ligações não covalentes e covalentes adicionais (teorias eletrônicas e de adsorção) (Smart, 2005; Khutoryanskiy, 2011).

FORMULAÇÕES FARMACÊUTICAS MUCOADESIVAS

Os materiais utilizados na obtenção de formulações mucoadesivas podem ser classificados quanto a sua natureza química, sendo eles: metálicos, cerâmicos e poliméricos. Polímeros são macromoléculas arranjadas por meio de ligações químicas entre pequenas unidades repetidas, os monômeros. Estas moléculas são a base das formulações mucoadesivas, devido à sua capacidade de formar ligações químicas com outras superfícies. Polímeros mucoadesivos devem ser não tóxicos, não irritantes, podem ser solúveis ou insolúveis em água e devem interagir com a mucosa rapidamente (Patil et al., 2016). Eles podem também ser divididos quanto as suas propriedades (Quadro 2).

Quadro 2 – Classificação dos polímeros mucoadesivos quanto as suas propriedades.

Natural	Alginato de sódio, pectina, gelatina, carragenina, goma xantana, goma Guar
Sintético	Polivinil álcool (PVA), poliamidas, policarbonatos, polimetacrilatos
Biocompatível	Ésteres de ácido hialurônico, polivinil acetato, polietilenoglicol
Biodegradável	Polilactatos, quitosana, policaprolactona (PCL), poliglicoides, óxido de polietileno

Adaptado de (Lohani e Chaudhary, 2012)

As formulações farmacêuticas mucoadesivas podem estar na forma sólida, líquida e semissólida. No estado sólido, os comprimidos mucoadesivos são aplicados, principalmente, na cavidade oral, mas podem também ter aplicação ginecológica (Kharenko et al., 2009). Os comprimidos que se ligam à mucosa bucal tem sido bem sucedidos comercialmente, como as formulações de testosterona (Striant®, Columbia Laboratories Inc, EUA) e nitroglicerina (Nitrogard®, Forest Pharmaceuticals Inc., USA). Com o objetivo de melhorar as propriedades mucoadesivas destes comprimidos, polímeros mucoadesivos

como carbomeros, gomas, resinas naturais e derivados de celulose são adicionados à formulação. Apesar da eficácia dos comprimidos mucoadesivos para aplicação local, a principal restrição à sua ampla utilização decorre do seu tamanho e forma (Van Roey et al., 2004).

Filmes poliméricos mucoadesivos também são comumente propostos para aplicação oral e oftálmica (Okamoto et al., 2001; Chun et al., 2003; Ahuja et al., 2006). Ao contrário dos comprimidos, os filmes têm maior flexibilidade para se adequarem à superfície de aplicação. Eles também apresentam algumas vantagens em comparação a formulações semissólidas (cremes e géis), uma vez que podem manter uma dose precisa de fármaco no local de aplicação (Birudaraj et al., 2005; Salamat-Miller et al., 2005). Filmes para aplicação ocular, em comparação às formulações líquidas, apresentam vantagens como maior tempo de retenção, maior tempo de meia vida de eliminação, maior precisão da dosagem e maior estabilidade (Ludwig, 2005).

As formulações no estado líquido são utilizadas normalmente com finalidade terapêutica ou protetora (Batchelor, 2004b). Lágrimas artificiais e saliva artificial, por exemplo, são formulações líquidas a base de polímeros mucoadesivos (carbomeros e carboximetilcelulose de sódio), cuja função é proteger os olhos e a boca ou auxiliar no tratamento da síndrome do olho seco e na secura da boca (xerostomia) (Albietz e Douglas, 2003; Preetha e Banerjee, 2005).

Os líquidos mucoadesivos também são utilizados para a proteção da mucosa esofágica. Por exemplo, o medicamento Gaviscon (Gaviscon Liquid®, Reckitt Benckiser Healthcare, Reino Unido), que usa alginato de sódio como polímero mucoadesivo, pode se aderir à mucosa esofágica durante 1 hora após o uso, proporcionando proteção ao esôfago contra o suco gástrico em casos de refluxo estomacal (Batchelor, 2004b; Yadav e Deshmukh, 2016). Formulações mucoadesivas para aplicação no esôfago têm sido estudadas para o tratamento de disfunções motoras, infecções fúngicas e tumores esofágicos (Batchelor, 2005; Zhang et al., 2008).

Formulações contendo líquidos formadores de géis têm sido propostas para tratamento ocular, nasal e transdérmico (Lee et al., 2000; Ugwoke et al., 2005; Kharenko et al., 2009). Estas formulações contêm poloxamer, pectina, carbopol ou ácido hialurônico (Willats et al., 2006; Géraud et al., 2017; Sousa et al., 2017), que são polímeros caracterizados por transições de fase e a formação de géis viscoelásticos em resposta a temperatura, força iônica ou pH (Ludwig, 2005). A adição de polímeros mucoadesivos aumenta o tempo de contato do gel com o local de ação, melhorando a eficácia terapêutica. Os produtos NyoGel® (timolol, Novartis, Suíça, contendo um carbomero e álcool polivinílico) e Pilogel® (cloridrato

de pilocarpina, Alcon Laboratories, Suíça, contendo carbopol 940) são exemplos comerciais de géis poliméricos mucoadesivos para tratamento oftálmico. Um outro exemplo de formação de gel mucoadesivo é o Zilactin® B (Zilactin®, Zila Pharmaceuticals, EUA), produto contendo benzocaína e lidocaína, indicado para o tratamento sintomático do herpes nos lábios (Ludwig, 2005; Valenta, 2005; Zhang et al., 2008).

Sistemas micro e nanoestruturados também têm sido desenvolvidos para aplicação em formulações mucoadesivas (Patil et al., 2016). Micro e nanopartículas oferecem a possibilidade de aumentar a superfície e o tempo de contato do fármaco com o local de ação, proporcionando vantagens adicionais à terapia medicamentosa (Nappinnai e Sivaneswari, 2013). Essas partículas podem ser obtidas a partir de polímeros biocompatíveis (derivados de celulose e amido, polietilenoglicol e seus copolímeros, álcool polivinílico, ácido hialurônico e seus ésteres) e polímeros biodegradáveis (polilactatos, poliglicólidos, policaprolactonas e quitosana) bem como misturas de polímeros e complexos polieletrólitos (Vasir et al., 2003; Costantino et al., 2007). A maior parte dos estudos de sistemas micro e nanoestruturados mucoadesivos ainda é realizada em centros de pesquisa. A complexidade do escalonamento do nível laboratorial para o industrial é atualmente o principal desafio para sua ampla comercialização (Kharenko et al., 2009; Laffleur, 2016).

ENSAIOS DE MUCOADESÃO *IN VITRO*

Os ensaios de mucoadesão são importantes para quantificar a eficácia da formulação em aderir ao muco. Variados métodos de caracterização, desenvolvidos em diferentes centros de pesquisa, estão descritos na literatura. Contudo, um método de ensaio normatizado e padrão para os ensaios de mucoadesão ainda não foi definido (Peppas e Sahlin, 1996; Davidovich-Pinhas e Bianco-Peled, 2010), devido à grande variabilidade entre as formulações e possibilidade de avaliação da mucoadesão. De forma geral, estas técnicas podem ser classificadas em medidas diretas e indiretas, e estão apresentadas nesta seção. A Figura 3 apresenta de forma esquemática exemplos de método direto e indireto, texturômetro e ângulo de contato, respectivamente.

Figura 3 – Representação esquemática de métodos direto e indireto que medem a mucoadesão *in vitro*; (a) equipamento texturômetro; (b) gráfico força x tempo do texturômetro; (c) medição por ângulo de contato.

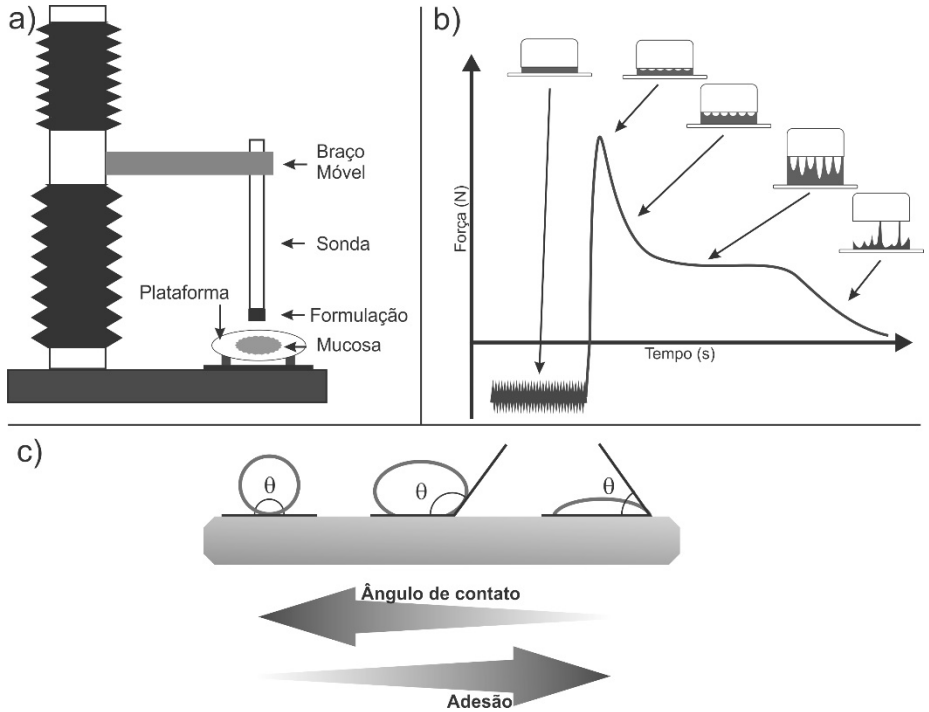

Adaptado com autorização de Springer (Alam et al., 2007) e Wolters Kluwer Medknow Publications (Latheeshjal et al., 2011)

MÉTODOS DIRETOS

A determinação direta da mucoadesão de uma formulação normalmente envolve a quantificação da força necessária para separar a superfície mucoadesiva do muco. Outra abordagem possível é a determinação de outro parâmetro quantitativo envolvido nesta separação, como o tempo. Estes ensaios de mucoadesão *in vitro* são comumente realizados em modo de tensão, no qual a força aplicada atua na direção axial, ou no modo de cisalhamento, no qual a força atua na direção tangencial (Figura 4).

Figura 4 – Tipos de forças aplicadas em ensaios de mucoadesão *in vitro*.

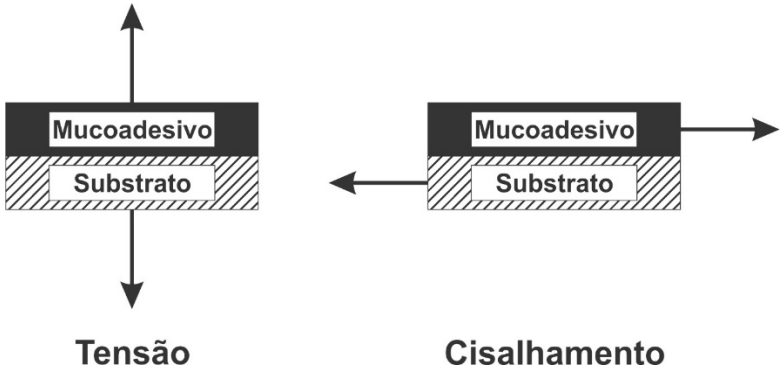

Adaptado com autorização de Taylor & Francis (Davidovich-Pinhas e Bianco-Peled, 2010)

O ensaio de tensão é realizado utilizando instrumentos comercialmente disponíveis, tal como máquinas de ensaios mecânicos ou analisadores de textura (texturômetros). Os

resultados são normalmente apresentados como força de desprendimento máxima e trabalho total de adesão, que significam a força máxima necessária para quebrar a ligação adesiva e a área sob a curva representando o trabalho de desprendimento, respectivamente (Baloğlu et al., 2003). O tipo de substrato utilizado para o teste é um parâmetro que influencia diretamente nos resultados obtidos. O substrato mais próximo das condições fisiológicas é a superfície mucosa fresca, obtida de fonte animal. Devido à sua disponibilidade limitada, a utilização de outras superfícies é comum (Grabovac et al., 2005; Venter et al., 2006). Os pós de mucina, por exemplo, são comercialmente disponíveis e amplamente usados na pesquisa. Eles podem ser preparados como solução aquosa concentrada (gel), disco comprimido parcialmente hidratado, filme hidratado ou podem ainda ser utilizados para embeber discos de papel de filtro com solução de mucina (Munasur et al., 2007; Fransén et al., 2008). Neste tipo de teste há uma variedade de fatores que afetam os resultados, como o tipo de amostra (estado físico, geometria), condições ambientes (seco ou úmido) até os parâmetros de análise (velocidade de desprendimento, força de pré-carga e tempo de contato) (Peppas e Sahlin, 1996; Patil et al., 2016).

O ensaio dinâmico sob força de cisalhamento pode ser realizado por tempo de duração de mucoadesão, com o método do cilindro rotativo, ou como ensaio de fluxo contínuo. No primeiro, avalia-se a capacidade de formulações mucoadesivas sólidas ou semissólidas de manter contato com a superfície mucosa sob forças de cisalhamento. O parâmetro quantitativo mensurado é o tempo de desprendimento, desintegração e/ou erosão da formulação (Bernkop-Schnürch e Steininger, 2000). No ensaio de fluxo contínuo, a capacidade de um polímero para manter a ligação com a superfície da mucosa sob força de cisalhamento, quando submetida a um fluxo contínuo, é quantificada (Belgamwar et al., 2009).

A microscopia de força atômica também permite que as forças moleculares e superficiais sejam mensuradas em uma escala quase molecular, sendo, portanto, adequada para o monitoramento da interação mucina-polímero. O uso dessa técnica se estende ainda à caracterização da alteração na rugosidade da superfície que ocorre com ligações entre o polímero adesivo e o tecido mucoso (Cleary et al., 2004; Bassi Da Silva et al., 2017).

MÉTODOS INDIRETOS

Os ensaios de reologia, espectroscópicos e de energia de superfície / ângulo de contato são uns dos principais métodos indiretos de quantificação da mucoadesividade de uma formulação. Por meio da reologia é possível monitorar a força de interação das cadeias

poliméricas com a mucina e prever a capacidade de mucoadesão. Dois tipos de experimentos reológicos são empregados, a medida de viscosidade e a relação entre o módulo elástico (G') e o módulo viscoso (G") (Hay et al., 2017), módulos viscosimétricos que relacionam o comportamento viscoelástico da formulação e sua capacidade de armazenamento e perda de energia frente à deformação (Bassi Da Silva et al., 2017).

O método espectroscópico detecta a interação do polímero e do muco a nível de ligações químicas. Por meio de um espectrômetro de infravermelho com transformada de Fourier (FTIR) acoplado ao modo de reflexão total atenuada (ATR) é possível analisar as interações interfaciais ou a interpenetração entre o filme polimérico e amostra de mucina hidratada (Cilurzo et al., 2005; Sriamornsak et al., 2008). Já as medições dos ângulos de contato podem predizer a natureza mucoadesiva da amostra devido ao papel da energia superficial no processo de mucoadesão. Ângulos de contato menores são indicativos de melhor molhabilidade, e indicam o aumento da adesão (Santos et al., 2003; Davidovich-Pinhas e Bianco-Peled, 2010).

CONCLUSÃO

A superfície úmida e aderente da camada mucosa contribui para a aplicação de sistemas mucoadesivos. Estas formulações apresentam-se como alternativas promissoras para o transporte de fármacos para epitélios cobertos por muco, já que podem ser delineadas para promoverem proteção da mucosa, liberação controlada e direcionamento de agentes ativos a sítio-alvos específicos. Deve-se ter em mente, durante o desenvolvimento de formulações mucoadesivas, quais são as características particulares da mucosa alvo na qual a formulação será administrada, e como adaptar a formulação para seu alvo. Diversos métodos para avaliar o desempenho mucoadesivo de formulações são descritos na literatura. Sua padronização e validação, a fim de se obter resultados mais confiáveis e intercambiáveis entre diferentes estudos e centros de pesquisa são fundamentais, e devem acompanhar a evolução da pesquisa na área.

REFERÊNCIAS BIBLIOGRÁFICAS

AHUJA, A.; ALI, J.; RAHMAN, S. Biodegradable periodontal intrapocket device containing metronidazole and amoxycillin: formulation and characterisation. **Die Pharmazie-An International Journal of Pharmaceutical Sciences,** v. 61, n. 1, p. 25-29, 2006. ISSN 0031-7144.

AHUJA, A.; KHAR, R. K.; ALI, J. Mucoadhesive drug delivery systems. **Drug Development and industrial pharmacy,** v. 23, n. 5, p. 489-515, 1997. ISSN 0363-9045.

ALAM, M. A.; AHMAD, F. J.; KHAN, Z. I.; KHAR, R. K.; ALI, M. Development and evaluation of acid-buffering bioadhesive vaginal tablet for mixed vaginal infections. **AAPS PharmSciTech,** v. 8, n. 4, p. 229-236, 2007.

ALBIETZ, D. J.; DOUGLAS, I. Ocular therapeutics. **Clinical and Experimental Optometry,** v. 86, n. 2, p. 131-132, 2003. ISSN 1444-0938.

BALOĞLU, E.; ÖZYAZıCı, M.; HıZARCıOĞLU, S.; KARAVANA, H. An in vitro investigation for vaginal bioadhesive formulations: bioadhesive properties and swelling states of polymer mixtures. **Il Farmaco,** v. 58, n. 5, p. 391-396, 2003. ISSN 0014-827X.

BASSI DA SILVA, J.; FERREIRA, S. B. D. S.; DE FREITAS, O.; BRUSCHI, M. L. A critical review about methodologies for the analysis of mucoadhesive properties of drug delivery systems. **Drug Development and Industrial Pharmacy**, n. just-accepted, p. 1-67, 2017. ISSN 0363-9045.

BATCHELOR, H. The Drug Delivery Companies Report. **Autumn/Winter, Pharma Ventures Ltd,** v. 16, 2004a.

BATCHELOR, H. Novel bioadhesive formulations in drug delivery. **The Drug Delivery Companies Report Autumn/Winter, Pharma Ventures Ltd**, p. 17-21, 2004b.

BATCHELOR, H. Bioadhesive dosage forms for esophageal drug delivery. **Pharmaceutical research,** v. 22, n. 2, p. 175-181, 2005. ISSN 0724-8741.

BELGAMWAR, V.; SHAH, V.; SURANA, S. Formulation and evaluation of oral mucoadhesive multiparticulate system containing metoprolol tartarate: an in vitro-ex vivo characterization. **Current drug delivery,** v. 6, n. 1, p. 113-121, 2009. ISSN 1567-2018.

BERNKOP-SCHNÜRCH, A.; STEININGER, S. Synthesis and characterisation of mucoadhesive thiolated polymers. **International journal of pharmaceutics,** v. 194, n. 2, p. 239-247, 2000. ISSN 0378-5173.

BIRUDARAJ, R.; MAHALINGAM, R.; LI, X.; JASTI, B. R. Advances in buccal drug delivery. **Critical Reviews™ in Therapeutic Drug Carrier Systems,** v. 22, n. 3, 2005. ISSN 0743-4863.

CAMBLIN, M.; BERGER, B.; HASCHKE, M.; KRÄHENBÜHL, S.; HUWYLER, J.; PUCHKOV, M. CombiCap: A novel drug formulation for the basel phenotyping cocktail. **International Journal of Pharmaceutics,** v. 512, n. 1, p. 253-261, 2016. ISSN 0378-5173.

CHUN, M.-K.; KWAK, B.-T.; CHOI, H.-K. Preparation of buccal patch composed of carbopol, poloxamer and hydroxypropyl methylcellulose. **Archives of pharmacal research,** v. 26, n. 11, p. 973-978, 2003. ISSN 0253-6269.

CILURZO, F.; SELMIN, F.; MINGHETTI, P.; MONTANARI, L. The effects of bivalent inorganic salts on the mucoadhesive performance of a polymethylmethacrylate sodium salt. **International journal of pharmaceutics,** v. 301, n. 1, p. 62-70, 2005. ISSN 0378-5173.

CLEARY, J.; BROMBERG, L.; MAGNER, E. Adhesion of polyether-modified poly (acrylic acid) to mucin. **Langmuir,** v. 20, n. 22, p. 9755-9762, 2004. ISSN 0743-7463.

COSTANTINO, H. R.; ILLUM, L.; BRANDT, G.; JOHNSON, P. H.; QUAY, S. C. Intranasal delivery: physicochemical and therapeutic aspects. **International journal of pharmaceutics,** v. 337, n. 1, p. 1-24, 2007. ISSN 0378-5173.

DAVIDOVICH-PINHAS, M.; BIANCO-PELED, H. Mucoadhesion: a review of characterization techniques. **Expert opinion on drug delivery,** v. 7, n. 2, p. 259-271, 2010. ISSN 1742-5247.

FRANSÉN, N.; BJÖRK, E.; EDSMAN, K. Changes in the mucoadhesion of powder formulations after drug application investigated with a simplified method. **Journal of pharmaceutical sciences,** v. 97, n. 9, p. 3855-3864, 2008. ISSN 1520-6017.

GARTI, N. **Delivery and controlled release of bioactives in foods and nutraceuticals**. Elsevier, 2008.

GÉRAUD, B.; JØRGENSEN, L.; YBERT, C.; DELANOË-AYARI, H.; BARENTIN, C. Structural and cooperative length scales in polymer gels. **The European Physical Journal E,** v. 40, n. 1, p. 5, 2017. ISSN 1292-8941.

GRABOVAC, V.; GUGGI, D.; BERNKOP-SCHNÜRCH, A. Comparison of the mucoadhesive properties of various polymers. **Advanced drug delivery reviews,** v. 57, n. 11, p. 1713-1723, 2005. ISSN 0169-409X.

HAY, W. T.; BYARS, J. A.; FANTA, G. F.; SELLING, G. W. Rheological characterization of solutions and thin films made from amylose-hexadecylammonium chloride inclusion complexes and polyvinyl alcohol. **Carbohydrate Polymers**, 2017. ISSN 0144-8617.

KHARENKO, E.; LARIONOVA, N.; DEMINA, N. Mucoadhesive drug delivery systems (Review). **Pharmaceutical chemistry journal,** v. 43, n. 4, p. 200-208, 2009. ISSN 0091-150X.

KHUTORYANSKIY, V. V. Advances in mucoadhesion and mucoadhesive polymers. **Macromolecular bioscience,** v. 11, n. 6, p. 748-764, 2011. ISSN 1616-5195.

LAFFLEUR, F. Mucoadhesive therapeutic compositions: a patent review (2011-2014). **Expert opinion on therapeutic patents,** v. 26, n. 3, p. 377-388, 2016. ISSN 1354-3776.

LATHEESHJAL, L.; MURALA, S.; VAIDYA, M.; SWETHA, G. Mucoadhesive Drug Delivery System: An Overview. **International Journal of PharmTech Research,** v. 3, n. 1, p. 42-49, 2011.

LEE, J. W.; PARK, J. H.; ROBINSON, J. R. Bioadhesive- based dosage forms: The next generation. **Journal of Pharmaceutical Sciences,** v. 89, n. 7, p. 850-866, 2000. ISSN 1520-6017.

LOHANI, A.; CHAUDHARY, G. P. Mucoadhesive microspheres: A novel approach to increase gastroretention. **Chronicles of Young Scientists,** v. 3, n. 2, p. 121, 2012. ISSN 2229-5186.

LONGER, M.; ROBINSON, J. Fundamental-aspects of bioadhesion. **Pharmacy International,** v. 7, n. 5, p. 114-117, 1986. ISSN 0167-3157.

LUDWIG, A. The use of mucoadhesive polymers in ocular drug delivery. **Advanced drug delivery reviews,** v. 57, n. 11, p. 1595-1639, 2005. ISSN 0169-409X.

MUNASUR, A. P.; GOVENDER, T.; MACKRAJ, I. Using an experimental design to identify and quantify the effects of environment related test parameters on the in vitro mucoadhesivity testing of

a propanolol buccal tablet. **Drug development and industrial pharmacy,** v. 33, n. 7, p. 709-716, 2007. ISSN 0363-9045.

NAPPINNAI, M.; SIVANESWARI, S. Formulation optimization and characterization of gastroretentive cefpodoxime proxetil mucoadhesive microspheres using 3 2 factorial design. **Journal of Pharmacy Research,** v. 7, n. 4, p. 304-309, 2013. ISSN 0974-6943.

OKAMOTO, H.; TAGUCHI, H.; IIDA, K.; DANJO, K. Development of polymer film dosage forms of lidocaine for buccal administration: I. Penetration rate and release rate. **Journal of controlled release,** v. 77, n. 3, p. 253-260, 2001. ISSN 0168-3659.

PATIL, H.; TIWARI, R. V.; REPKA, M. A. Recent advancements in mucoadhesive floating drug delivery systems: A mini-review. **Journal of Drug Delivery Science and Technology,** v. 31, p. 65-71, 2// 2016. ISSN 1773-2247. Disponível em: < http://www.sciencedirect.com/science/article/pii/S1773224715300642 >.

PEPPAS, N. A.; SAHLIN, J. J. Hydrogels as mucoadhesive and bioadhesive materials: a review. **Biomaterials,** v. 17, n. 16, p. 1553-1561, 1996. ISSN 0142-9612.

PREETHA, A.; BANERJEE, R. Comparison of artificial saliva substitutes. **Trends Biomater Artif Organs,** v. 18, n. 2, p. 178-186, 2005.

RAJARAM, D. M.; LAXMAN, S. D. Buccal Mucoadhesive Films: A Review. **Systematic Reviews in Pharmacy,** v. 8, n. 1, 2017.

REINEKE, J.; CHO, D.; DINGLE, Y.; CHEIFETZ, P.; LAULICHT, B.; LAVIN, D.; FURTADO, S.; MATHIOWITZ, E. Can bioadhesive nanoparticles allow for more effective particle uptake from the small intestine? **Journal of Controlled Release,** v. 170, n. 3, p. 477-484, 2013. ISSN 0168-3659.

SALAMAT-MILLER, N.; CHITTCHANG, M.; JOHNSTON, T. P. The use of mucoadhesive polymers in buccal drug delivery. **Advanced drug delivery reviews,** v. 57, n. 11, p. 1666-1691, 2005. ISSN 0169-409X.

SANTOS, C.; FREEDMAN, B.; GHOSN, S.; JACOB, J.; SCARPULLA, M.; MATHIOWITZ, E. Evaluation of anhydride oligomers within polymer microsphere blends and their impact on bioadhesion and drug delivery in vitro. **Biomaterials,** v. 24, n. 20, p. 3571-3583, 2003. ISSN 0142-9612.

SHANKAR, N. B.; KUMAR, R. P.; KUMAR, N. U.; BRATA, B. B. Development and characterization of bioadhesive gel of microencapsulated metronidazole for vaginal use. **Iranian journal of pharmaceutical research: IJPR,** v. 9, n. 3, p. 209, 2010.

SMART, J. D. The basics and underlying mechanisms of mucoadhesion. **Advanced drug delivery reviews,** v. 57, n. 11, p. 1556-1568, 2005. ISSN 0169-409X.

SOUSA, J.; ALVES, G.; OLIVEIRA, P.; FORTUNA, A.; FALCÃO, A. Intranasal delivery of ciprofloxacin to rats: A topical approach using a thermoreversible in situ gel. **European Journal of Pharmaceutical Sciences,** v. 97, p. 30-37, 2017. ISSN 0928-0987.

SRIAMORNSAK, P.; WATTANAKORN, N.; NUNTHANID, J.; PUTTIPIPATKHACHORN, S. Mucoadhesion of pectin as evidence by wettability and chain interpenetration. **Carbohydrate polymers,** v. 74, n. 3, p. 458-467, 2008. ISSN 0144-8617.

UGWOKE, M. I.; AGU, R. U.; VERBEKE, N.; KINGET, R. Nasal mucoadhesive drug delivery: background, applications, trends and future perspectives. **Advanced drug delivery reviews,** v. 57, n. 11, p. 1640-1665, 2005. ISSN 0169-409X.

VALENTA, C. The use of mucoadhesive polymers in vaginal delivery. **Advanced drug delivery reviews,** v. 57, n. 11, p. 1692-1712, 2005. ISSN 0169-409X.

VAN ROEY, J.; HAXAIRE, M.; KAMYA, M.; LWANGA, I.; KATABIRA, E. Comparative efficacy of topical therapy with a slow-release mucoadhesive buccal tablet containing miconazole nitrate versus systemic therapy with ketoconazole in HIV-positive patients with oropharyngeal candidiasis. **JAIDS Journal of Acquired Immune Deficiency Syndromes,** v. 35, n. 2, p. 144-150, 2004. ISSN 1525-4135.

VASIR, J. K.; TAMBWEKAR, K.; GARG, S. Bioadhesive microspheres as a controlled drug delivery system. **International Journal of Pharmaceutics,** v. 255, n. 1, p. 13-32, 2003. ISSN 0378-5173.

VENTER, J.; KOTZE, A.; AUZELY-VELTY, R.; RINAUDO, M. Synthesis and evaluation of the mucoadhesivity of a CD-chitosan derivative. **International journal of pharmaceutics,** v. 313, n. 1, p. 36-42, 2006. ISSN 0378-5173.

WILLATS, W. G.; KNOX, J. P.; MIKKELSEN, J. D. Pectin: new insights into an old polymer are starting to gel. **Trends in Food Science & Technology,** v. 17, n. 3, p. 97-104, 2006. ISSN 0924-2244.

YADAV, A. J.; DESHMUKH, G. A Comprehensive Review on Gastro-retentive Drug Delivery System. 2016. ISSN 7: 001-028.

YANG, X.; ROBINSON, J. Bioadhesion in mucosal drug delivery. **Biorelated Polymers and Gels, Academic Press, San Diego, CA**, p. 135-192, 1998.

ZHANG, L.; RUSSELL, D.; CONWAY, B. R.; BATCHELOR, H. Strategies and therapeutic opportunities for the delivery of drugs to the esophagus. **Critical Reviews™ in Therapeutic Drug Carrier Systems,** v. 25, n. 3, 2008. ISSN 0743-4863.

CAPÍTULO 02

THERMOREVERSIBLE MUCOADHESIVE POLYMER-DRUG DISPERSION FOR SUSTAINED LOCAL DELIVERY OF BUDESONIDE TO TREAT INFLAMMATORY DISORDERS OF THE GI TRACT

Capítulo publicado como artigo original na revista Journal of Controlled Release, 2019, doi.org/10.1016/j.jconrel.2019.04.011.

Autores: Rayane S. C. M. Q. Antonino[1], Thais L. Nascimento[1], Edilson R. de Oliveira Júnior[1], Leonardo G. Souza[1], Aline C. Batista[2], Eliana M. Lima[1*]

[1]Laboratório de Nanotecnologia Farmacêutica e Sistemas de Liberação de Fármacos, FarmaTec, Faculdade de Farmácia, Universidade Federal de Goiás – UFG, Goiânia, Goiás, Brasil;
[2]Laboratório de Patologia Bucal, Faculdade de Odontologia, Universidade Federal de Goiás – UFG, Goiânia, Goiás, Brasil.

RESUMO

As formulações mucoadesivas com fármacos foram estudadas e utilizadas como alternativas às formulações convencionais, de modo a obter uma retenção prolongada no local pretendido. Além de fornecer liberação controlada do medicamento, vários medicamentos e doenças podem se beneficiar de formulações mucoadesivas, contribuindo para melhores resultados terapêuticos. Aqui, nós descrevemos o desenvolvimento e a caracterização *in vitro* / *in vivo* de uma formulação gelificante *in situ* mucoadesiva usando PF127, um polímero termorreversível, capturando budesonida (BUD), potente corticosteróide usado para o tratamento de uma ampla gama de doenças inflamatórias, incluindo aqueles que afetam mucosas, como no trato gastrointestinal. As formulações de PF127 (15-17%) foram preparadas com sucesso por um método a frio como uma dispersão gelificante *in situ* reversível para administração de fármaco na mucosa, como confirmado por DSC. As temperaturas de sol-gel das formulações de PF127 (25-39 °C) foram observadas por gelificação dinâmica e determinadas por microrreologia e reometria oscilatória. Difratogramas de raios X e imagens de TEM mostraram que a BUD foi completamente solubilizada dentro das micelas poliméricas. *In vitro*, os géis mostraram 5-14 g de força de mucoadesão, e os estudos *ex vivo* confirmaram que a formulação aderiu eficientemente à mucosa. A análise histopatológica combinada com imagens de fluorescência e permeação intestinal *ex vivo* confirmaram que a formulação permaneceu na mucosa TGI por pelo menos 4 h após a administração. Estudos *in vivo* conduzidos em modelo murino de mucosite intestinal demonstraram que a formulação de 16% PF127BUD foi capaz de resolver a lesão inflamatória na mucosa intestinal. Os resultados demonstraram que o ajuste fino das formulações de PF127 juntamente com a seleção adequada do agente farmacológico, caracterização completa das dispersões e suas interações com interfaces biológicas conduzem ao desenvolvimento de sistemas eficazes de administração controlada de fámacos direcionados para doenças inflamatórias do GI.

Palavras-Chave: TGI; doenças inflamatórias; mucoadesão; microrreologia; reometria oscilatória; micelas.

ABSTRACT

Mucoadhesive drug formulations have been studied and used as alternatives to conventional formulations in order to achieve prolonged retention at the intended site. In addition to providing a controlled drug release, several drugs and disease conditions might benefit from mucoadhesive formulations, contributing to better therapeutic outcomes. Here, we describe the development and the *in vitro/in vivo* characterization of a mucoadhesive *in situ* gellifying formulation using PF127, a thermo reversible polymer, entrapping budesonide (BUD), a potent corticosteroid used for the treatment of a wide range of inflammatory diseases, including those affecting mucosas, such as in the GI tract. PF127 formulations (15-17%) were successfully prepared by a cold method as a thermo reversible *in situ* gelling dispersion for mucosal drug delivery, as confirmed by DSC. Sol-gel temperatures of PF127 formulations (25-39°C) were observed by dynamic gelation and determined by microrheology and oscillatory rheometry. X-ray diffractograms and TEM images showed that BUD was completely solubilized within the polymeric micelles. *In vitro*, the gels showed 5-14 g force of mucoadhesion, and the *ex vivo* studies confirmed that the formulation efficiently adhered to the mucosa. Histopathological analysis combined with fluorescence images and *ex vivo* intestinal permeation confirmed that the formulation remained on the TGI mucosa for at least 4 h after administration. *In vivo* studies conducted in a murine model of intestinal mucositis demonstrated that the 16% PF127 BUD formulation was able to resolve the inflammatory injury in the intestinal mucosa. Results demonstrate that fine-tuning of PF127 formulations along with adequate selection of the drug agent, thorough characterization of the dispersions and their interactions with biological interfaces leads to the development of effective controlled drug delivery systems targeted to GI inflammatory diseases.

Keywords: TGI; inflammatory diseases; mucoadhesion; microrheology; oscillatory rheometry; micelles

GRAPHICAL ABSTRACT

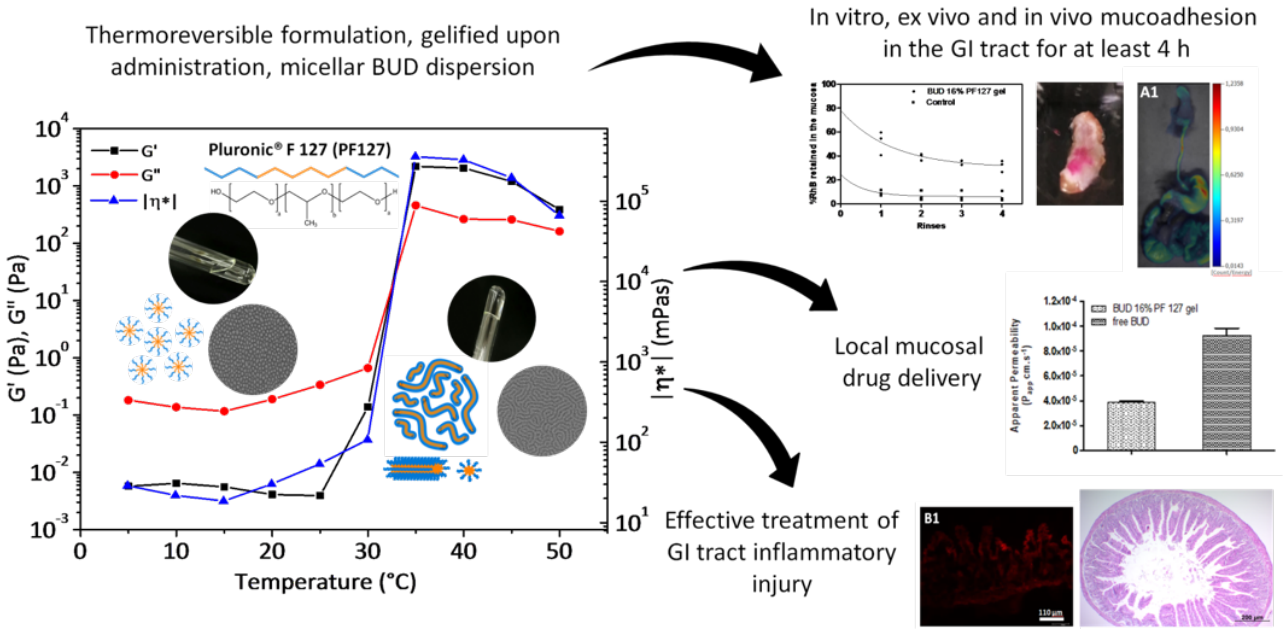

INTRODUCTION

Budesonide (BUD) is a glucocorticoid with high local anti-inflammatory activity and low systemic absorption (Popov *et al.*, 2016). Its limited bioavailability is also due to the rapid conversion of the molecule in the liver into metabolites with little or no steroid activity (Edsbäcker and Andersson, 2004). This reduces the adverse effects inherent to systemic corticosteroids, such as suppression of the hypothalamic-pituitary adrenal axis, making BUD a favorable therapeutic option for the treatment of inflammatory diseases of the gastrointestinal tract (GI) such as Crohn's disease, ulcerative colitis, mucositis of the upper and lower intestinal tract and esophageal eosinophilia (Varshosaz *et al.*, 2010; Akkari, A. C. S. *et al.*, 2016; Laubitz *et al.*, 2017). Despite widespread clinical use, BUD has low aqueous solubility (Zhang *et al.*, 2011) and extensive first pass biotransformation (Zhang and Zhang, 2015). It exhibits a high ratio of topical-to-systemic activity, which is attributed to its strong local anti-inflammatory effect and extensive first-pass elimination (up to 90%), which considerably limits its systemic bioavailability and effects (Sharma *et al.*, 2005). Inflammatory disorders of the TGI mucosa affect an increasingly large number of patients (Prasad *et al.*, 2007; González-Cervera *et al.*, 2017). The treatment of these conditions still lack therapeutic efficacy, and is limited to the administration of oral medications in the form of anti-inflammatory solutions and/or suspensions (Furuta *et al.*, 2007; Laubitz *et al.*, 2017). The possibility of enabling mucus retention and site-specific drug release, achieved by formulations with distinctive physical and chemical properties (Wang *et al.*, 2018), has directed the use of mucoadhesive formulations to achieving therapeutic effect directly on the affected mucosa (Laffleur and Bernkop-Schnürch, 2013). We explored this approach, focusing on providing local and controlled drug release (Boateng *et al.*, 2015), therefore limiting systemic absorption and reducing side effects associated with the conventional oral administration of drugs.

Pluronic® F127 (PF127; Poloxamer 407) is a mucoadhesive synthetic copolymer composed of bound triblock (ABA) polyoxyethylene (PEO) and polyoxypropylene (PPO) chains (PEO100-PPO70-PEO100) (Akkari, A. C. *et al.*, 2016; Ban *et al.*, 2017). One of the main advantages of this triblock polymer is its thermo reversible behavior in aqueous solutions (Akash and Rehman, 2015). At low temperatures, PF127 is in a liquid state, and as temperature increases, the phase transition occurs and the polymer dispersion becomes a gel (Bruschi *et al.*, 2007; Bhowmik *et al.*, 2013). Liquids with *in situ* gelification have been proved to be more convenient forms of drug delivery for local application, since they are

easy to administer in the body cavities (Masteikova *et al.*, 2003; Karavana, 2012). The aim of this study was to develop a suitable mucoadhesive *in situ* gelifying formulation of BUD using Pluronic® F127, with adequate mechanical and rheological properties that will result in a prolonged retention of the formulation on the TGI mucosa for local treatment of inflammatory conditions.

MATERIALS AND METHODS

Materials

Pluronic® F-127 Bioreagent (PF127, Mw 12,800 Da) was purchased from Sigma Aldrich (St Louis, MO, USA, batch nr. BCBC6633V). BUD was donated by Eurofarma (São Paulo, BR, batch nr. 401576). Propylene glycol 99.8% purity was purchased from Qhemis (Indaiatuba, São Paulo, BR, batch nr. 13087865). Rhodamine B and mucin from porcine stomach (Type II) were purchased from Sigma Aldrich (St Louis, MO, USA, batch nrs. SLBN9463V and SLBL3184V, respectively). Other reagents and solutions used were of analytical grade or superior.

Preparation of the polymer-drug dispersion

Different concentrations of PF127 (15, 16 and 17% w/w) were dissolved in ultrapurified water previously equilibrated at 4-8 °C. The solutions were kept under magnetic stirring at 700 rpm for 2 h at 4 °C. For the preparation of BUD gels, the drug was first dissolved in propylene glycol then added to the PF127 solution for the final concentrations of 0.5 mg/mL BUD and 5% w/w propylene glycol. Formulations were then stirred at 700 rpm at approximately 30 °C until complete micellar solubilization of BUD.

Quantitative determination of BUD in formulations

To analyze the amount of BUD present in the formulations, 200 mg of each gel were dissolved in 1.8 mL methanol:Hepes buffer 5 mM (70:30 v/v). Samples (n=3) were vortex mixed for 1 minute, and aliquots were filtered using 0.45 µm PVDF filters prior to quantification.

The concentration of BUD was determined using a reversed-phase high-performance liquid chromatography (HPLC) system (1260 Infinity, Agilent Technologies, Santa Clara, California, USA) equipped with a 1260 quaternary pump, 1260 DAD detector and 1260 ALS flow cell, following the method previously described by Naikwade e Bajaj, 2009 (Naikwade

and Bajaj, 2009). Chromatographic separation was achieved using a Zorbax Extend C18 analytical column (150 mm x 4.6 mm, 5 µm) (Agilent Technologies, Santa Clara, California, USA). The mobile-phase consisted of a mixture of methanol:water (80:20 v/v) with flow rate of 1.0 mL/min. The detection wavelength was 244 nm (λ_{max} for BUD) and the injection volume was 10 µL. A calibration curve was obtained from 40-60 µg/mL with r>0.99. Run time was 5 min, and BUD elution was observed at 3 min. The method was validated according to ICH recommendations (Guideline, 2005). Total amount of the drug in each formulation was determined as the experimental concentration of BUD obtained by HPLC.

Differential Scanning Calorimetry (DSC)

DSC was used to study the critical micellization temperature (CMT) or micellization temperature (Tm) of the polymer-drug dispersions. 10 mg of each sample were placed in sealed aluminum pans and submitted to heating from 0-50 °C at a rate of 10 °C/min under N_2 atmosphere (20 mL/min), using a DSC 8500 with HyperDSC™/Intracooler 3 (Perkin Elmer, Norwalk, USA). An empty pan was used as reference. Analysis were performed in triplicate and DSC curves were represented by heat flow (mW) *versus* temperature (°C).

X-ray powder diffraction (XRPD)

XRPD was performed using an XRD7000 X-ray diffractometer (Shimadzu, Japan) using Cu Kα radiation (λ = 1.54 Å), and acceleration voltage and current of 40 kV and 30 mA, respectively. The powder sample and the gels samples were scanned in reflectance mode from 2 to 60° 2θ with a scan speed of 1° 2θ/min and a step size of 0.02° 2θ.

Microrheology

A microrheometer based on diffusing wave spectroscopy (DWS) was used for the measurements of PF127 dispersions. This technique corresponds to photon correlation spectroscopy in concentrated media and measures the Brownian motion of particles, which depends on the viscoelastic structure of the sample. The determination of Sol-gel transition (Tsol-gel) temperature was obtained using a Rheolaser LAB™ (Formulaction, Toulouse, France). 20 mL of the samples were subjected to heating for evaluation of the viscoelastic parameters G' (elastic modulus) and G" (viscous modulus). Tsol-gel was determined as the temperature at which the values of the viscoelastic modules were between the solid-like and

the liquid-like behavior (Pasqua *et al.*, 2014). Measurements were performed in triplicates for each formulation (n=3).

Oscillatory rheometry

Tsol-gel temperatures of the polymer-drug dispersions were also measured using an oscillatory rheometer with plate-plate geometry (Haake Mars III, Thermo Fisher Scientific Inc, Karlsruhe, Germany). Aliquots of each formulation (n=3) were carefully applied to the lower plate and the temperature sweep analysis was performed over the range of 5-50 °C with heating rate of 2 °C/min and frequency of 1 Hz. G', G" and η* were calculated using the Rheowin MARS III (Haake, Karlsruhe, Germany) software. The Tsol-gel was defined as the point at which G' was halfway between the values for the solution and the gel, and was calculated for the systems that had significantly increased η* with increasing temperature (Jones *et al.*, 2009).

***In vitro* dynamic gelation**

In vitro dynamic gelation time was measured at 37 °C, after application of the 15, 16 and 17% (w/w) PF127 formulations in vertically positioned glass pipettes. Distance run and time were recorded for a comparison between formulations.

***In vitro* mucoadhesion**

Mucoadhesion of 16% PF127 BUD gel formulations was measured using a TA-XT plus texturometer (Stable Micro Systems, Surrey, UK). Mucin discs were prepared by compressing 250 mg of mucin with 140-150 kg force. The discs were then fixed on the 0.5 R cylindrical probe and hydrated with 5% mucin solution for 2 minutes. After the excess solution was dried from the discs, the force needed to remove the formulations after contact with the artificial mucosa (disk) surface was recorded. 10 mL of each sample were placed in Petri dishes and equilibrated at 37 °C ± 0.5 for the test. The contact with the mucin probe was made at a constant speed of 0.1 mm/s and 5 g force, for 60 s, after which the probe dislocated 15 mm upwards. Measurements were performed in triplicates.

TEM

Transmission electron microscopy (TEM) imaging was conducted using a Tecnai F20 Electron Microscope (FEI Company, Hillsboro, Oregon), with an accelerating voltage of 120 kV, equipped with a 4k x 4k UltraScan CCD camera. Samples of 16% PF127 – BUD dispersions were negatively stained with 2% (w/v) uranyl acetate solution for observation. Samples were prepared at room temperature and at 37 °C for comparison.

Animals

Male Wistar rats (350-400 g) were used for the *ex vivo* mucoadhesion experiments and intestinal permeation assay, while male swiss mice (8-10 weeks old) were used for the *in vivo* GI mucosal inflammatory model. The oral cavity and esophagus of both mice and rats have a mucosa lined by a stratified squamous epithelium with a keratinized surface, exhibiting similar anatomical, histological, biochemical and physiological properties. The intestinal part of the GI tract in both rodents is also very similar, down to the histological morphology (Nolte *et al.*, 2016). Due to these similarities and to the easier handling of the rat duodenum, we chose this species to perform the *ex vivo* mucoadhesion and intestinal permeation studies.

All animals were obtained from the Central Animal Facility at Federal University of Goiás (UFG). Animals were acclimatized for a week prior to the beginning of experiments and kept under 12:12 h light-dark cycles and controlled temperature. Food and water were provided *ad libitum*. Experiments were conducted according to the UFG Animal Research Ethics Committee guidelines (approved protocol nr. 001/17) and the principles of laboratory animal care and legislation in Brazil (Law 11794, October 8, 2008).

E*x vivo* esophageal mucoadhesion

BUD 16% PF127 gels were fluorescently labeled with rhodamine B at 2 mg/mL for the *ex vivo* esophagus mucoadhesion study. Animals (n=3) were anesthetized by intraperitoneal injection of ketamine 50 mg/kg and xylazine 10 mg/kg and then euthanized before the removal of the tissues. Esophageal tissue segments were cut longitudinally and kept at 37 °C in Hartmann solution before use. Formulation aliquots of 10 µL were deposited on top of the esophageal mucosal surface, which was positioned at a 45 degree angle and maintained at 37 °C in a temperature controlled chamber. A solution of rhodamine B 2 mg/mL in Hartmann was used as the non-mucoadhesive control for comparison. One minute after

application of either formulation or rhodamine solution, the tissues were rinsed 4 times with 1 mL Hartmann's solution at 2 min intervals. The washing solutions were then analyzed using a fluorescence spectrophotometer (Cary Eclipse, Varian Inc., Palo Alto, CA, USA) with excitation at 540 nm and emission at 625 nm. The difference between the amount of rhodamine B applied to the esophageal tissue and the amount present in the washing solutions was considered as the fraction that adhered to the esophageal mucosa.

In vivo total GI mucoadhesion studies

In vivo mucoadhesion of BUD 16% PF127 polymer-drug dispersions was evaluated using fluorescence molecular tomography (FMT, Fluorescence Tomography *in vivo* Imaging Systems, Perkin Elmer, USA). The formulation was labeled with IR780 at 25 mg/ml. Animals received orally 20 µL of the formulation. Four hours after administration, animals were euthanized and the GI tract was imaged to visualize the formulation distribution.

Ex vivo intestinal permeation

The ex vivo intestinal permeation study was carried out to evaluate the retention of BUD inside the intestinal mucosa, since the decreased drug permeation would be desirable to favor the local inflammatory effect. Intestinal segments of 10 cm/each, representing the duodenum were removed from the animals (n=6) after euthanasia and kept in lactated Ringer’s solution before preparation. The interior of each intestinal segment was filled with 500 µL of either BUD 16% PF127 polymer-drug dispersion (Group A) BUD solution (0.5% BUD in 5% DMSO) (Group B). The segments were then submerged in 20 mL lactated Ringer's solution. Experiments were performed in triplicates. A segment of the medial jejunum immersed in lactated Ringer's solution was used as control. The experiment was carried under gentle magnetic stirring, at 37 ± 0.5 ° C for 2 h. The Ringer’s lactated solution was withdrawn, stored and replaced from each system at 15-minute intervals up to 2 h. BUD permeated through the intestine wall and present in the external medium was quantified by HPLC. For this experiment, a new calibration curve for BUD was obtained, with the range of 0.1 to 4 μg/mL and linearity of r=0.9954.

Experimental intestinal mucositis model and *in vivo* treatment

To evaluate the *in vivo* therapeutic effect of the BUD-gel formulation on a GI inflammatory disorder, an animal model for intestinal mucositis was used as previously described (Dos Santos Filho *et al.*, 2016; Santos Filho, Arantes*, et al.*, 2018; Santos Filho, Da Silva*, et al.*, 2018). 5-FU was diluted in sterile water and administered i.p. (300 µL, 200 mg/Kg), for 3 consecutive days for all groups except the negative control. Animals were divided into 4 groups (n=5) and were, during the same period, treated orally by gavage with: water (negative and positive controls); blank formulation (placebo) and BUD-gel formulation (treated group). On day 4 animals were anesthetized i.p. with 10 mg/Kg xylazine and 100 mg/Kg of ketamine hydrochloride and euthanized by cervical dislocation. 10 cm of the duodenum proximal portions were immediately immersed in 10% phosphate buffered formalin pH 7.4 and kept at room temperature for 48 h before histophatological analysis.
For imaging the mucosal adherence of the formulation, rhodamine B was used as fluorescent label to visualize the formulation distribution in the duodenum epithelial mucosa. Animals were treated as described above with the fluorescent formulation. 10 cm portions of the duodenum were removed 1 h after treatment, immediately embedded in OCT media (Sakura, Torrance, CA, USA) and frozen at −80 °C. Sections of 5 µm were then obtained using a cryostat microtome (Leica Microsystems, Bannockburn, IL, USA), transferred to microscopy slides, covered with coverslips and analyzed using the N21 filter for rhodamine detection in a fluorescence microscope (DMI 4000B Leica Microsystems, Bannockburn, IL, USA).

Histopathological evaluation

Two mid-sagittal macroscopic cross sections from each animal were dehydrated in graded ethanol (70-100%), cleared in xylene and paraffin-embedded using an automatic tissue processor (OMA DM40, São Paulo, SP, Brazil). Paraffin-embedded duodenum samples (5 µm thickness) were obtained using a microtome (Leica RM 2155, Heidelberg, BW, Germany). After mounting, slides were dewaxed in xylene, hydrated using graded ethanol and stained with haematoxylin and eosin (H&E). The slides were observed using a light microscope (Axio Scope A1 Carl Zeiss, Jena, TH, Germany) and 5x and 10x objectives. The following microscopic characteristics were evaluated: integrity of the epithelial lining, duodenum crypts atrophy, inflammatory infiltrate and necrotic tissue damage.

Statistical analysis

Statistical analysis was performed using GraphPad Prism 5.03 (San Diego, CA, USA). Variation between groups was measured by two-way Analysis of Variance (ANOVA) followed by Bonferroni's test. Statistical significance was established as $p<0.05$.

RESULTS AND DISCUSSION

Polymer-drug dispersion preparation and BUD content

The method to prepare the polymer-drug dispersion used in this work is simple, quick and does not require the use of specific equipment or specialized techniques, making it ideal for production scale-up. The cold method is widely cited in the literature for obtaining PF127 gels (Altuntaş and Yener, 2017; Ban *et al.*, 2017; Fathalla *et al.*, 2017; Pitorre *et al.*, 2017; Rao *et al.*, 2017). Here, we optimized this technique by increasing the system temperature after BUD incorporation to induce the micellization. As a result, the transparent aspect of the final dispersions confirmed the absence of BUD crystals and therefore the complete solubilization of the drug inside PF127 micelles. All of the formulations, 15, 16 and 17% (w/w) PF127, showed pHs around 7.4-7.6.

HPLC calibration curve, BUD chromatogram and BUD content of PF127 gels are shown in Figure S1. BUD contents of 0.49-0.5 mg/mL were obtained for all three formulations proposed. The one-pot formulation preparation method was decisive for a nearly 100% actual yield of the drug initially added to the mixture. This highlights another advantage of promoting the micellization and solubilization of BUD only by adjusting polymer concentration and temperature, without additional components, such as cyclodextrins, commonly used to improve the incorporation and solubilization of hydrophobic drugs in PF127 (Akkari, A. C. S. *et al.*, 2016). In addition, a one-pot procedure enables for easier scaling-up processes and ensures total yield of the drug amount.

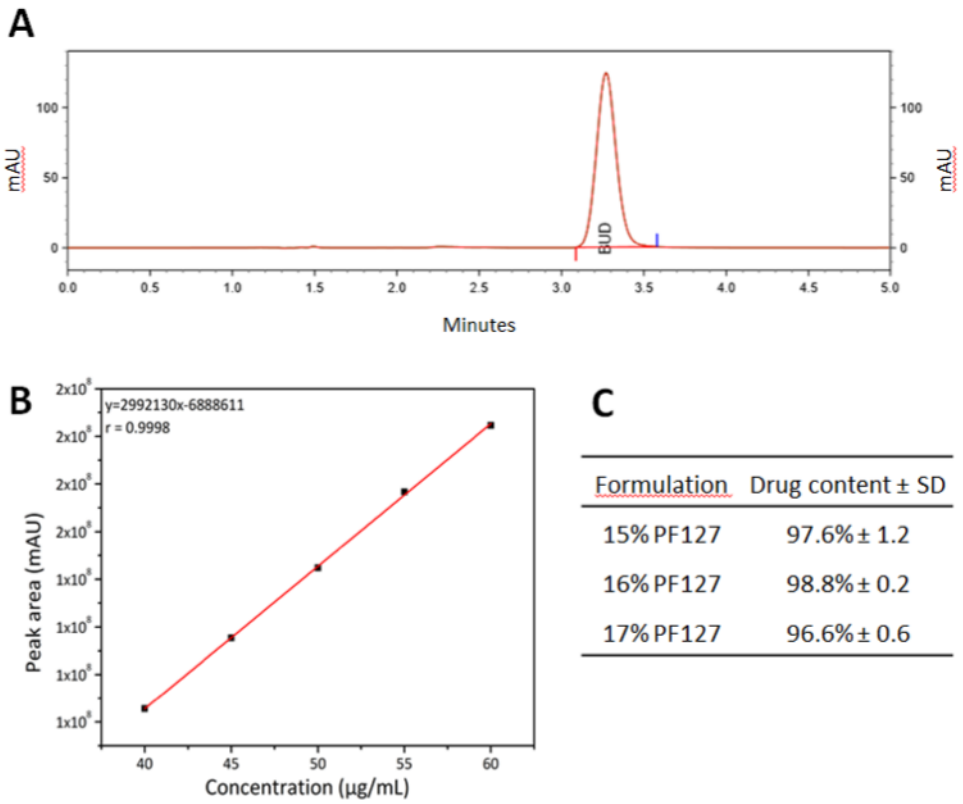

Formulation	Drug content ± SD
15% PF127	97.6% ± 1.2
16% PF127	98.8% ± 0.2
17% PF127	96.6% ± 0.6

Figure S1. HPLC calibration curve, chromatogram and BUD content of PF127 gels. A. BUD calibration curve (40-60 µg/mL). B. Representative BUD chromatogram. Chromatographic separation was achieved using C18 150 x 4.6 mm, 5 µm column. Mobile phase was methanol:water (80:20 v/v) with 1.0 mL/min flow. The wavelength of 244 nm was used for detection, and injection volume was 10 µL. C. Budesonide content of the gel formulations prepared with 15%, 16% and 17% PF127, presented as percentage of the theoretical yield of the 0.5mg/mL drug concentration in the formulations.

The hydrophobic nature of BUD favored its partition into the hydrophobic portion of the PF127 chain (PPO). With the increase in temperature, the polymer structure organization rearranged to a micellar assembly, with the drug being solubilized within the micelles (Figure 1).

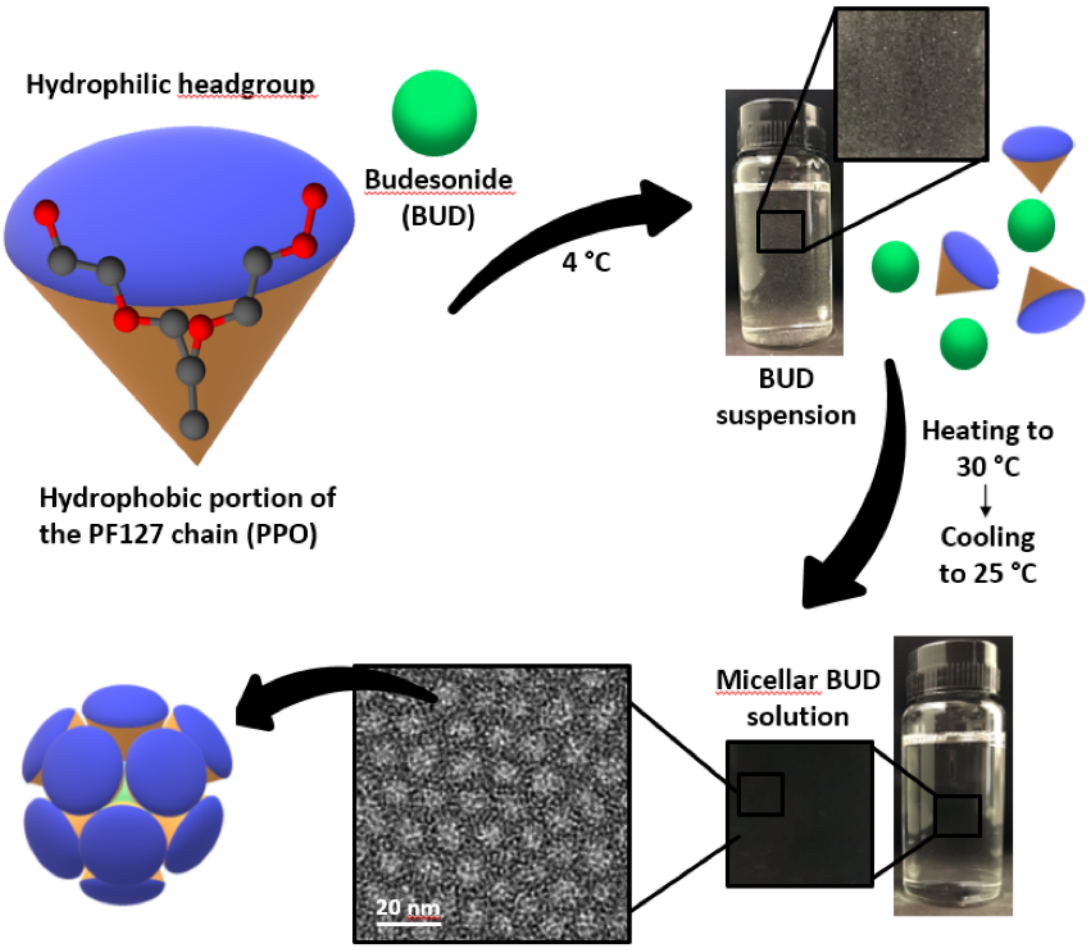

Figure 1. BUD solubilization inside PF127 micelles. Schematic illustration of the PF127 structure and its conical shape, where brown and blue parts represent hydrophobic and hydrophilic regions, respectively. Thermally induced micelle formation allows BUD, represented in green, to be solubilized within PF127 hydrophobic regions. BUD solubilization within PF127 micelles was visually observed, as depicted in the photo of the formulation, which turned from a translucid suspension to a completely transparent colloidal dispersion. BUD solubilization was corroborated by high-resolution TEM images evidencing the absence of BUD drug crystals in the formulation.

DSC and XRPD

The micellization or critical micellization temperature of the formulations was determined by DSC. Since the formation of micelles is the prerequisite for PF127 gelation, it was essential to study this process and characterize the formulations containing or not BUD. DSC curves for 15, 16 and 17% PF127 gels are shown in Figure 2A. Large endothermic peaks around 16-20 °C were observed for all formulations, with or without the drug, showing that BUD addition to the gel did not change the enthalpic behavior of the formulations. The presence of endothermic peaks is a result of the dewatering of PPO blocks with the increasing temperature (Jiang *et al.*, 2008). Since dewatering of PPO blocks leads to the formation of

micelles, the endothermic peak can be attributed to the Tm (Wanka *et al.*, 1994; Pragatheeswaran and Chen, 2013).

The Tm values found for the different formulations (Figure 2A) were inversely proportional to the polymer concentration (Trong *et al.*, 2008), with lower Tm values being observed for higher concentrations of PF127 (Akkari, A. C. *et al.*, 2016). As expected, upon addition of BUD, a decrease in Tm values was observed for all PF127 concentrations tested. This is related to the hydrophobic nature of BUD (logP 3.2) (Bandi *et al.*, 2004) and its low solubility in water at physiological pH (20 µg/ml) (Dudognon *et al.*, 2006), which probably helped strengthen the hydrophobic interactions of PPO chains, thereby decreasing the thermal energy required for micellization (Akkari, A. C. *et al.*, 2016).

XRPD diffractograms for powder budesonide and freshly prepared 15, 16 and 17% PF127 formulations are presented in Figure 2B. A diffraction pattern which corresponds to the crystalline state of budesonide is shown. In contrast, no Bragg reflections was observed for all PF127 formulations. This confirms our previous observations that evidence BUD solubilization by PF127 micelles upon preparation of the formulation (Ali *et al.*, 2016).

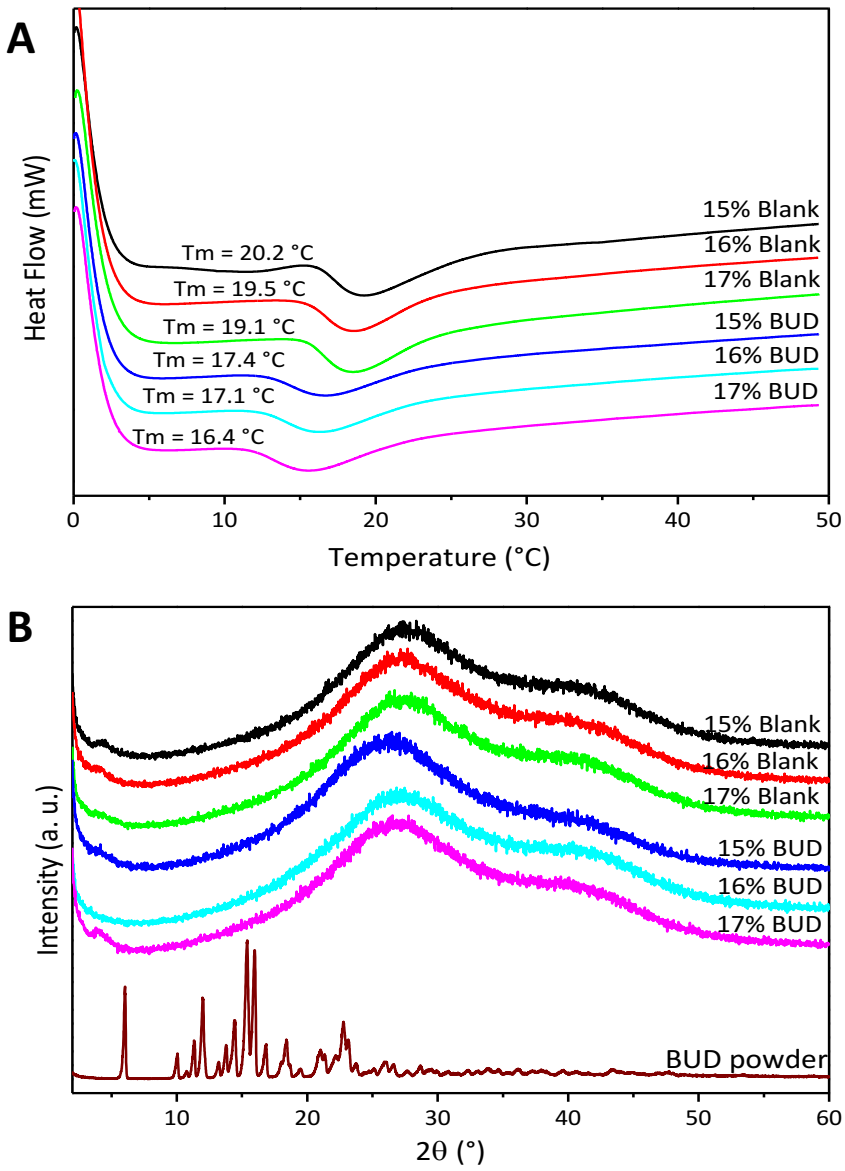

Figure 2. A. DSC curves obtained for 15%, 16% and 17% PF127 formulations in the absence (Blank) and presence (BUD) of budesonide, evidencing the different critical micellization temperatures (Tm). B. X-ray diffractograms of BUD and the PF127 formulations in the absence (Blank) and presence (BUD) of budesonide, indicating drug solubilization.

Microrheology, oscillatory rheometry and dynamic gelation

A non-destructive technique that determines rheological properties, such as microrheology, provides results by monitoring the Brownian motion of the sample droplets. Since this method does not promote any type of alteration in the sample structure (Corredig and Alexander, 2008; Tisserand *et al.*, 2012; Xu *et al.*, 2016) when compared to the classical rheology technique, which has been reported to induce structural shear degradation of the sample analyzed (Batista et al., 2006), we chose to analyze the PF127 gels formulations

using microrheology. Tsol-gel temperatures of the formulations with and without BUD are shown in Figure 3G. 15% PF127 formulation without BUD (15% Blank) did not show sol-gel transition until 40 °C. Since this concentration is at the critical gelling concentration (CGC) limit for PF127, and can be affected by the type of polymer and the size of the polymer chain (Attwood et al., 1985; Lenaerts et al., 1987), the transition may not happen. An exponential ratio between the viscosity of the polymer and the Tsol-gel temperature was observed for the other formulations, with the curve slope being dependent on the concentration of PF127 (Lenaerts et al., 1987). The higher the concentration of PF127, the lower was the measured Tsol-gel temperature. This phenomenon can be explained based on the previously reported observation that PF127 micelles in aqueous solution undergo thermally induced swelling and desolvation. This hypothesis, therefore, proposes the creation of an interconnected network (Escobar-Chávez et al., 2006), and was confirmed in this work through the DSC results and TEM micrographs, which will be discussed below. In addition, a slight decrease in the Tsol-gel temperature (~1 °C) was observed for all formulations when BUD was added. The alteration of Tsol-gel temperature by the addition of active substances of additives has been previously described in the literature (Mazia et al., 2016). As observed for Tm, where the hydrophobic nature of BUD lowered the micellization temperature, it also hastened the sol-gel transition.

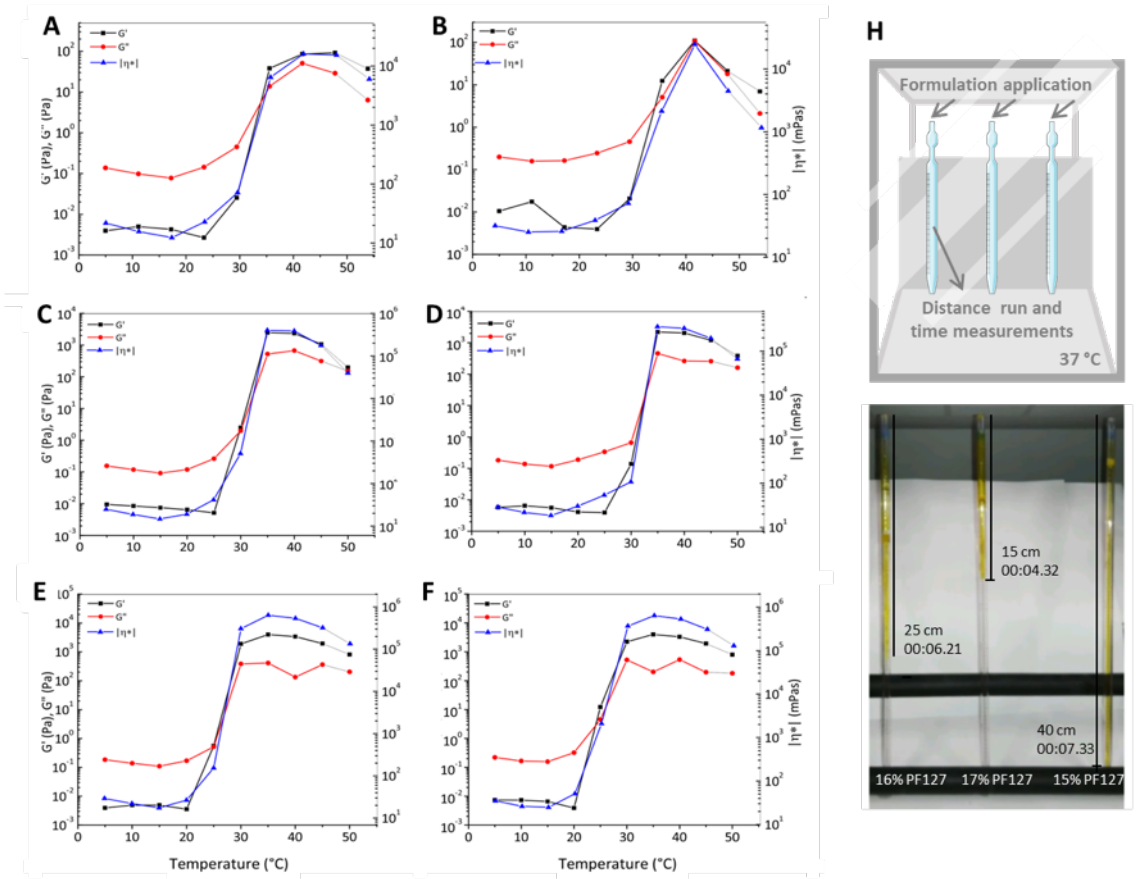

G

Formulation	G'max* (Pa)	G"max* (Pa)	|η|min* (mPas)	|η|max* (mPas)	$T_{sol-gel}$ (°C)	$T_{sol-gel}$ (°C)**
15%Blank	171	40	16.6	10,977	-	-
15%BUD	48	34	27.6	10,051	35.5	38.7
16%Blank	1,510	413	19.5	250,253	30.2	32.2
16%BUD	1,459	285	25.2	237,532	30.0	31.7
17%Blank	3,222	299	30.4	515,862	25.1	29.7
17%BUD	2,865	309	43.7	460,556	25.3	28.8

*Min = values before Tsol-gel /Max = values after of Tsol-gel
**Result obtained by microrheology

Figure 3. Rheograms with elastic (G') and viscous (G") modulus, viscosity |η*| vs. temperature (°C) obtained by oscillatory rheometry at 1Hz for the PF127 formulations containing budesonide (BUD) or not (Blank). Formulations were prepared with 15, 16 or 17% polymer. A = 15% Blank, B = 15% BUD, C = 16% Blank, D = 16% BUD, E= 17% Blank and F = 17% BUD. G" values before gelation were higher than G' at all measured temperatures. G = Elastic modulus (G'), viscous modulus (G"), viscosity |η| and Sol-gel transition temperatures for blank and BUD formulations. Rheological parameters were determined before and after Tsol-gel temperature. Tsol-gel measurements were made using microrheology. *Formulation did not show sol-gel transition until 40 °C, ** SD = Standard Deviation. H. Schematic representation and results obtained from the dynamic gelation study. Distance run and gelification time were measured for 15, 16 and 17% BUD formulations.

Rheological analysis was performed considering the different compositions and the presence or absence of BUD. The elastic (G') and viscous (G") modulus, viscosity (η*) and Tsol-gel temperature were determined for all formulations. Figure 3 (A, B, C, D, E, F) shows the rheograms with variations of G' and G" in relation to the temperature range (5-50 °C) as well as the variation in viscosity. All formulations exhibited a non-Newtonian behavior. The viscoelastic characteristic of the gels causes them to exhibit a liquid behavior at low temperatures and a gel behavior with the increase of the system temperature, in which the viscosity is considerably increased (Junqueira *et al.*, 2016). Before the sol-gel transition all formulations had greater G" values compared to G' (Figure 3G). The increased value of the viscous modulus before transition characterizes the liquid state of the formulations (Tisserand *et al.*, 2012). With the temperature increase, an inversion of G' and G" values was observed. After the sol-gel transition G' values were considerably elevated, as was the system viscosity, which characterizes the gel behavior of the formulations (Junqueira *et al.*, 2016).

In agreement with the microrheology results, the sol-gel transition was not observed for the 15% Blank formulation, as visualized through the dynamic gelation experiment (Figure 3H). Variations of 1-2 °C were observed between rheology and microrheology analysis regarding the Tsol-gel temperature. These variations do not indicate a disagreement between the results, but are rather a reflection of the different techniques used for the measurement of Tsol-gel temperature. As mentioned previously, classical rheology applies shear stress to measure rheological properties. In general, this stress causes a progressive degradation of the polymer molecular entanglement (Lee *et al.*, 2016). Thus, modifications in the formulation microstructure may promote changes in the rheological properties, one of them being the sol-gel transition (Çelebi *et al.*, 2015; Dewan *et al.*, 2015).

Microrheology is a passive technique, i.e., there is neither contact, forces or external stress being applied to the sample (Bellour *et al.*, 2002; Tisserand *et al.*, 2012). It is therefore a more sensitive and accurate technique for determining the Tsol-gel temperature (Pasqua *et al.*, 2014). Ideally, the Tsol-gel temperature of formulations for mucosal application should be between 30-35 °C (Miyazaki *et al.*, 1998; Jones *et al.*, 2003; Karavana, 2012). For this reason, we considered the 16% PF127 BUD formulation as the most promising for *in vivo* application. This formulation was then further characterized for its microstructure, mucoadhesion and *in vivo* efficacy.

TEM

TEM images of 16% PF127 BUD were obtained at 25 and 37 °C (Figure 4). The individual organization of ~10 nm micelles, as well as the spherical shape and core-shell structure of the PF127 formulations were observed (Lam *et al.*, 1999). It is possible to visualize in Figure 4 (A, B, C, D) the micelle formation and the homogeneity in size and shape of the micelles at 25 °C. At this temperature, all three formulations were in a fluid, liquid form. In addition, it was possible to confirm through the absence of drug crystals (also demonstrated by XRD) that BUD was completely solubilized and molecularly dispersed in the formulation. This represents a considerable advantage of the formulation from the pharmacotherapeutic point of view, since BUD is fully available when in contact with the mucosa to perform its biological activity.

The micellar organization of PF127 is mentioned in the literature as a reflection of its structural organization in triblocks (Akkari, A. C. *et al.*, 2016; Rençber *et al.*, 2017; Varaprasad *et al.*, 2017). This microstructure has been described as long range orders of micelles, where each micelle is well separated from the surrounding ones (Pragatheeswaran and Chen, 2013; Eshel-Green and Bianco-Peled, 2016). At 37 °C (Figure 4, E and F), the polymer molecules exhibit a different arrangement. The micrographs show the formation of interconnected networks of the polymer assembly, which leads to the formation of the gel. For PF127, the CGC is reported as >15% (mass) (Pragatheeswaran and Chen, 2013). Above this concentration, when the temperature is increased, the hydrophilic chains of the copolymer are desolvated as a result of the breakdown of hydrogen bonds previously established between the solvent and the hydrophilic chains. This phenomenon favors the hydrophobic interactions between polyoxypropylene (PPO) domains, and leads to the formation of gel (Escobar-Chávez *et al.*, 2006).

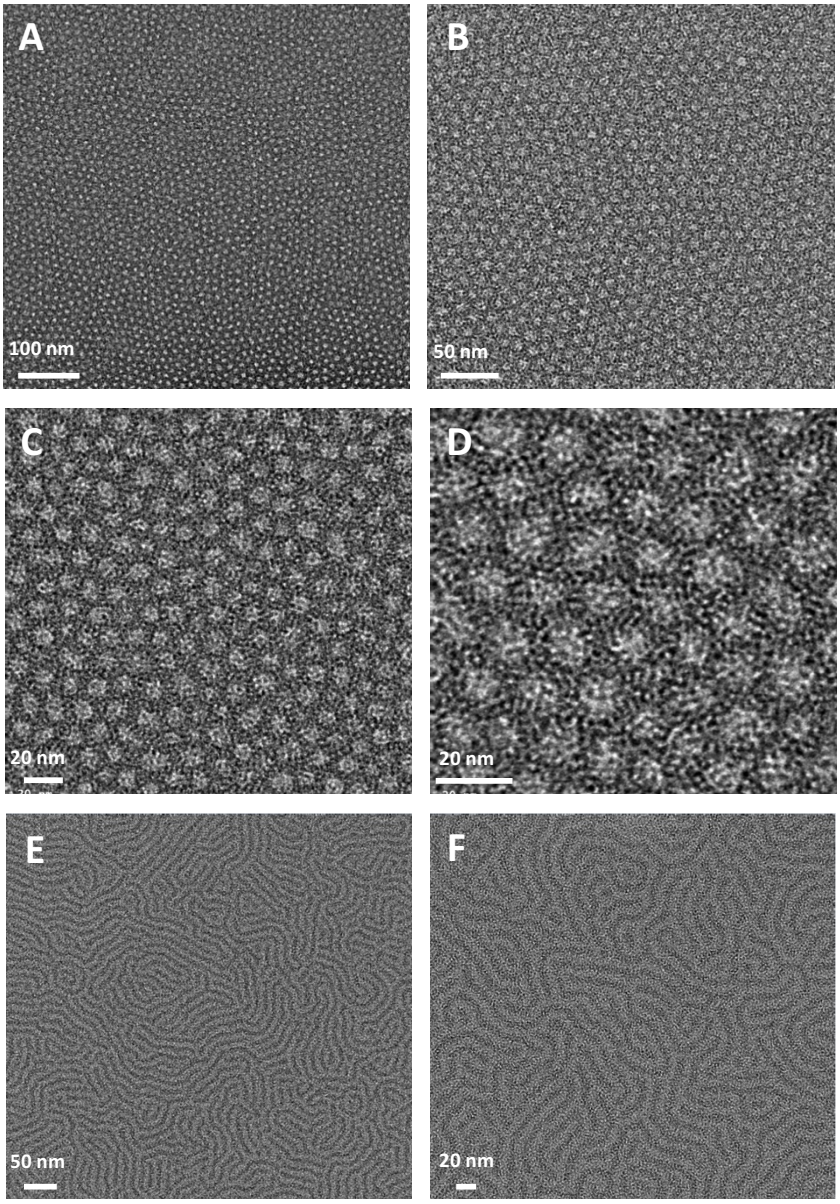

Figure 4. TEM images of 16% PF127 formulation containing BUD at 0.5 mg/mL. Images made at 25 °C (A, B, C, D) show the individual micellar organization. Images made at 37 °C (E, F) show the interconnected networks of the co-polymer assembly following thermogelling. Magnifications: A) 29000x; B) 62000x; C) 100000x; D) 200000x; E) 62000x; F) 100000x.

In vitro and *ex vivo* mucoadhesion

Figure 5A shows the mucoadhesive force measured *in vitro* of the 16% PF127 sample, as well as the 15% and 17% samples used for comparison. The assay was performed at 37 °C to simulate body temperature. For this reason, 15% PF127 gels were still liquid as they had not reached their Tsol-gel temperature, as shown by microrheology, oscillatory rheometry and DSC. Mucoadhesive strength values were around 5 g for the 15% PF127 formulations, and increased significantly (p<0.001) with the increase of polymer content until 11-14 g for

gels with 17% PF127. The presence of BUD increased the adhesion strength, indicating a possible formation of secondary bonds between the mucoadhesive polymer and the mucus glycoproteins (Pereira *et al.*, 2013).

The *in vitro* mucoadhesion assay was used as a preliminary study to compare between the 3 different formulations with varying concentrations of PF127. *Ex vivo* esophageal mucoadhesion was then studied for the 16% PF127 BUD formulation, which presented the most suitable Tsol-gel temperature range for mucosal application. Experimental setup is schematized in Figure 5B, calculated amounts of rhodamine B adhered to the esophageal mucosa after consecutive rinses are shown in Figure 5C and representative images of the trachea sections throughout the analysis are shown in Figure 5D. The control, a 2 mg/mL rhodamine B Hartmann solution, did not adhere to the mucosa and was rapidly and almost completely rinsed off. For the formulation, on the other hand, the fraction which remained adhered to the esophageal tissue decreased exponentially as a function of the number of successive rinses with the Hartmann solution. Around 50% of the formulation remained in contact after the first rinse. After the second rinse, over 40% was still retained by the mucosa, and after the third rinse almost 40% of the formulation was retained. After 4 rinses, ~30% of the formulation was still in contact with the esophageal mucosa. The higher amount of formulation lost after the first rinse is probably due to the portion of the formulation that did not interact directly with the esophageal mucosa, and was therefore washed away with the rinsing solution (Richardson *et al.*, 2005). Similarly, a two-stage retention profile, dependent on the ability of the polymer to interact with the gastric mucosa, has been observed for polyacrylic acid dispersions (Riley *et al.*, 2002; Smart *et al.*, 2003).

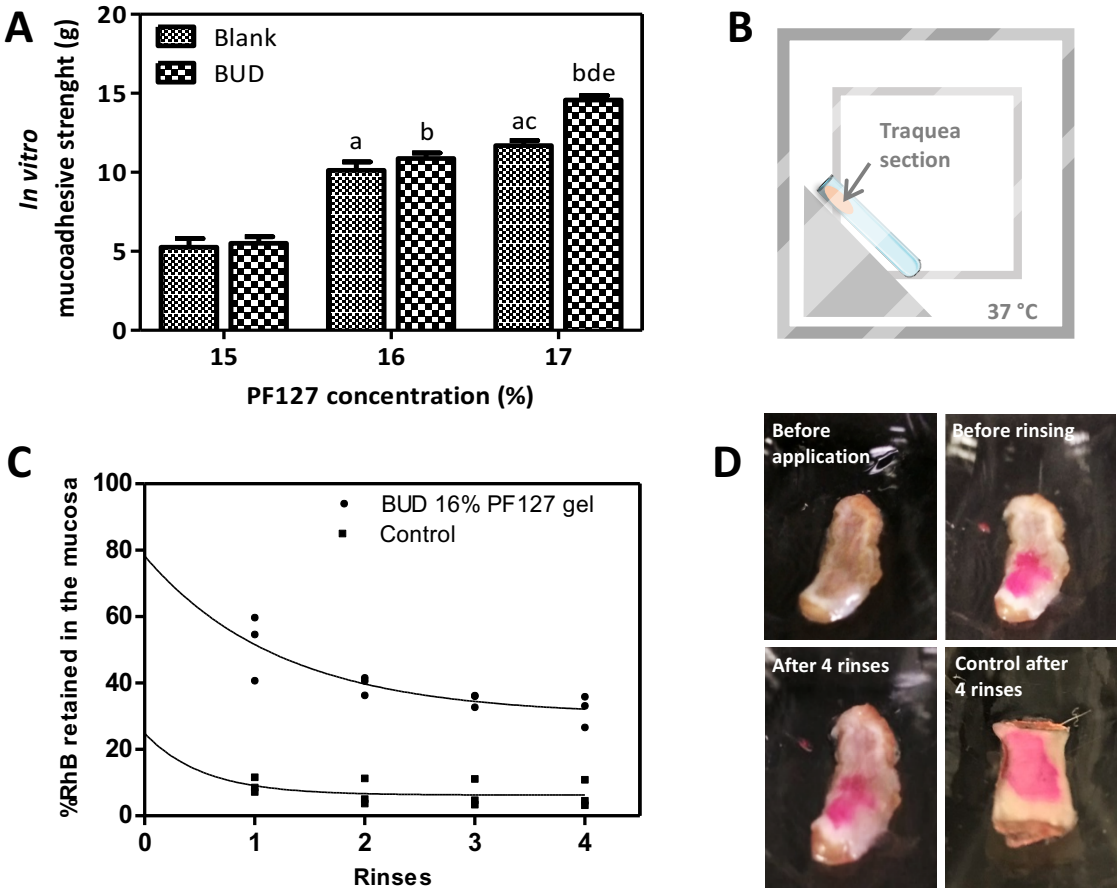

Figure 5. A. *In vitro* mucoadhesive strength of 15, 16 and 17% PF127 formulations, without and with BUD. Measurements were made at 37 °C using a texturometer. Each bar presents mean ± SD of 3 independent experiments. [a]p<0.05 *vs* blank 15% PF127; [b]p<0.05 *vs* BUD 15% PF127; [c]p<0.05 *vs* blank 16% PF127; [d]p<0.05 *vs* BUD 16%; [e]p<0.05 *vs* blank 17% PF127. B. Schematic representation of the experimental setup used for measuring formulation retention on the esophageal mucosa surface. C. *Ex vivo* mucoadhesion of the rhodamine B-labeled 16% PF127 BUD formulation. Rhodamine B that remained adhered to the esophageal mucosa was quantified after 4 consecutive rinses. Temperature was mantained at 37°C, and the test was perfomed in triplicate. D. Representative images of the trachea sections throughout the *ex vivo* analysis.

In vivo **mucoadhesion in the TGI and** ***ex vivo*** **intestinal permeation**

The potential of PF127 formulations to adhere to the esophageal mucosa is considered superior when compared to solutions, suspensions and non-adhesive formulations (Richardson *et al.*, 2005). Combination strategies with mucoadhesive polymers have also been explored to improve PF127 ability to adhere to mucosal surfaces, e.g. with carpobol 934P (Junqueira *et al.*, 2016), xanthan gum (Bhowmik *et al.*, 2013) and chitosan (Caramella *et al.*, 2015).

The *in vivo* mucoadhesion of the formulation was evaluated throughout the TGI using fluorescence tomography after oral administration of the formulation. A broad distribution of gel through the TGI tract was observed (Figure 6A1). This indicated that the formulation moved in a slow rate from the mouth to the lower intestines. *Ex vivo* images also evidenced the presence of the formulation in the esophagus region after 4 hours (Figure 6A2), while normal total TGI transit time for fluids in mice is around 1.5 h (Schwarz *et al.*, 2002; Padmanabhan *et al.*, 2013; Woting and Blaut, 2018). This indicates that the formulation mucoadhesion might have contributed to the prolonged retention of the formulation on the esophagus (Collaud *et al.*, 2007). Fluorescence imaging confirmed the presence of the formulation in proximal and distal regions of the intestinal mucosa 1 h after treatment (Figure 6B).

Reduced permeation of BUD from the PF127 gel through the intestinal wall *ex vivo*, compared to BUD solution, indicates that the formulation favors the localized effect of BUD (Figure 6C). Micellization of BUD within the self-assembled polymer structures slows down the drug release and consequently the permeation through the intestinal barrier, in addition to promoting mucoadhesion and a prolonged retention on the intestinal mucosa. Contributing to the localized effect of BUD and reducing its systemic bioavailability are additional advantages of this formulation, also leading to the reduction of adverse effects.

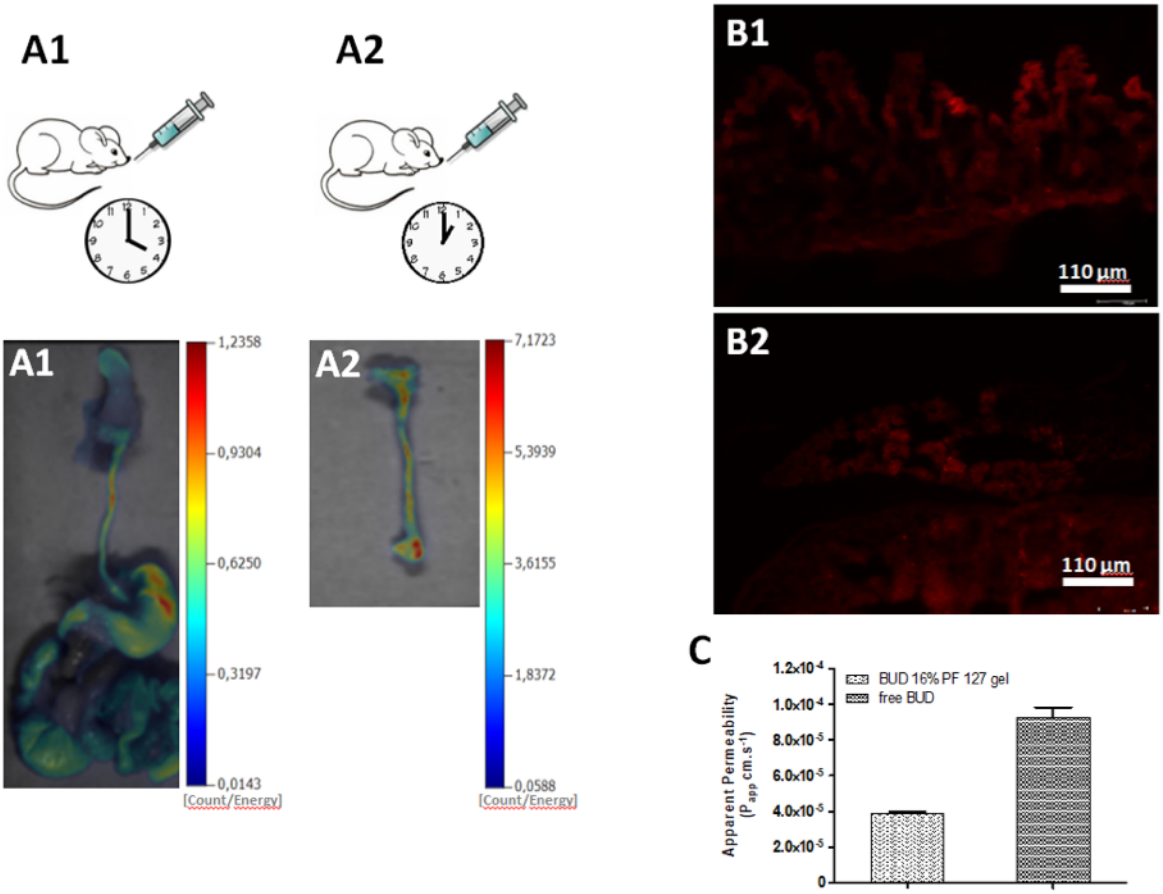

Figure 6. A. *Ex vivo* images representing the TGI tract and esophagus of animals treated orally with 20 µl of 16% PF127 BUD formulation, euthanized 4 and 1 h after treatment, respectively (n=2). B. Representative fluorescence microscopy images of B1: Proximal portion and B2: Distal portion of mice duodenum 1 h after administration of BUD-gel labeled with rhodamine B by gavage. The coverage of the intestinal crypts by the gel evidences the formulation mucoadhesiveness. C. Apparent intestinal permeability of the 16% PF127 BUD formulation compared to the free drug, indicating decreased passage of the formulation through the intestinal barrier.

In vivo therapeutic efficacy against mucositis

Since gelation and mucoadhesive behavior of the formulation are dependent on the total concentration of the polymer, contents of the GI fluid might influence these properties in vivo. Nevertheless, the contents of the GI tract are generally semi-solid, and excess water is not available to interact and promote dilution of the formulation. Very low levels of fluid are present in the mouse GI tract (less than 1mL total), making the choice of this animal model very suitable for the in vivo experiments conducted in this work (Mcconnell *et al.*, 2008). Intestinal mucositis is an inflammation and/or ulcerative injury that can be caused by infectious diseases, immune system deficiency or specific medications (Peterson *et al.*, 2011). It is known that during chemotherapy treatments, such as with 5-FU, interruptions in

cell division occur in the intestinal crypts and in the renewal of the epithelium villi, leading to a rapid loss of intestinal structure and functionality (Keefe *et al.*, 2000). Histopathological analysis results (Figure 7) showed that animals which received 5-FU (positive control, C and D), compared to the negative controls (A and B), presented short crypts, ulceration areas, intense inflammatory infiltrate and vacuolated epithelial lining cells with water accumulation, indicating hydropic degeneration. The intestinal mucositis evidences found in the present study were similar to those found in other studies where 5-FU was used as a model to evaluate possible treatments for the disease (Wu *et al.*, 2011; Soares *et al.*, 2013; De Ávila *et al.*, 2015; Bastos *et al.*, 2016; Dos Santos Filho *et al.*, 2016).

It was also possible to observe, in animals treated with the blank formulation (Figure 7, E and F), areas with crypts atrophy, resulting in localized ulceration and vacuolization of the epithelial lining. On the other hand, images of animals treated with BUD-gel showed preserved crypt sizes, absence of ulceration and vacuolization in the lining epithelium, and a decrease in inflammatory infiltrate (Figure 7, G and H). These results demonstrate that the formulation was able to reduce the injury caused by 5-FU. This can be explained by the local anti-inflammatory activity of BUD and the adhesion of the formulation to the intestinal mucosa.

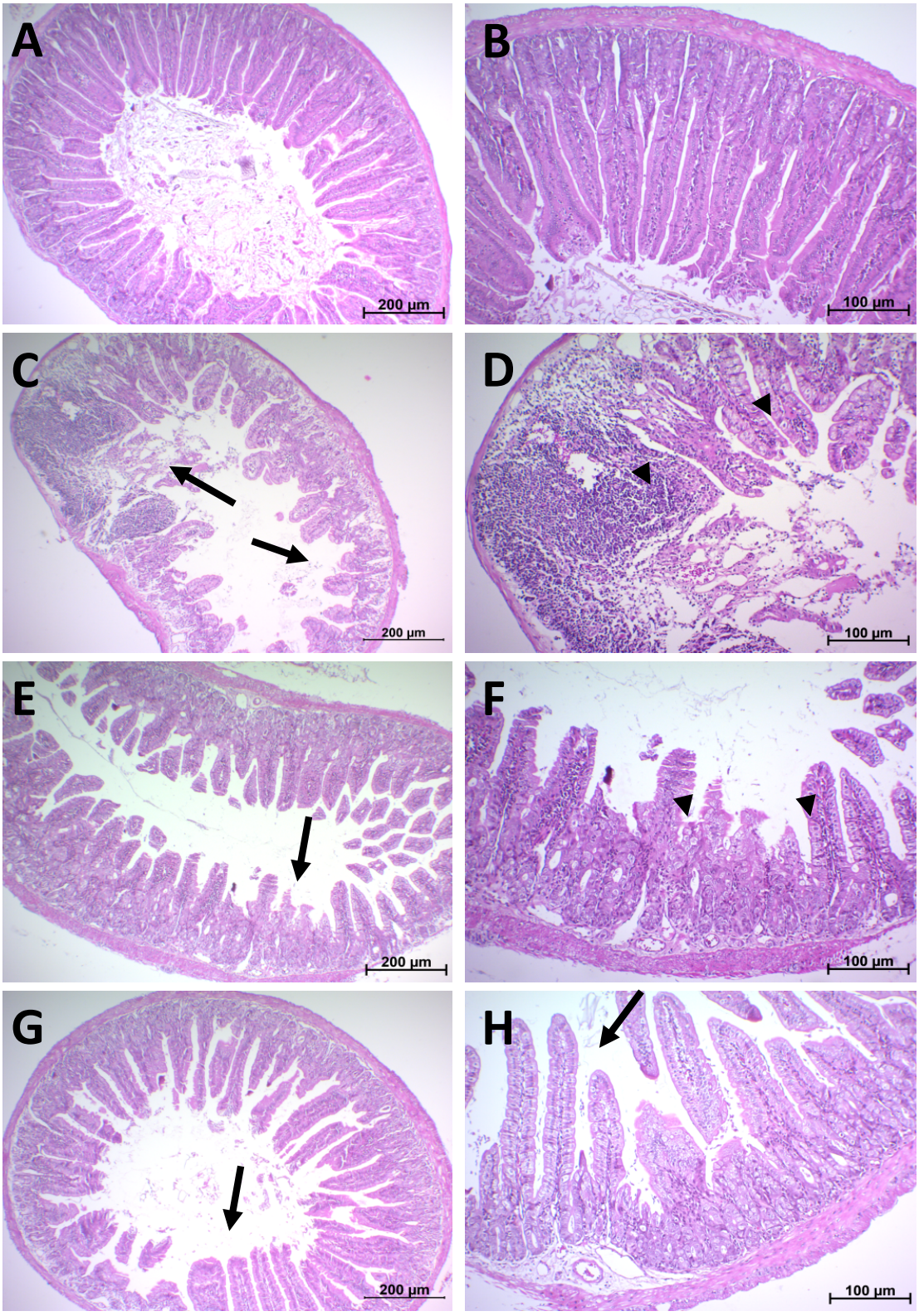

Figure 7. Histological sections of mice duodenum after induction of intestinal mucositis with 5-FU and treatment with BUD gel. A/B: Negative control showing long and normal crypts; C/D: Positive control showing short crypts and ulceration area (arrows), intense inflammatory infiltrate and vacuolized lining cells (arrowheads); E/F: Placebo treated duodenums showing areas with crypt atrophy resulting in ulceration (arrow) and vacuolization of epithelial lining cells (arrowheads); G/H: BUD-gel treated duodenums showing preserved crypts and absence of ulceration (arrows).

Induction of intestinal mucositis and treatment were done simultaneously for 3 days. Duodenum samples were removed for histopathological analysis 24 h after the last treatment. Slides were stained using HE. Magnification: 5X right row (A C, E, G), 10X left row (B, D, F, H).

It should be noted that the formulation containing BUD also had an effect on the animals weight loss during treatment with 5-FU. Positive control group (induced mucositis, treated with water) had an average weight loss of 20%. The group treated with the blank formulation (placebo) exhibited 18% of weight loss. Conversely, the weight loss of animals treated with BUD gel was approximately 11%; nearly half of that of the positive control ($p<0.05$). The destruction of the gastrointestinal epithelium contributes to poor absorption of nutrients and, consequently, weight loss (Keefe, 2007). Treatment with 5-FU can directly induce loose and aqueous bowel movements, and could have prolonged negative effects on homeostasis or reduction of food intake (Sakai et al., 2014). Therefore, the results reinforce that our mucoadhesive formulation could actually protect the intestinal mucosa preventing or reducing lesions and weight loss. The histopathological results combined with the fluorescence and FMT images indicate the mucoadhesion of the formulation and its effectiveness for in situ treatment of intestinal mucositis. The beneficial effect of this new formulation for the treatment of experimental mucositis is of clear clinical relevance, since mucositis is a common dose-limiting toxic effect of chemotherapy, for which there is no standard therapy or preventive measures (Sharma et al., 2005). Additionally, as demonstrated by FMT (Figure 6), the prolonged residence time of the formulation throughout the entire GI mucosa, highlights its potential application for a wider range of inflammatory disorders, from the esophagus though the colon. The protective effect of Poloxamer 407 mucoadhesive formulations in the TGI has been shown previously (Bastos et al., 2016; Dos Santos Filho et al., 2016). Here, we go further to show, besides the protective effect, the advantages of a system that can be used to prolong the contact of non-soluble drugs with the TGI mucosa.

There are approximately 110 marketed products of budesonide worldwide (DrugBank, 2019) (Wishart *et al.*, 2017). With the exception of an aerosol foam/emulsion for rectal administration, all the other dosage forms intended for oral, nasal or the respiratory (inhalation) route present budesonide in its solid form (either as a dry powder or in suspension). This could be expected since budesonide, a BCS Class II drug, is practically insoluble in water. More recent approaches to address local delivery of budesonide to treat inflammatory bowel disease also present the drug in the form of nanoparticles either

nanostructured into polymeric systems (Odabasi *et al.*, 2014) or milled to the nanometer range (Van Schandevyl and Bauters, 2016). This is the first report of a budesonide formulation with mucoadhesive characteristics proven to treat intestinal mucositis. Also, there are no records in the literature or in the documentation of budesonide marketed products of an aqueous formulation in which the drug is molecularly dispersed, as demonstrated in this work. In addition to an extensive characterization of the dispersions, as well as on the in vivo and ex vivo mucoadhesive properties of the formulation, we could demonstrate the prolonged retention of the formulation on the mucosa, from the esophagus to the small intestine, leading to the resolution of the induced mucositis. The formulation proposed here can be applied as a potential platform for treating diverse TGI inflammatory pathologies. The idea applied in the development of the dispersion can be used for the incorporation of drugs that are poorly soluble, due to the mucoadhesive properties and drug solubilization within the polymer micelles. These outputs contribute to the development of more effective formulations for treating TGI diseases.

CONCLUSION

Pluronic® F127 was successfully formulated as a thermo reversible *in situ* gel former for mucosal application through the oral route. The method used for the preparation of the formulation allowed the solubilization and molecular dispersion of BUD, observed by TEM and confirmed by DSC and XRPD, allowing the direct contact of the drug with the mucosa after *in vivo* application. Mucoadhesion and Tsol-gel temperature results indicated 16% PF127 as the most adequate for a possible application in the mucosa, in accordance to the microrheology and rheometry results. *Ex vivo and in vivo* studies showed that the formulation was able to efficiently adhere to the TGI mucosa and resolve local inflammatory injury.

Using the 16% PF127 gel we can enable the effective availability of BUD at the inner surface of the TGI mucosa, and the micellization / solubilization aspect might qualify this system as a platform for other non-soluble molecules. Furthermore, the formulation proposed in this work stands out for being easily scaled up, and for not requiring complex components or preparations steps.

ACKNOWLEDGMENTS

This work was financially supported by the Brazilian research funding agencies *Conselho Nacional de Desenvolvimento Científico e Tecnológico* (CNPq), *Financiadora de Estudos e Pesquisas* (FINEP), *Coordenação de Aperfeiçoamento de Pessoal de Nível Superior* (CAPES), *Fundação de Apoio à Pesquisa da Universidade Federal de Goiás* (FUNAPE), *Fundação de Apoio à Pesquisa do Estado de Goiás* (FAPEG), and by Ferring Pharmaceuticals.

The EM work was conducted at the Molecular Electron Microscopy Core facility at the University of Virginia, which is supported by the School of Medicine and built with NIH grant (G20-RR31199). The authors would like to thank Professor Marcus Vinicius Lia Fook from CERTBIO at Federal University of Campina Grande for DSC and rheological analysis, and Lílian Cristina Rosa Santos for her aid with the *ex vivo* permeation experiment.

COMPETING INTERESTS

The authors declare no competing interests.

REFERENCES

AKASH, M. S. H.; REHMAN, K. Recent progress in biomedical applications of Pluronic (PF127): pharmaceutical perspectives. **Journal of Controlled Release,** v. 209, p. 120-138, 2015. ISSN 0168-3659.

AKKARI, A. C. et al. Poloxamer 407/188 binary thermosensitive hydrogels as delivery systems for infiltrative local anesthesia: Physico-chemical characterization and pharmacological evaluation. **Materials Science and Engineering: C,** v. 68, p. 299-307, 2016. ISSN 0928-4931.

AKKARI, A. C. S. et al. Budesonide-hydroxypropyl-β-cyclodextrin inclusion complex in binary poloxamer 407/403 system for ulcerative colitis treatment: A physico-chemical study from micelles to hydrogels. **Colloids and Surfaces B: Biointerfaces,** v. 138, p. 138-147, 2016. ISSN 0927-7765.

ALI, H. et al. Budesonide loaded PLGA nanoparticles for targeting the inflamed intestinal mucosa—Pharmaceutical characterization and fluorescence imaging. **Pharmaceutical research,** v. 33, n. 5, p. 1085-1092, 2016. ISSN 0724-8741.

ALTUNTAŞ, E.; YENER, G. Formulation and Evaluation of Thermoreversible In Situ Nasal Gels Containing Mometasone Furoate for Allergic Rhinitis. **AAPS PharmSciTech**, p. 1-10, 2017. ISSN 1530-9932.

ATTWOOD, D.; COLLETT, J.; TAIT, C. The micellar properties of the poly (oxyethylene)-poly (oxypropylene) copolymer Pluronic F127 in water and electrolyte solution. **International journal of pharmaceutics,** v. 26, n. 1-2, p. 25-33, 1985. ISSN 0378-5173.

BAN, E. et al. Poloxamer-Based Thermoreversible Gel for Topical Delivery of Emodin: Influence of P407 and P188 on Solubility of Emodin and Its Application in Cellular Activity Screening. **Molecules,** v. 22, n. 2, p. 246, 2017.

BANDI, N. et al. Preparation of budesonide–and indomethacin–hydroxypropyl-β-cyclodextrin (HPBCD) complexes using a single-step, organic-solvent-free supercritical fluid process. **European journal of pharmaceutical sciences,** v. 23, n. 2, p. 159-168, 2004. ISSN 0928-0987.

BASTOS, C. C. C. et al. Use of Bidens pilosa L.(Asteraceae) and Curcuma longa L.(Zingiberaceae) to treat intestinal mucositis in mice: Toxico-pharmacological evaluations. v. 3, p. 279-287, 2016. ISSN 2214-7500.

BATISTA, A. P. et al. Rheological characterization of coloured oil-in-water food emulsions with lutein and phycocyanin added to the oil and aqueous phases. **Food Hydrocolloids,** v. 20, n. 1, p. 44-52, 2006. ISSN 0268-005X.

BELLOUR, M. et al. Brownian motion of particles embedded in a solution of giant micelles. **The European Physical Journal E: Soft Matter and Biological Physics,** v. 8, n. 4, p. 431-436, 2002. ISSN 1292-8941.

BHOWMIK, M. et al. Effect of xanthan gum and guar gum on in situ gelling ophthalmic drug delivery system based on poloxamer-407. **International journal of biological macromolecules,** v. 62, p. 117-123, 2013. ISSN 0141-8130.

BOATENG, J.; OKEKE, O.; KHAN, S. Polysaccharide based formulations for mucosal drug delivery: A review. **Current pharmaceutical design,** v. 21, n. 33, p. 4798-4821, 2015. ISSN 1381-6128.

BRUSCHI, M. L. et al. Semisolid systems containing propolis for the treatment of periodontal disease: in vitro release kinetics, syringeability, rheological, textural, and mucoadhesive properties. **Journal of pharmaceutical sciences,** v. 96, n. 8, p. 2074-2089, 2007. ISSN 1520-6017.

CARAMELLA, C. M. et al. Mucoadhesive and thermogelling systems for vaginal drug delivery. **Advanced drug delivery reviews,** v. 92, p. 39-52, 2015. ISSN 0169-409X.

ÇELEBI, N.; ERMIŞ, S.; ÖZKAN, S. Development of topical hydrogels of terbinafine hydrochloride and evaluation of their antifungal activity. **Drug development and industrial pharmacy,** v. 41, n. 4, p. 631-639, 2015. ISSN 0363-9045.

COLLAUD, S. et al. Clinical evaluation of bioadhesive hydrogels for topical delivery of hexylaminolevulinate to Barrett's esophagus. **Journal of Controlled Release,** v. 123, n. 3, p. 203-210, 2007. ISSN 0168-3659.

CORREDIG, M.; ALEXANDER, M. Food emulsions studied by DWS: recent advances. **Trends in food science & technology,** v. 19, n. 2, p. 67-75, 2008. ISSN 0924-2244.

DE ÁVILA, P. H. M. et al. Mucoadhesive formulation of Bidens pilosa L.(Asteraceae) reduces intestinal injury from 5-fluorouracil-induced mucositis in mice. v. 2, p. 563-573, 2015. ISSN 2214-7500.

DEWAN, M. et al. Effect of methyl cellulose on gelation behavior and drug release from poloxamer based ophthalmic formulations. **International journal of biological macromolecules,** v. 72, p. 706-710, 2015. ISSN 0141-8130.

DOS SANTOS FILHO, E. X. et al. Curcuminoids from Curcuma longaL. reduced intestinal mucositis induced by 5-fluorouracil in mice: Bioadhesive, proliferative, anti-inflammatory and antioxidant effects. v. 3, p. 55-62, 2016. ISSN 2214-7500.

DUDOGNON, E. et al. Formation of budesonide/α-lactose glass solutions by ball-milling. **Solid State Communications,** v. 138, n. 2, p. 68-71, 2006. ISSN 0038-1098.

EDSBÄCKER, S.; ANDERSSON, T. J. C. P. Pharmacokinetics of budesonide (Entocort™ EC) capsules for Crohn's disease. v. 43, n. 12, p. 803-821, 2004. ISSN 0312-5963.

ESCOBAR-CHÁVEZ, J. J. et al. Applications of thermo-reversible pluronic F-127 gels in pharmaceutical formulations. **Journal of Pharmacy & Pharmaceutical Sciences,** v. 9, n. 3, p. 339-58, 2006. ISSN 1482-1826.

ESHEL-GREEN, T.; BIANCO-PELED, H. Mucoadhesive acrylated block copolymers micelles for the delivery of hydrophobic drugs. **Colloids and Surfaces B: Biointerfaces,** v. 139, p. 42-51, 2016. ISSN 0927-7765.

FATHALLA, Z. M. et al. Poloxamer-based thermoresponsive ketorolac tromethamine in situ gel preparations: Design, characterisation, toxicity and transcorneal permeation studies. **European Journal of Pharmaceutics and Biopharmaceutics,** v. 114, p. 119-134, 2017. ISSN 0939-6411.

FURUTA, G. T. et al. Eosinophilic esophagitis in children and adults: a systematic review and consensus recommendations for diagnosis and treatment: sponsored by the American Gastroenterological Association (AGA) Institute and North American Society of Pediatric Gastroenterology, Hepatology, and Nutrition. **Gastroenterology,** v. 133, n. 4, p. 1342-1363, 2007. ISSN 0016-5085.

GONZÁLEZ-CERVERA, J. et al. Association between atopic manifestations and eosinophilic esophagitis: A systematic review and meta-analysis. **Annals of Allergy, Asthma & Immunology,** v. 118, n. 5, p. 582-590. e2, 2017. ISSN 1081-1206.

GUIDELINE, I. H. T. Validation of analytical procedures: text and methodology. **Q2 (R1),** v. 1, 2005.

JIANG, J. et al. The effect of physiologically relevant additives on the rheological properties of concentrated Pluronic copolymer gels. **Polymer,** v. 49, n. 16, p. 3561-3567, 2008. ISSN 0032-3861.

JONES, D. S.; BROWN, A. F.; DAVID WOOLFSON, A. Solute and solvent effects on the thermorheological properties of poly (oxyethylene)–poly (oxypropylene) block copolymers: implications for pharmaceutical dosage form design. **Journal of applied polymer science,** v. 87, n. 6, p. 1016-1026, 2003. ISSN 1097-4628.

JONES, D. S. et al. Rheological, mechanical and mucoadhesive properties of thermoresponsive, bioadhesive binary mixtures composed of poloxamer 407 and carbopol 974P designed as platforms for implantable drug delivery systems for use in the oral cavity. **International journal of pharmaceutics,** v. 372, n. 1, p. 49-58, 2009. ISSN 0378-5173.

JUNQUEIRA, M. V. et al. Evaluation of the methylene blue addition in binary polymeric systems composed by poloxamer 407 and Carbopol 934P using quality by design: rheological, textural, and mucoadhesive analysis. **Drug development and industrial pharmacy,** v. 42, n. 12, p. 2009-2019, 2016. ISSN 0363-9045.

KARAVANA, S. Y. A new in-situ gel formulation of Itraconazole for vaginal administration. **Pharmacology & Pharmacy,** v. 3, n. 04, p. 417, 2012.

KEEFE, D. et al. Chemotherapy for cancer causes apoptosis that precedes hypoplasia in crypts of the small intestine in humans. v. 47, n. 5, p. 632-637, 2000. ISSN 0017-5749.

KEEFE, D. M. J. C. O. I. O. Intestinal mucositis: mechanisms and management. v. 19, n. 4, p. 323-327, 2007. ISSN 1040-8746.

LAFFLEUR, F.; BERNKOP-SCHNÜRCH, A. Strategies for improving mucosal drug delivery. **Nanomedicine,** v. 8, n. 12, p. 2061-2075, 2013. ISSN 1743-5889.

LAM, Y.-M.; GRIGORIEFF, N.; GOLDBECK-WOOD, G. Direct visualisation of micelles of Pluronic block copolymers in aqueous solution by cryo-TEM. **Physical Chemistry Chemical Physics,** v. 1, n. 14, p. 3331-3334, 1999.

LAUBITZ, D. et al. Mucosal Inflammation, not Microbiome, Drives the Development Colorectal Cancer During Colitis-Associated Microbial Dysbiosis. **Gastroenterology,** v. 152, n. 5, p. S357, 2017. ISSN 0016-5085.

LEE, S. G. et al. Enhanced topical delivery of tacrolimus by a carbomer hydrogel formulation with transcutol P. **Drug development and industrial pharmacy,** v. 42, n. 10, p. 1636-1642, 2016. ISSN 0363-9045.

LENAERTS, V. et al. Temperature-dependent rheological behavior of Pluronic F-127 aqueous solutions. **International journal of pharmaceutics,** v. 39, n. 1-2, p. 121-127, 1987. ISSN 0378-5173.

MASTEIKOVA, R.; CHALUPOVA, Z.; SKLUBALOVA, Z. Stimuli-sensitive hydrogels in controlled and sustained drug delivery. **Medicina,** v. 39, n. 2, p. 19-24, 2003.

MAZIA, R. S. et al. Formulation and Evaluation of a Mucoadhesive Thermoresponsive System Containing Brazilian Green Propolis for the Treatment of Lesions Caused by Herpes Simplex Type I. **Journal of pharmaceutical sciences,** v. 105, n. 1, p. 113-121, 2016. ISSN 0022-3549.

MCCONNELL, E. L. et al. Measurements of rat and mouse gastrointestinal pH, fluid and lymphoid tissue, and implications for in-vivo experiments. v. 60, n. 1, p. 63-70, 2008. ISSN 0022-3573.

MIYAZAKI, S. et al. Thermally reversible xyloglucan gels as vehicles for rectal drug delivery. **Journal of Controlled Release,** v. 56, n. 1, p. 75-83, 1998. ISSN 0168-3659.

NAIKWADE, S.; BAJAJ, A. Preparation and in vitro evaluation of budesonide spray dried microparticles for pulmonary delivery. **Sci Pharm,** v. 77, p. 419-441, 2009.

NOLTE, T. et al. Nonproliferative and Proliferative Lesions ofthe Gastrointestinal Tract, Pancreas andSalivary Glands of the Rat and Mouse. v. 29, n. 1_Suppl, p. 1S-125S, 2016. ISSN 0914-9198.

ODABASI, M. et al. Prophylactic and therapeutic effects of oral budesonide for acute radiation-induced enteritis and colitis in rats. v. 7, n. 4, p. 940, 2014.

PADMANABHAN, P. et al. Gastrointestinal transit measurements in mice with 99m Tc-DTPA-labeled activated charcoal using NanoSPECT-CT. v. 3, n. 1, p. 60, 2013. ISSN 2191-219X.

PASQUA, A. et al. Potential application of micro-rheology-Rheolaser Lab R in food sciences. **Advances in Food Safety and Health**, p. 60-69, 2014.

PEREIRA, R. R. D. A. et al. Preparation and characterization of mucoadhesive thermoresponsive systems containing propolis for the treatment of vulvovaginal candidiasis. **Journal of pharmaceutical sciences,** v. 102, n. 4, p. 1222-1234, 2013. ISSN 1520-6017.

PETERSON, D. et al. Management of oral and gastrointestinal mucositis: ESMO Clinical Practice Guidelines. v. 22, n. suppl_6, p. vi78-vi84, 2011. ISSN 1569-8041.

PITORRE, M. et al. Recent advances in nanocarrier-loaded gels: Which drug delivery technologies against which diseases? **Journal of Controlled Release**, 2017. ISSN 0168-3659.

POPOV, T. A.; NIET, S. D.; VANDERBIST, F. Budesonide/Salmeterol in Fixed-Dose Combination for the Treatment of Asthma. **Expert review of respiratory medicine**, n. just-accepted, 2016. ISSN 1747-6348.

PRAGATHEESWARAN, A. M.; CHEN, S. B. Effect of chain length of PEO on the gelation and micellization of the Pluronic F127 copolymer aqueous system. **Langmuir,** v. 29, n. 31, p. 9694-9701, 2013. ISSN 0743-7463.

PRASAD, G. A. et al. Prevalence and predictive factors of eosinophilic esophagitis in patients presenting with dysphagia: a prospective study. **The American journal of gastroenterology,** v. 102, n. 12, p. 2627, 2007. ISSN 0002-9270.

RAO, M.; AGRAWAL, D. K.; SHIRSATH, C. Thermoreversible mucoadhesive in situ nasal gel for treatment of Parkinson's disease. **Drug development and industrial pharmacy,** v. 43, n. 1, p. 142-150, 2017. ISSN 0363-9045.

RENÇBER, S. et al. Mucoadhesive in situ gel formulation for vaginal delivery of clotrimazole: formulation, preparation, and in vitro/in vivo evaluation. **Pharmaceutical development and technology,** v. 22, n. 4, p. 551-561, 2017. ISSN 1083-7450.

RICHARDSON, J. C. et al. Oesophageal bioadhesion of sodium alginate suspensions: 2. Suspension behaviour on oesophageal mucosa. **European journal of pharmaceutical sciences,** v. 24, n. 1, p. 107-114, 2005. ISSN 0928-0987.

RILEY, R. G. et al. An in vitro model for investigating the gastric mucosal retention of 14 C-labelled poly (acrylic acid) dispersions. **International journal of pharmaceutics,** v. 236, n. 1, p. 87-96, 2002. ISSN 0378-5173.

SAKAI, H. et al. Neutrophil recruitment is critical for 5-fluorouracil-induced diarrhea and the decrease in aquaporins in the colon. v. 87, p. 71-79, 2014. ISSN 1043-6618.

SANTOS FILHO, E. X. et al. Randomized clinical trial of a mucoadhesive formulation containing curcuminoids (Zingiberaceae) and Bidens pilosa Linn (Asteraceae) extract (FITOPROT) for prevention and treatment of oral mucositis-phase I study. **Chemico-biological interactions**, 2018. ISSN 0009-2797.

SANTOS FILHO, E. X. et al. Chemopreventive effects of FITOPROT against 5-fluorouracil-induced toxicity in HaCaT cells. **Life sciences,** v. 193, p. 300-308, 2018. ISSN 0024-3205.

SCHWARZ, R. et al. Gastrointestinal transit times in mice and humans measured with 27Al and 19F nuclear magnetic resonance. v. 48, n. 2, p. 255-261, 2002. ISSN 0740-3194.

SHARMA, R.; TOBIN, P.; CLARKE, S. J. J. T. L. O. Management of chemotherapy-induced nausea, vomiting, oral mucositis, and diarrhoea. v. 6, n. 2, p. 93-102, 2005. ISSN 1470-2045.

SMART, J. D. et al. The retention of 14 C-labelled poly (acrylic acids) on gastric and oesophageal mucosa: an in vitro study. **European journal of pharmaceutical sciences,** v. 20, n. 1, p. 83-90, 2003. ISSN 0928-0987.

SOARES, P. M. et al. Inflammatory intestinal damage induced by 5-fluorouracil requires IL-4. v. 61, n. 1, p. 46-49, 2013. ISSN 1043-4666.

TISSERAND, C. et al. Passive microrheology for measurement of the concentrated dispersions stability. In: (Ed.). **UK colloids 2011**: Springer, 2012. p.101-105.

TRONG, L. C. P.; DJABOUROV, M.; PONTON, A. Mechanisms of micellization and rheology of PEO–PPO–PEO triblock copolymers with various architectures. **Journal of colloid and interface science,** v. 328, n. 2, p. 278-287, 2008. ISSN 0021-9797.

VAN SCHANDEVYL, G.; BAUTERS, T. J. J. O. O. P. P. Formulation of budesonide mouthwash for the treatment of oral chronic graft-versus-host disease. v. 22, n. 1, p. 82-85, 2016. ISSN 1078-1552.

VARAPRASAD, K. et al. A mini review on hydrogels classification and recent developments in miscellaneous applications. **Materials Science and Engineering: C**, 2017. ISSN 0928-4931.

VARSHOSAZ, J. et al. Effectiveness of budesonide-succinate-dextran conjugate as a novel prodrug of budesonide against acetic acid-induced colitis in rats. **International journal of colorectal disease,** v. 25, n. 10, p. 1159-1165, 2010. ISSN 0179-1958.

WANG, L. et al. Functional nanocarrier for drug and gene delivery via local administration in mucosal tissues. **Nanomedicine,** v. 13, n. 1, p. 69-88, 2018. ISSN 1743-5889.

WANKA, G.; HOFFMANN, H.; ULBRICHT, W. Phase diagrams and aggregation behavior of poly (oxyethylene)-poly (oxypropylene)-poly (oxyethylene) triblock copolymers in aqueous solutions. **Macromolecules,** v. 27, n. 15, p. 4145-4159, 1994. ISSN 0024-9297.

WISHART, D. S. et al. DrugBank 5.0: a major update to the DrugBank database for 2018. v. 46, n. D1, p. D1074-D1082, 2017. ISSN 0305-1048.

WOTING, A.; BLAUT, M. J. N. Small Intestinal Permeability and Gut-Transit Time Determined with Low and High Molecular Weight Fluorescein Isothiocyanate-Dextrans in C3H Mice. v. 10, n. 6, p. 685, 2018.

WU, Z. et al. Interleukin 1 receptor antagonist reduces lethality and intestinal toxicity of 5-fluorouracil in a mouse mucositis model. v. 65, n. 5, p. 339-344, 2011. ISSN 0753-3322.

XU, D. et al. Influence of microcrystalline cellulose on the microrheological property and freeze-thaw stability of soybean protein hydrolysate stabilized curcumin emulsion. **LWT-Food Science and Technology,** v. 66, p. 590-597, 2016. ISSN 0023-6438.

ZHANG, P. et al. Preparation and characterization of budesonide-loaded solid lipid nanoparticles for pulmonary delivery. **J Chin Pharm Sci,** v. 20, n. 4, p. 390-6, 2011.

ZHANG, Y.; ZHANG, J. Preparation of budesonide nanosuspensions for pulmonary delivery: Characterization, in vitro release and in vivo lung distribution studies. **Artificial cells, nanomedicine, and biotechnology**, p. 1-5, 2015. ISSN 2169-1401.

PARTE II

1. AMORFIZAÇÃO – SÍLICA MESOPOROSA

O elevado número de novos compostos químicos com baixa solubilidade aquosa associados à descoberta de novos fármacos tem promovido a pesquisa e o desenvolvimento de meios eficazes para ultrapassar a sua baixa biodisponibilidade (Engers *et al.*, 2010; Kawabata *et al.*, 2011). Uma das ferramentas mais promissoras é a conversão de fármacos cristalinos na sua forma amorfa, quando comparado a outras ferramentas, como formação de sal, que tem muitas limitações práticas (Serajuddin, 2007; Laitinen *et al.*, 2013).

O material amorfo apresenta organização estrutural com ordem de curto alcance no arranjo atômico, além de ser a forma com mais alta energia interna em um material sólido (Jenkins e Snyder, 1996). Como resultado de sua alta energia interna, materiais amorfos geralmente têm maior movimento molecular vibracional (relaxamento) e propriedades termodinâmicas melhoradas em comparação com o estado cristalino, levando a maior solubilidade aparente e taxa de dissolução (Hancock e Zografi, 1997). A alta energia interna e a mobilidade molecular aumentada de materiais amorfos também são responsáveis por sua maior reatividade química e tendência à recristalização, que pode ocorrer durante a fabricação, armazenamento ou dissolução no momento da administração (Vasconcelos *et al.*, 2007; Aaltonen e Rades, 2009).

Neste contexto, muito esforço tem sido feito para obter uma melhor compreensão dos fatores críticos na recristalização e encontrar métodos para a estabilização de formas amorfas de fármacos, a fim de se beneficiar de suas vantagens quanto à taxa de solubilidade e dissolução.

Na década de 60, as dispersões, polímero-sólido, tornaram-se o método preferido para estabilizar a forma amorfa e aumentar a dissolução do fármaco, método este introduzido por Sekiguchi e Obi (Sekiguchi *et al.*, 1961). Os aspectos associados à estabilidade das dispersões sólidas ainda não são totalmente compreendidos e esses sistemas ainda não são capazes de garantir a manutenção do estado amorfo (Janssens *et al.*, 2009).

As formas amorfas podem ser preparadas por transformação inicial do material cristalino em uma forma não cristalina termodinamicamente estável como, fusão ou

obtenção de solução, ou por conversão direta de sólidos cristalinos em um sólido amorfo (Laitinen *et al.*, 2013). Por fusão o sólido fundido é resfriado rapidamente (Vasconcelos *et al.*, 2007), por solução promove-se a precipitação rápida da solução como na secagem por *spray-drying* (Corrigan *et al.*, 1984). Já a conversão direta utiliza-se da ativação mecânica por moagem (Dudognon *et al.*, 2006).

A adição de certos excipientes, tais como tensoativos, anti-plastificantes e outros inibidores de recristalização, pode proporcionar melhoria significativa na estabilidade física de fármacos amorfos. O interesse pelo potencial de sistemas amorfos binários, compreendendo pequenas moléculas ao invés de polímeros, tem aumentado consideravelmente (Laitinen *et al.*, 2013). Tem sido relatado que moléculas pequenas, como ácido cítrico, açúcares, uréia e nicotinamida podem ser usadas como veículos em dispersões sólidas (Ahuja *et al.*, 2007; Masuda *et al.*, 2012).

Outra alternativa aos sistemas de fármaco-polímero na obtenção de sistemas amorfos é a aplicação de meios porosos ou adsorventes como a sílica mesoporosa (Laitinen *et al.*, 2013; Bremmell e Prestidge, 2019). A sílica mesoporosa (SM) refere-se a materiais porosos que exibem poros com diâmetros entre 2 e 50 nm (Prestidge *et al.*, 2007).

A alta energia livre de superfície, devido à grande área superficial do material poroso, permite que o sistema seja transferido para um estado de energia livre mais baixo após a adsorção de moléculas de fármaco na SM (Prestidge *et al.*, 2007). O fármaco adsorvido à superfície da SM perde sua estrutura cristalina. Devido à diminuição da energia livre de Gibbs, o sistema amorfo é fisicamente estável e a cristalização ocorre apenas se o estado termodinâmico do sistema for alterado. Além dos fatores termodinâmicos, a nucleação e o crescimento de cristais são prejudicados por restrições espaciais, ou seja, os poros não são capazes de incorporar moléculas suficientes para alcançar um tamanho de nucleação crítico (Qian e Bogner, 2011; 2012).

A capacidade de carga de um fármaco na SM pode ser definida como, a quantidade de fármaco que está estabilizada na SM (Hempel *et al.*, 2018). O fármaco pode está confinado na SM formando a monocamada, ou seja, o fármaco que interage com os grupos funcionais (Si-OH) da superfície da SM, pode está também preenchendo os poros, o fármaco que não interage com a superfície da SM, mas está dentro dos poros. E o excesso de fármaco, que fica fora dos poros da SM (Andersson *et al.*, 2004).

Para determinar a capacidade de carga da monocamada na SM, Hempel introduziu um método mais sistemático e confiável, baseado na quantificação da fração do fármaco que não interage com a superfície da SM, através da detecção da transição vítrea no DSC

(Hempel *et al.*, 2018). O método proposto baseia-se na fusão do fármaco no ciclo de aquecimento-resfriamento-aquecimento no DSC, sem utilização de solventes. No aquecimento no DSC, o fármaco se fundirá nos poros da SM através de forças capilares. Como as moléculas do fármaco adsorvidas na superfície da SM não contribuem para nenhum evento térmico, pois estão interagindo com os grupos funcionais da superfície da SM, a quantidade de fármaco em excesso pode ser quantificada, simplesmente pela determinação da variação da capacidade calorífica (ΔC_p) da fase restante.

Como a ΔC_p é uma propriedade extensiva e aditiva da matéria, o valor de ΔC_p é proporcional à fração amorfa do sistema e diminuirá linearmente com a diminuição do conteúdo do fármaco. Assim, a capacidade de carga da monocamada na SM pode ser determinada extrapolando ΔC_p (J/gºC) para zero (Saunders *et al.*, 2004).

Assim a aplicação de meios porosos, especialmente a SM é uma alternativa tecnológica e promissora para amorfização de fármacos. Uma vez que, obter o fármaco na sua forma amorfa é um dos meios mais efetivos para melhorar a baixa solubilidade aquosa, taxa de dissolução e, consequentemente a biodisponibilidade (Bremmell e Prestidge, 2019).

CAPÍTULO 03

IMPACT OF DRUG LOADING IN MESOPOROUS SILICA-AMORPHOUS FORMULATIONS ON THE PHYSICAL STABILITY OF DRUGS WITH HIGH RECRYSTALLIZATION TENDENCY

Capítulo publicado na forma de artigo original na revista International Journal of Pharmaceutics: X, 2019, doi.org/10.1016/j.ijpx.2019.100026.

Autores: Rayane S. C. M. Q. Antonino[1;2], Michael Ruggiero[3], Zihui Song[3], Thais Leite Nascimento[2], Eliana Martins Lima[2], Adam Bohr[1], Matthias Manne Knopp[4], Korbinian Löbmann[1]

[1]Department of Pharmacy, University of Copenhagen, Copenhagen, Denmark
[2]Laboratório de Nanotecnologia Farmacêutica e Sistemas de Liberação de Fármacos, Faculdade de Farmácia, Universidade Federal de Goiás – UFG, Goiânia, Goiás, Brazil
[3]Department of Chemistry, University of Vermont, Burlington, Vermont, USA.
[4]Bioneer:FARMA, Department of Pharmacy, University of Copenhagen, Copenhagen, Denmark

RESUMO

Neste estudo, descreve-se um método para determinar a capacidade de carga em monocamada (MLC) dos fármacos naproxeno e ibuprofeno, ambos com alta tendência de recristalização, em sílica mesoporosa (MS), um transportador bem conhecido que é capaz de estabilizar a forma amorfa de um fármaco. A estabilização tem sido sugerida como sendo devida à adsorção direta das moléculas do fármaco na superfície MS, isto é, a monocamada do fármaco. Além disso, o fármaco que não está em contato direto com a superfície da MS pode preencher os poros até sua capacidade de preenchimento de poros (PFC) e é potencialmente estabilizada pelo confinamento devido ao tamanho do poro ser menor que um núcleo de cristal. Para fármacos com alta tendência de recristalização, qualquer fármaco fora dos poros cristaliza devido à sua baixa estabilidade física. A monocamada do fármaco não contribui para a temperatura de transição vítrea (T_g) no DSC, no entanto, o fármaco amorfo confinado acima de MLC tem uma T_g e a variação da capacidade calorífica (ΔC_p) sobre a T_g aumenta com uma fração crescente de fármaco amorfo confinado. Assim, vários valores de carga de fármaco acima da MLC foram investigados para a presença de uma T_g e ΔC_p utilizando calorimetria exploratória diferencial (DSC). Uma correlação linear entre a quantidade de fármaco amorfo confinado e sua ΔC_p foi identificada para as misturas entre o MLC e o PFC. Por extrapolação subsequente para zero ΔC_p, a MLC experimental poderia ser determinada. Usando a teoria do funcional da densidade teórica (DFT) e dinâmica molecular *ab initio* (AIMD), as energias de ligação para a monocamada sugerem que a monocamada é termodinamicamente mais favorável do que a forma cristalina, enquanto que a forma amorfa confinada é termodinamicamente menos favorável. Consequentemente, um estudo de estabilidade física mostrou que os fármacos amorfos confinados acima do MLC eram termodinamicamente instáveis e, consequentemente, fluindo para fora dos poros, a fim de cristalizar, enquanto a monocamada permaneceu fisicamente estável.

Palavras-Chave: Sílica mesoporosa; capacidade de carregamento; calorimetria exploratória diferencial (DSC); amorfo.

ABSTRACT

In this study, a method is described to determine the monolayer loading capacity (MLC) of the drugs naproxen and ibuprofen, both having high recrystallization tendencies, in mesoporous silica (MS), a well known carrier that is able to stabilize the amorphous form of a drug. The stabilization has been suggested to be due to direct adsorption of the drug molecules onto the MS surface, i.e. the drug monolayer. In addition, drug that is not in direct contact with MS surface can fill the pores up to its pore filling capacity (PFC) and is potentially stabilized by confinement due to the pore size being smaller than a crystal nuclei. For drugs with high recrystallization tendencies, any drug outside the pores crystallizes due to its poor physical stability. The drug monolayer does not contribute to the glass transition temperature (T_g) in the DSC, however, the confined amorphous drug above MLC has a T_g and the heat capacity (ΔC_p) over the T_g increases with an increasing fraction of confined amorphous drug. Hence, several drug loading values above the MLC were investigated towards the presence of a T_g and ΔC_p using differential scanning calorimetry (DSC). A linear correlation between the amount of confined amorphous drug and its ΔC_p was identified for the mixtures between the MLC and PFC. By subsequent extrapolation to zero ΔC_p the experimental MLC could be determined. Using theoretical density functional theory (DFT) and *ab initio* Molecular Dynamics (AIMD), the binding energies for the monolayer suggested that the monolayer in fact is thermodynamically more favorable than the crystalline form, whereas the confined amorphous form is thermodynamically less favorable. Consequently, a physical stability study showed that the confined amorphous drugs above the MLC were thermodynamically unstable and consequently flowing out of the pores in order to crystallize, whereas the monolayer remained physically stable.

Keywords: Mesoporous silica; loading capacity; differential scanning calorimetry (DSC); amorphous.

GRAPHICAL ABSTRACT

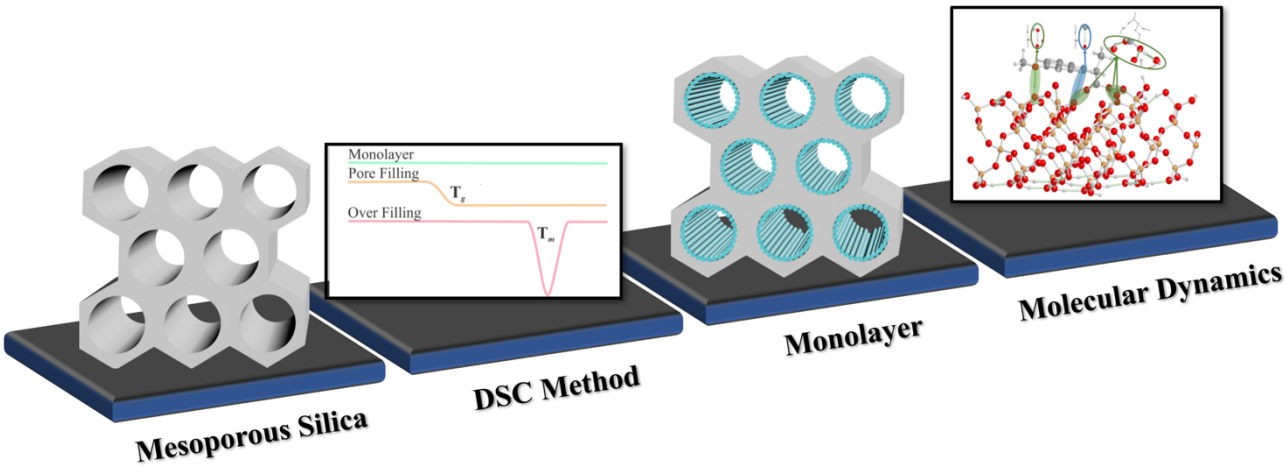

1. Introduction

Amorphous formulations are one of the most efficient ways of improving bioavailability in an era of drug discovery where a large percentage of new molecules have solubility-limited dissolution rates (Riikonen et al., 2018; Sayed et al., 2018). In this context, mesoporous silica (MS), having small pores (e.g., pore diameter between 2 and 50 nm) and large specific surface areas (e.g., often greater than 300 m^2/g) (Andersson et al., 2004), have received quite some attention, due to their ability to stabilize the amorphous form of a drug within their mesopores (Kumar et al., 2014; Laitinen et al., 2013; Rouquerol et al., 1994).

Inhibition of drug crystallization through adsorption to a MS has generally been explained by two responsible mechanisms: i) molecular interactions (e.g., hydrogen bonding) between functional groups of the drug molecules and the surface of the MS, and ii) confinement and spatial separation of the drug in the pores of MS, since the diameter of the mesopores is smaller than a critical crystalline nuclei of the drug (Azaïs et al., 2006; Rengarajan et al., 2008). With respect to i), the large MS surface area provides additional surface free energy, and it has been suggested that the adsorption of the drug in the amorphous form is actually thermodynamically favorable because of the lower free energy state than the crystalline drug (Andersson et al., 2004; Qian and Bogner, 2011, 2012). When all binding sites on the MS surface are occupied by drug molecules and an excess amount of drug is present in the system, it cannot be in direct contact with the MS surface anymore, and it will start to form additional layers on top of the initial drug monolayer (Genina et al., 2018; Hempel et al., 2018). In this case, the drug will start filling up the pores and this excess amount of amorphous drug may be stabilized by being physically restrained from crystallization, in the case of ii). Thus, the surface area and pore volume of a given MS influence the loading capacity of a given drug (Bavnhøj et al., 2019; Yani et al., 2016).

Accordingly, the loading capacity of a drug in a MS can be differentiated into two different classes, i.e. the drug in direct contact with the MS surface forming a drug monolayer and any excess drug filling up the pores. The former loading limit is dependent on the available surface area of the MS and is referred to as monolayer loading capacity (MLC). The latter is dependent on the pore volume of the MS and is referred to as pore filling capacity (PFC). Any further addition of drug will result in an overloading, i.e. drug being present outside of the pores (Bavnhøj et al., 2019; Choudhari et al., 2014).

The MLC can be determined experimentally by a differential scanning calorimetry (DSC) based method recently introduced by Hempel et al. (Hempel et al., 2018). This method is

based on deliberately overloading the MS with the drug upon melting and quenching (using drug loadings of 50-90 wt%), and subsequently determining the heat capacity change (ΔC_p) over the glass transition temperature (T_g) of the excess drug (i.e. excess to the monolayer) upon reheating. Since the monolayer is not contributing to the T_g signal in the DSC (Shen et al., 2010), the MLC can be obtained by extrapolating the ΔC_p values for the different drug loadings to zero (x-intercept). Since the method relies on the presence of an excess amorphous phase providing a T_g signal, it works well for drugs with good or medium glass forming ability (GFA). Generally, drugs can be classified into three classes of GFA according to their tendency to crystallize from the undercooled melt (Baird et al., 2010), i.e. based on the presence/absence of observable crystallization during a heat-cool-heat cycle using DSC. Briefly, class I drugs are classified as poor glass formers and crystallize upon cooling of the melt, class II are medium glass formers that do not crystallize upon cooling from the melt but upon reheating above their T_g and class III are good glass formers that neither crystallize upon cooling and reheating (Avramov et al., 2003). In other words, the approach of Hempel et al. (Hempel et al., 2018) is not feasible drugs with poor GFA since these drugs would crystallize outside the MS pores (at least above PFC), making a meaningful determination of the ΔC_p over the T_g of the excess drug at high drug loadings above 50 wt% not possible. On the other hand, it has been suggested that at concentrations above the MLC but below the PFC, the drug will be constrained within the pores and a crystallization cannot occur within the pores due to the pore diameter being smaller than a crystal nuclei (Qian and Bogner, 2012).

Consequently, the aim of this study was to investigate whether the MLC of a class I drug with poor GFA, namely naproxen, can experimentally be determined by extending the drug-MS ratios to lower drug loadings to cover the region between MLC and PFC. Furthermore, the impact of different degrees of drug loadings, i.e. monolayer, pore filling and overfilling, on the physical stability of such a system was studied and compared to ibuprofen, a drug with good GFA (class III). Lastly, the impact of drug loading upon storage below and above the T_g was investigated, in particular with a focus on the amorphous (in)stability of the confined drug above MLC but below PFC, both for poor and good glass formers.

2. Methods and Materials

2.1. Materials

Naproxen (NAP; M_w = 230.26 g/mol, minimal projection area 34.77 Å^2, maximal projection area 72.19 Å^2, molecular density 1.081 g/cm^3) and ibuprofen (IBU; M_w = 206.28 g/mol, minimal projection area 35.44 Å^2, maximal projection area 64.57 Å^2, molecular density 0.974 g/cm^3) were purchased from Fagron (Barsbüttel, Germany). Syloid® 72 FP (SYL; average pore diameter 10 nm, pore volume 1.20 cm^3/g, surface area 350 m^2/g) was received as a generous gift from Grace GmbH (Worms, Germany). All chemicals were used as received.

2.2. Experimental MLC determination

Based on a method proposed by Hempel et al. (Hempel et al., 2018), the MLC was determined from physical mixtures of the crystalline drugs with SYL. Physical mixtures of drug and SYL (15-100 wt% drug for IBU and 10-100 wt% drug for NAP) were prepared by weighing in a total of 200 mg of the material followed by gentle mixing using a mortar and pestle. The mixing procedure was repeated three times in order to ensure proper mixing before the powder was collected and stored in an airtight container at room temperature until use. The thermal properties of the samples were analyzed using a Discovery DSC from TA Instruments (New Castle, DE, USA). The physical mixtures of the IBU samples (~5 mg) and NAP samples (~14 mg) were analyzed in Tzero aluminum pans with a perforated lid under 50 mL/min nitrogen gas purge. The T_g (midpoint) and the heat capacity change over the glass transition (ΔC_p) were determined using the TA Instruments TRIOS (version 4.1.1) software.

For the determination of the MLC of IBU in SYL, the physical mixtures were exposed to a heat-cool-heat cycle using standard DSC. The physical mixtures were first annealed at ~5 °C above the melting point (T_m) of the drug for 5 minutes to ensure complete fusion of the drug into the pores and then quench cooled at a ballistic rate (maximum cooling rate of the instrument) to -80 °C. The samples were subsequently heated at a rate of 20 °C/min to 30 °C above the T_m of the drug. Each experiment was conducted in duplicate.

For the determination of the MLC of NAP in SYL, the physical mixtures were exposed to a heat-cool-heat cycle using modulated DSC. The physical mixtures were first annealed at ~5 °C above the T_m of the drug for 5 minutes to ensure complete fusion of the drug into the pores and then cooled to -80 °C at 10 °C/min. Subsequently, a modulated temperature DSC was used to determine the T_g and ΔC_p (J/g °C) due to the higher sensitivity compared to

standard DSC. The samples were analyzed from -80 °C to 80 °C at a heating rate of 2 °C/min with an underlying modulated temperature amplitude of 1.0 °C and a period of 50 s. The T_g and ΔC_p were determined from the reversing heat flow signal. Each experiment was conducted in duplicate.

The MLC was determined by a linear fitting of ΔC_p as a function of drug loading in the physical mixtures. For IBU and NAP, the linear fitting was performed on the drug loadings from 30-100 (wt%) and 20-50 (wt%), respectively. The experimental MLC is then obtained from the x-intercept of the trendline. Furthermore, the prediction interval with the upper and lower limits based on a 95% confidence interval were determined considering each replicate of ΔC_p as individual data point.

2.3. Theoretical determination of the MLC and PFC

The theoretical MLC and PFC were based on a previous publication by Bavnhøj et al. (Bavnhøj et al., 2019). Briefly, the theoretical MLC is based on the minimum projected surface area of the drug molecules and was calculated from equation 1 and 2:

$$MLC_w = \frac{A_{MS} \cdot M_{w(drug)}}{A_{drug} \cdot N_A} \quad \text{Equation 1}$$

Where A_{MS} is the surface area of the respective MS (m^2/g), A_{drug} is the minimal or maximal projection (surface) area of the respective drug (m^2/molecule) estimated using MarvinSketch version 18.12 from ChemAxon (Budapest, Hungary), N_A is the Avogadro constant ($6.022 \cdot 10^{23}$ mol^{-1}) and $M_{w(drug)}$ is the molecular weight (g/mol) of the respective drug. Equation 1 calculates the MLC as w_{drug}/w_{MS} (MLC_w). The theoretical MLC as wt% of the entire formulation, i.e. $w_{drug}/(w_{drug}+w_{MS})$, was calculated using equation 2:

$$MLC_{wt\%} = \frac{MLC_w}{1+ MLC_w} * 100\% \quad \text{Equation 2}$$

The theoretical PFC was calculated based on the amorphous/molecular densities of the drugs and pore volume of the MS, according to the equation 3:

$$PFC = \frac{V_{MS\,pore} * \rho_{drug}}{1+ V_{MS\,pore} * \rho_{drug}} * 100 \quad \text{Equation 3}$$

Where $V_{MS\ pore}$ is the pore volume of the MS (cm^3/g) and ρ_{drug} is the molecular density of the drug estimated using MarvinSketch version 18.12 from ChemAxon (Budapest, Hungary). The PFC includes the drug in the monolayer as well as the excess drug confined by the pores.

2.4. Theoretical *ab initio* Molecular Dynamics (AIMD) and density functional theory (DFT) simulations

The CP2k software package was used for all AIMD simulations, which incorporated three-dimensional periodic boundary conditions (Hutter et al., 2014; VandeVondele et al., 2005). With the AIMD method, the atomic dynamics are allowed to evolve in time according to Newton's equations of motion (*i.e. F* = *ma*), with the distinction between classical molecular dynamics being that the forces in AIMD are recomputed using quantum-mechanical simulations at each discrete timestep in the simulation. Thus, the AIMD technique enables the inclusion of temperature, providing a meaningful description of the structures and dynamics of materials at a high-level of theoretical accuracy. The simulations made use of the Perdew-Burke-Ernzerhof (PBE) density functional (Perdew et al., 1996) coupled with the dispersion correction of Grimme (Grimme-D3) (Grimme et al., 2010; Grimme et al., 2011). The electronic wavefunctions were represented using the double-zeta DZVP basis set (VandeVondele and Hutter, 2007). Simulations were performed within the canonical ensemble (NVT), with the temperature maintained at 200 K using a Nose-Hoover chain thermostat (Martyna et al., 1992; Nosé, 1984, 2002). The initial model involved loading the porous void with drug molecules to a loading limit of 10% less than the crystallographic density of the respective solids. The surface functionalization was set to an average OH-distribution of approximately 4.5 OH nm^{-1} to be as similar to the physically used SYL surface as possible. The CRYSTAL17 (Dovesi et al., 2018) software package was used for static DFT simulations to represent a two-dimensional periodic surface (periodic along the x and y axes corresponding to an infinite surface slab) with a single API molecule in the simulation cell. In order to match the AIMD simulations, parameters were kept as similar as possible. The D3-corrected PBE functional was coupled with the def2-SVP (Weigend and Ahlrichs, 2005) basis set for all atoms. Optimizations were performed at an effective temperature of 0 K to extract the fundamentally stable binding geometry of the adsorbed molecules.

2.5. Physical stability study

Physical mixtures of drug and SYL (15-60 wt% drug in 5 wt% increments for IBU and 10-60 wt% drug in 5 wt% increments for NAP) were prepared as described above and subsequently molten in a UF55 oven from Memmert (Schwabach, Germany) at 5 °C above T_m of the respective drug for 5 min. Subsequently, the mixture was removed from the oven, quench cooled to room temperature and gently mixed using a mortar and pestle. The

procedure was repeated once more to ensure that the mixture was homogeneous and the solid-state characteristics of the powder samples were then analyzed using an X'Pert Pro diffractometer from PANalytical (Almelo, the Netherlands) using CuKα radiation (λ = 1.5406 Å) at 45 kV and 40 mA. The freshly prepared samples were analyzed directly after preparation and after storage for 4 weeks under ambient conditions and at -80°C in a closed container. Approximately 3 mg of sample was placed on aluminum plates and measured over the angular range of 5-30° 2θ at a scanning rate of 4° 2θ/min and resolution of 0.001° 2θ. Results were analyzed using the X'Pert Data Viewer (version 1.2) software.

3. Results and Discussion

As mentioned in the introduction, it has previously been shown that a DSC based method can be used to determine the MLC of a drug with medium and good GFA in MS (Hempel et al., 2018). IBU is such a good glass former, however, NAP is a poor glass former and recrystallizes quickly already in the quenching step during the DSC run (Baird et al., 2010; Blaabjerg et al., 2017). Hence, any excess NAP outside of the pores would crystallize, which makes a meaningful determination of the ΔC_p over the T_g of the excess drug at high drug loadings above 50 wt% not possible. However, since the drug at concentrations above the MLC but below the PFC will be constrained within the pores, a crystallization can in theory not occur within the pores due to the pore diameter being smaller than a crystal nuclei (Qian and Bogner, 2012). For this purpose, we have extended the drug-MS ratios to lower drug loadings to cover the region between MLC and PFC in this study, i.e. 15-100 wt% for IBU and 10-100 wt% for NAP. It is suggested that such an approach will potentially allow the determination of ΔC_p values also for compounds with poor GFA, such as NAP (at least for drug loadings between MLC and PFC), allowing for a determination of their MLC. In this case, the confined drug (pore filling) above the MLC would remain amorphous, resulting in a T_g and ΔC_p signal in the DSC, while the drug outside the MS pores would crystallize.

For IBU-SYL, the experimentally determined MLC at zero ΔC_p (x-intercept) was found to be 26.6 wt% with a prediction interval from 22.6 to 29.9 wt% (Figure - **1**), which was supported by the absence of a T_g at a drug load of 25 wt% or below, suggesting that all drug was present as a monolayer for these drug loadings. The theoretical MLC based on minimum and maximum projected surface area was calculated at 25.3 and 15.9 wt%, respectively. The close agreement of the experimental MLC and the theoretical MLC based on minimum projected surface area suggest that the IBU molecules adsorb densely to the MS surface,

i.e. occupying as little as surface area as possible. The theoretical PFC was calculated to be 53.9 wt%. Since IBU is a good glass former, the amorphous fraction of the drug from the pore filling (between MLC and PFC) and outside the pores (overfilling), both contribute to the ΔC_p, resulting in a linear increase in the ΔC_p values over the entire sample set above MLC.

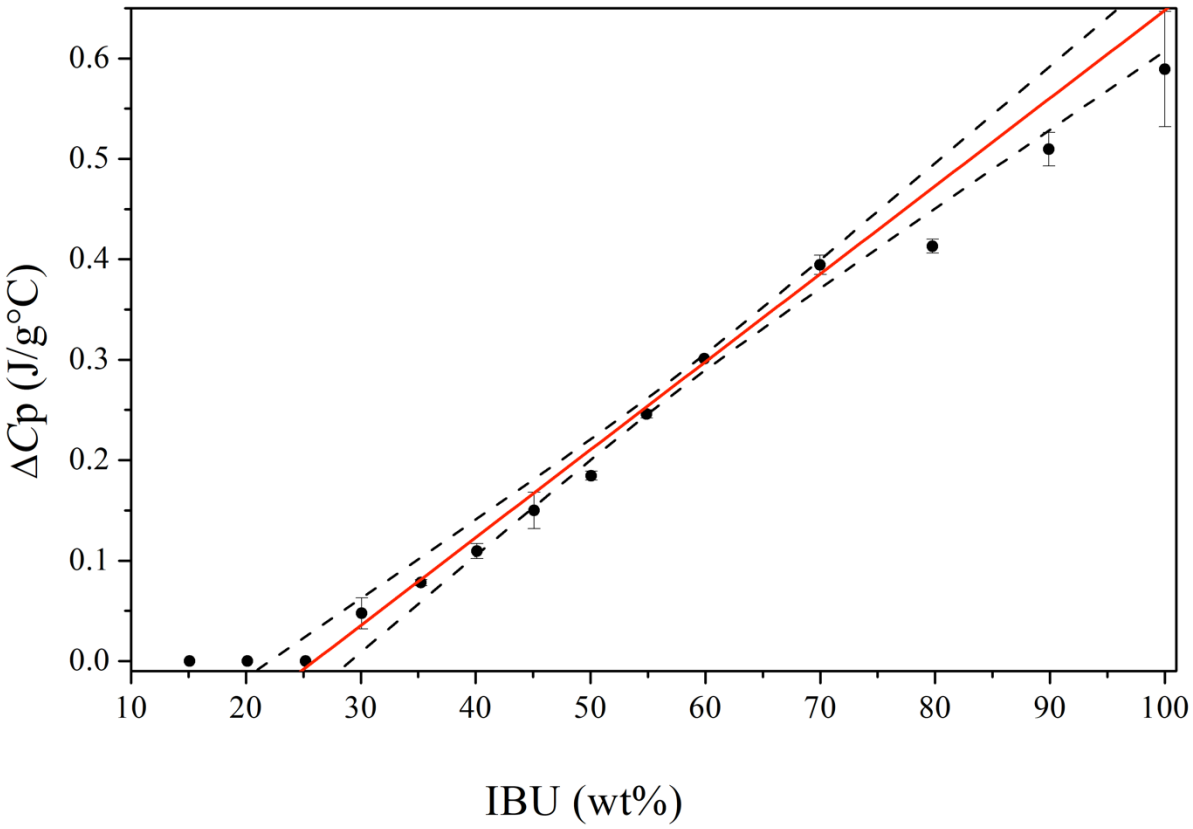

Figure - 1: Experimentally obtained ΔC_p (J/g °C) values over T_g as a function of IBU (wt%) loaded on SYL as well as their linear extrapolation between 30 and 100 wt% in SYL, r^2 = 0.99. The 95% confidence interval is represented in the dashed lines.

For NAP-SYL, a ΔC_p value may in theory only be obtained for the amorphous drug fraction between MLC and PFC. In other words, it is expected that a ΔC_p value is detectable for any drug loading above MLC and below PFC. For those drug loadings above PFC, one would assume that the pores are completely filled with drug and additionally excess drug would be on the outside of the pores. Since NAP is a poor glass former, the drug outside the pores should crystallize, however, the drug constrained inside the pores could be amorphous and should be detectable. From Figure 2, it can be seen that below 20 wt% drug loading, no T_gs or ΔC_p values were obtained. For the samples with drug loadings between 20 and 60 wt%, indeed ΔC_p values could be identified and a linear increase of ΔC_p was obtained for the samples between 20 and 50 wt%, suggesting that amorphous NAP is indeed filling up the pores. When using the ΔC_p values for the samples between 20 and 50 wt%, an experimental

MLC at zero ΔC_p (x-intercept) was determined at 20.6 wt% with a prediction interval from 19.1 to 22.2 wt%. The theoretical MLC based on the minimum and maximum projected surface area for NAP were calculated as 27.8 and 15.6 wt%, respectively. Since the experimental MLC lies in between these two theoretical MLC values, it is suggested that the NAP molecules are occupying a larger surface area on the MS surface than calculated from the minimal projected surface area of NAP. Hence, in contrast to IBU, the NAP molecules do not adsorb as densely to the MS surface.

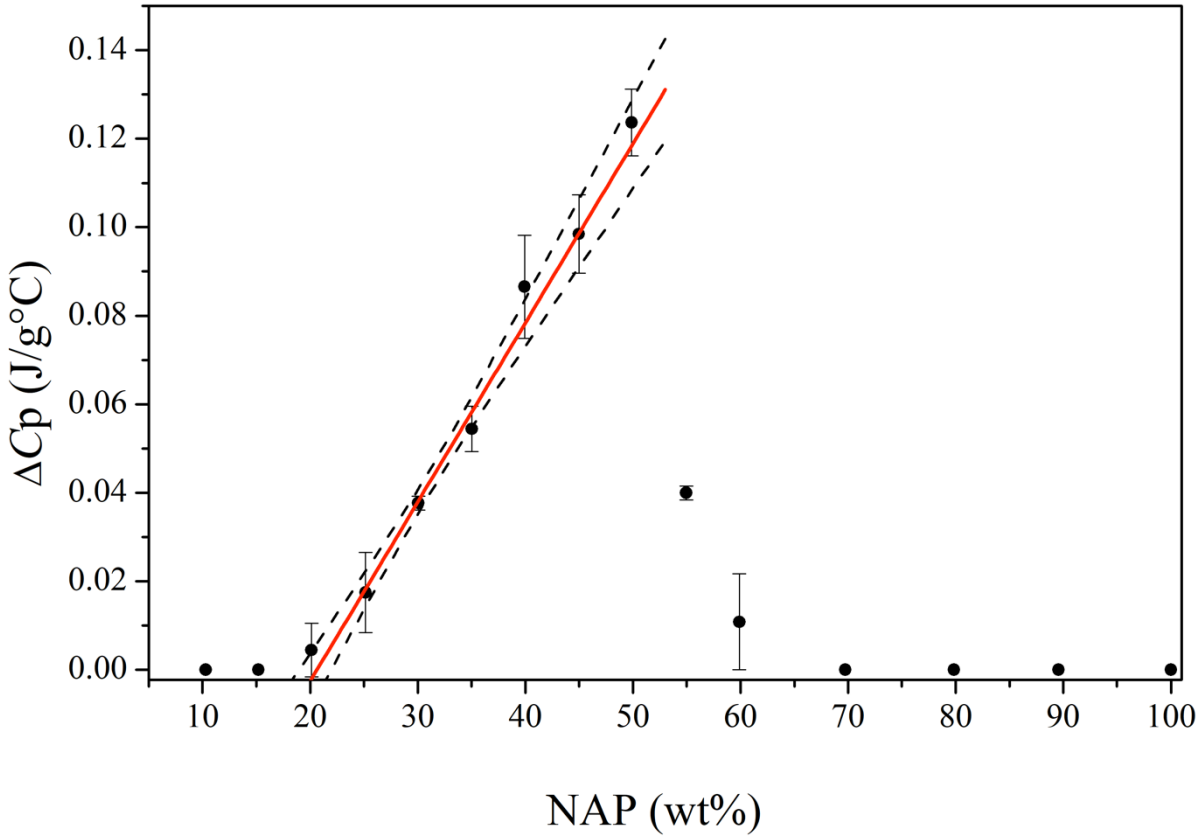

Figure - 2: Experimentally obtained ΔC_p (J/g °C) values over Tg as a function of NAP (wt%) loaded on SYL as well as their linear extrapolation between 20 and 50 wt% in SYL, r^2 = 0.99. The 95% confidence interval is represented in the dashed lines.

Interestingly, the ΔC_p decreases with increasing NAP load (55 and 60 wt%) and then disappears for samples with drug loadings >70 wt%, suggesting that a part or all of the drug above MLC is crystallizing during the timeframe of the heat-cool-heat cycle in the DSC. In other words, this suggests that the excess drug (above MLC and below PFC) must rather flow out of the pores and crystallize outside of the pores than remaining confined within the pores. To understand this finding one needs to consider that i) only the monolayer drug is thermodynamically favorable compared to the crystalline drug (Qian and Bogner, 2012), ii) the confined drug not in the monolayer is purely prevented from crystallization by the pore size being smaller than a crystal nuclei (Qian and Bogner, 2012) and iii) the crystalline form

of the drug is thermodynamically more stable than the pure amorphous form (Qian and Bogner, 2011) also when confined within the pores (above MLC and below PFC). The findings suggest that if there is a possibility for the drug to crystallize (drug loading above PFC), it will crystallize quickly and any drug confined in the pores will flow out of the pores and also crystallize. One may think of the drug crystallizing outside of the pores acting as seed for further crystal growth, dragging the confined drug out of the pores since it would be able to change into a thermodynamically more favorable form. This is further supported by the low T_g of NAP, its poor GFA and its inherent high tendency to crystallize. For the samples with a drug loading of 70 wt% and above, this effect becomes so pronounced that all of the confined drug (except the monolayer drug) recrystallizes on the outside of the pores. For the samples containing 55 and 60 wt% drug, i.e. close to the PFC, this effect is only partial, and some amorphous drug can remain within the pores during the timeframe of the DSC run, hence, contributing to the T_g and ΔC_p signal in the DSC measurement.

In order to investigate the underlying energetics driving intermolecular drug-surface and amorphous drug-drug interactions, the binding energies of the various phases of the drugs were determined using solid-state DFT and AIMD simulations. For these simulations, two distinct models were generated and used, the first was a physical representation of the studied systems, comprising of a MS model, which was loaded with drug to a density (within the pore) of 10% less than the crystallographic density of the respective drug molecules. The second was a two-dimensional periodic simulation where a drug molecule was fully docked to the surface and allowed to relax in order to strictly determine the potential of the drug-monolayer binding interaction. The results of the two analyses for the adsorbed drug were very similar; the ‘physical’ model yields a relative drug-monolayer binding energy (compared to the crystalline drug binding energy) for IBU of -32.93 kJ mol^{-1}, while the drug-surface 2D model yields a value of -31.98 kJ mol^{-1}. The results of the 2D monolayer model are provided in Table 1 for both studied materials.

Table - 1: Binding energies and relative binding energies (∆E, compared to the crystalline binding energies) for NAP and IBU for the monolayer and amorphous phases of the two materials calculated from DFT simulations. All energies are in units of kJ mol^{-1} $molecule^{-1}$.

	Naproxen 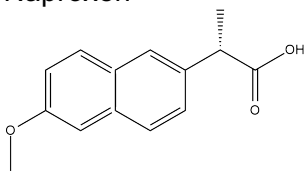		Ibuprofen 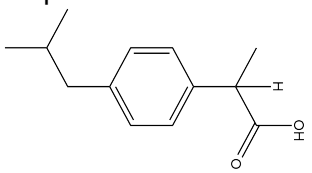	
	Binding Energy	∆E	Binding Energy	∆E
Crystal	-235.28	-	-136.61	-
Monolayer	-307.90	-72.62	-169.54	-32.93
Amorphous	-167.14	+68.14	-41.79	+94.82

In both cases, the energetics point to the previously observed effect that the drug-monolayer interaction is more stable than in the corresponding crystalline form. Moreover, a fully amorphous model yields net positive relative binding energies for the two materials, in line with experimental expectations of the instability of the amorphous form and the preference for crystallization. The simulations accurately confirm that monolayer adsorbed drugs are more stable than the corresponding crystalline counterparts, and a structural investigation provides some rationale for this effect. It is important to note that the binding energy is defined as:

$$E_{binding} = E_{drug+surface} - \left(E_{drug} + E_{surface}\right) \qquad \text{Equation 4}$$

such that the binding energy is not directly related to either the individual structures of the surface or drug on its own. However, the lack of a fully periodic and well-ordered crystalline structure indirectly improves the binding energy of the drug-surface interaction by enabling the drug molecules to adopt a conformation that maximizes each individual interaction while at the same time allowing for conformational freedom to adopt a more optimal molecular structure. For example, in the NAP system, the crystalline interactions are dominated by hydrogen bonding interactions between the carboxyl groups, with some weak London dispersion forces between the hydrophobic core of the molecule, and the individual molecular conformations are relatively stained in order to maximize and balance intermolecular interactions with the conformational strain. However, in the NAP-SYL system, the lack of well-defined order and the nature of the MS surface allows the NAP conformation more freedom to adopt a favorable structure, with the surface subsequently adapting its geometry to accommodate the NAP molecules. For example, hydrogen bonding interactions are maximized in the adsorbed system, including the carboxylic acid and ether groups of

NAP, as there are more hydrogen bond donors on the MS surface than what are present in crystalline NAP (Figure 3). Furthermore, non-classical interactions are present, for example weak C***H-O hydrogen bonds, which do not provide enough of an energetic stabilization to be observed in crystalline NAP, and are readily present due to the overabundance of hydrogen bond donors on the surface. Additionally, the increased dispersion forces due to the highly polar surface, and the more optimal binding geometry of the drugs all combine to drive the binding of the drugs and increased stability of the drug-SYL materials.

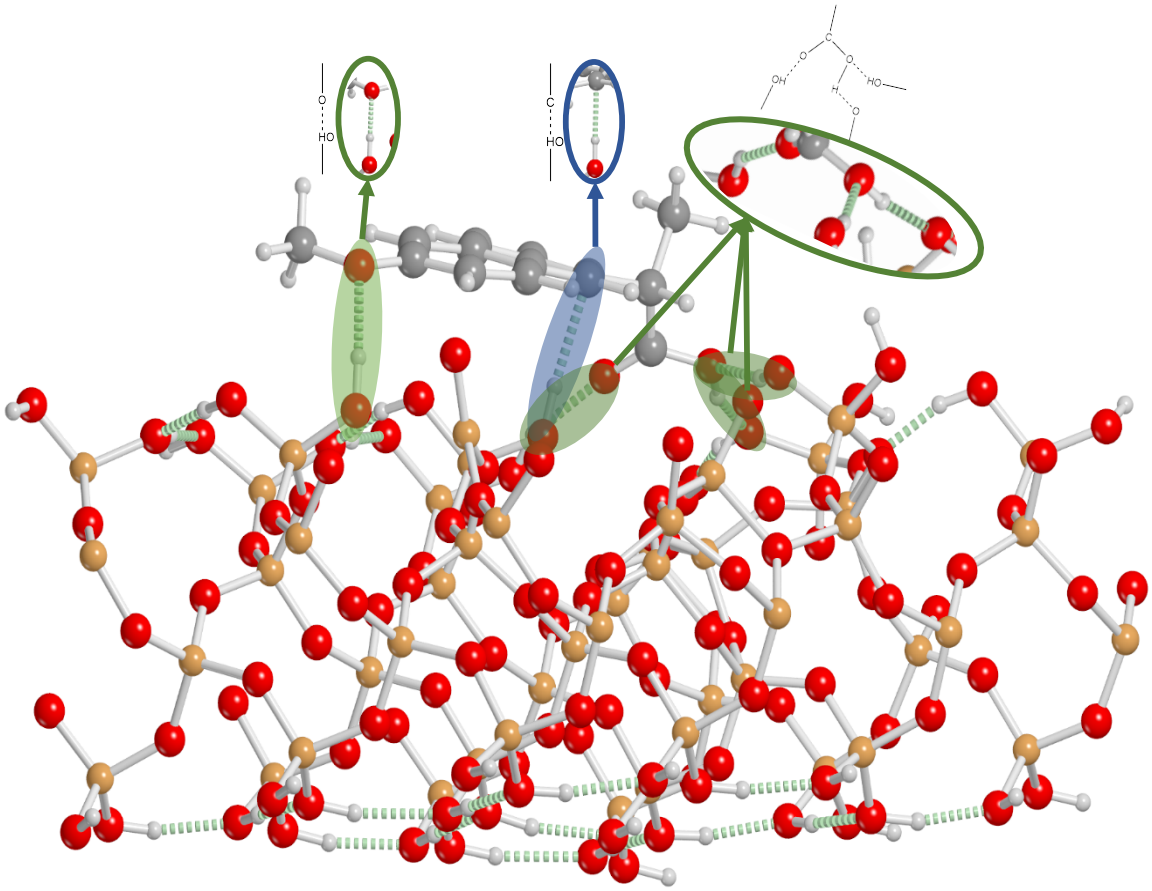

Figure - 3: Model of the NAP-SYL surface showing traditional hydrogen bonding (green circles), and non-traditional C***H-O hydrogen bond formation (blue circle).

Finally, the simulations provide a rationale for the theoretical determination of the MLC for NAP previously described. As described above, the experimental MLC value for NAP falls in between the predicted values using the minimum and maximum projected surface areas of the individual molecules. Since the projected surface areas of NAP in these calculations do not account for how the molecules bind to the surface, this observation is readily explained by investigating the binding geometry of the drug molecules with respect to the

surface (Figure 3). Due to the maximized hydrogen bonding of the NAP molecules on the MS surface, the drug molecules are not oriented completely orthogonal to the SYL surface, but are slightly rotated. Considering the hydrogen bonding pattern of the NAP molecules, the DFT calculations allow to project a minimum and maximum surface area of 51.33 $Å^2$ and 65.37 $Å^2$. These corrected values were used in equations 1 and 2, and the theoretical MLC based on the minimum and maximum projected surface area for NAP are now 20.7 and 17.0 wt%, respectively. The close agreement of the experimental MLC (20.6 wt%) to the corrected theoretical MLC based on minimum projected surface area suggest that the NAP molecules indeed are fulfilling their maximum hydrogen bonding possibilities and consequently adsorb densely to the MS surface, i.e. occupying as little as surface area as possible.

In order to investigate the effect of drug loading on the physical stability, drug-SYL systems were prepared with drug loadings between 15-60 wt% for IBU and 10-60 wt% for NAP and analyzed using XRPD directly after preparation and after 4 weeks of storage at -80°C (below the T_g of the drugs) or under ambient conditions (above the T_g of the drugs). It was assumed that below the MLC, these systems would be thermodynamically stable and between the MLC and PFC, they would be sterically stabilized (physically stable) by the drug confinement. Storing the samples below and above their respective T_g would potentially further contribute to stabilization or destabilization of the confined amorphous drug, since above the T_g, the drugs may possess enough mobility to leak from the pores and crystallize on the outside of the pores. The pure amorphous IBU and NAP are known to be highly unstable and rapidly recrystallize after preparation, mainly because of their very low T_g of -45 °C and 5 °C, respectively (Blaabjerg et al., 2017).

The XRPD diffractograms for the freshly prepared IBU-SYL systems showed that all drug loadings except 60 wt% were fully amorphous systems (Figure 4). This finding confirms that IBU was completely loaded into the pores of SYL up to 55 wt%. Since the theoretical PFC for IBU was found to be 53.9 wt%, it was expected that some crystallinity was observed for the 60 wt% due to being above the PFC and the poor physical stability of the pure amorphous IBU. The experimental MLC was 26.6 wt%, suggesting that samples with drug loadings ≤25 wt% are below the MLC and samples between 30 and 55 wt% represent those with pore filling. Upon storage, it was observed that the drug loadings below the MLC remained amorphous regardless of the storage conditions. However, for the samples between 30 and 55 wt% drug loading, Bragg peaks characteristic of crystalline IBU could be identified depending on the storage conditions. When storing the samples above the T_g of

IBU (ambient conditions) all samples above the MLC recrystallized, whereas when storing below its T_g (at -80°C) only the two samples close to the PFC, i.e. 50 and 55 (wt%), showed recrystallization (Figure 4).

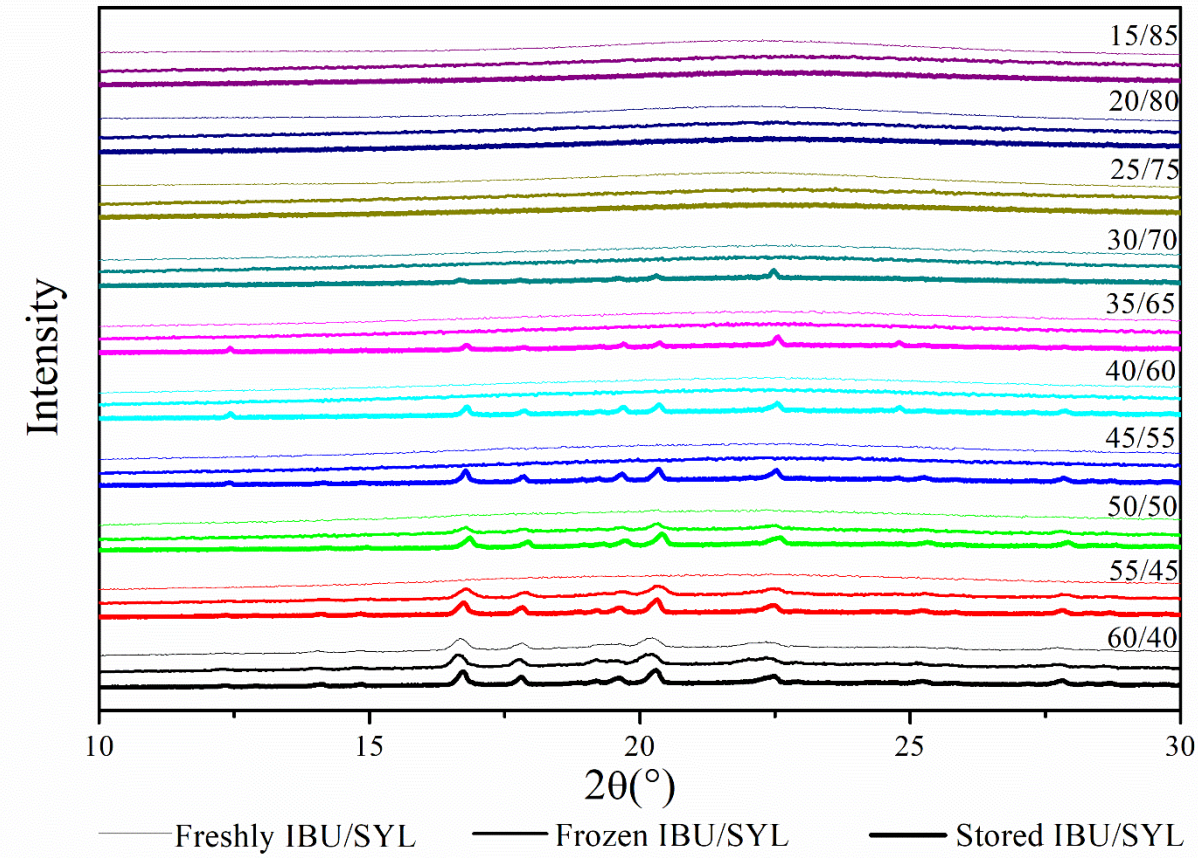

Figure - 4: X- rays diffractograms of IBU/SYL systems with different drug loadings freshly prepared (top diffractogram within a given drug loading XRPD set) and stored for 4 weeks either at -80 °C (middle diffractogram within a given drug loading XRPD set) or under ambient conditions (bottom diffractogram within a given drug loading XRPD set).

The XRPD patterns for the freshly prepared NAP-SYL systems show that fully amorphous systems can be prepared up to 35 wt% drug loading (Figure 5). This suggests that amorphous NAP-SYL systems can be prepared above the experimental MLC (20.6 wt%) but not entirely up to its PFC (56.5 wt%) as seen for IBU. Furthermore, given the linear increase of the ΔC_p up to a drug loading of 50 wt% in the DSC (see above), one may have expected that it would be possible to prepare fully amorphous samples also up to a drug loading of 50 wt%. However, the findings indicate that at loadings above 35 wt%, at least parts of the confined drug leaked out of the pores and crystallized as suggested above. Due to the longer experimental time frame from preparation to XRPD analysis compared to the rather short heat-cool-heat cycle during the DSC runs, this becomes now even more visible

also for drug loadings further away from the PFC (i.e. the samples with 40 to 55 wt% drug). Upon storage, this phenomenon becomes even more pronounced, since now all samples between MLC and PFC (25 to 55 wt%) showed recrystallization when stored above the T_g of NAP (ambient conditions) (Figure 5). Interestingly, also the sample with 20 wt% drug loading showed some recrystallization when stored under ambient conditions, suggesting that the MLC lies below 20 wt%. This was unexpected since the experimental MLC was 20.6 wt%, however, the 95% confidence interval (19.1 - 22.2 wt%) indicates that the experimental MLC may indeed be below 20 wt%. An MLC below 20 wt% is also supported by the finding that the storage time (4 weeks) did not cause recrystallization of the 10 and 15 (wt%) NAP samples regardless of the storage conditions. When stored below the T_g of NAP (at -80°C), the samples were generally more stable as expected, however, the sample with a drug loading of 35 wt% recrystallized (Figure 5), indicating that a confinement of the drug (loadings between MLC and PFC) can prolong stability below T_g for some time but cannot prevent crystallization over time.

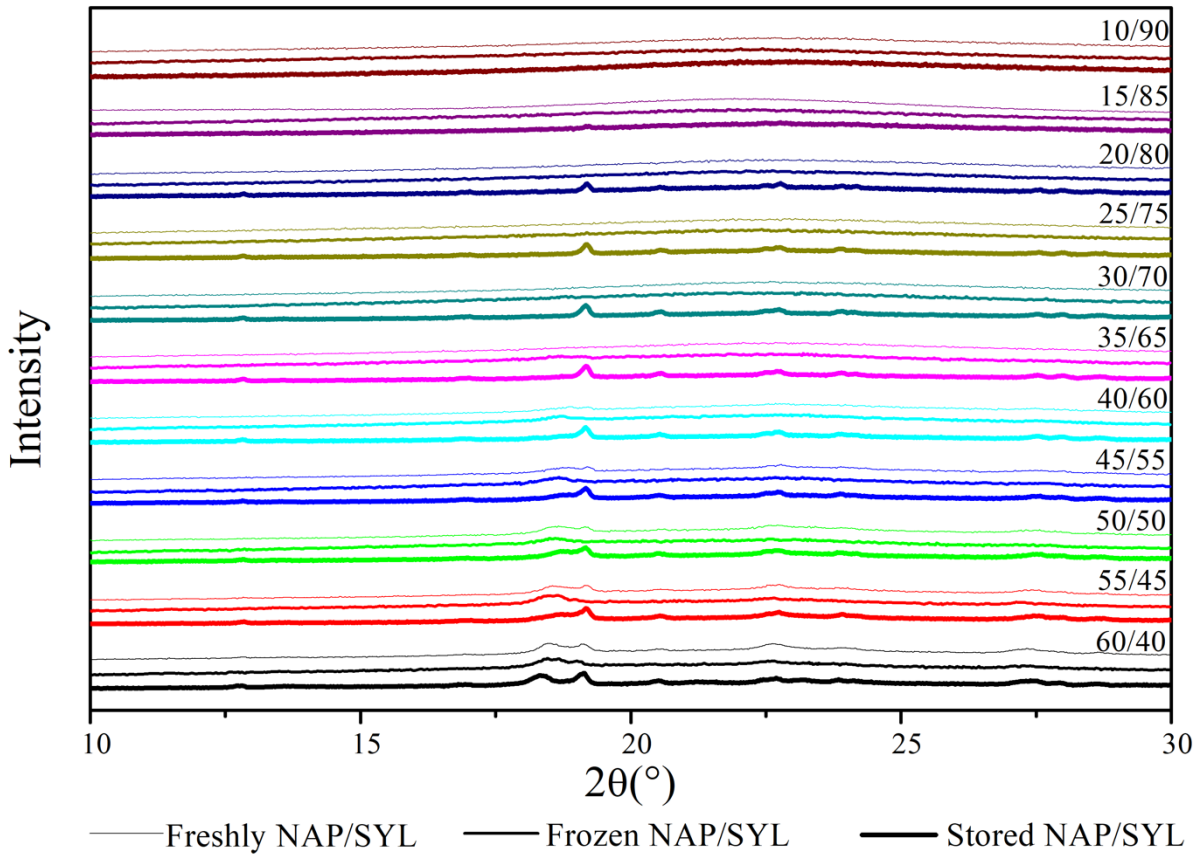

Figure - 5: X- rays diffractograms of NAP/SYL systems with different drug loadings freshly prepared (top diffractogram within a given drug loading XRPD set) and stored for 4 weeks either at -80 °C (middle diffractogram within a given drug loading XRPD set) or under ambient conditions (bottom diffractogram within a given drug loading XRPD set).

4. Conclusion

It was shown that the MLC can be experimentally determined also for drugs that are poor glass formers under the condition that the confined drug above MLC and below PFC remains amorphous in the heat-cool-heat cycle applied in the DSC run. Using solid-state DFT and AIMD simulations, it was confirmed that the drug-monolayer binding energies are more favorable than those found in the crystalline state of the drugs, which was reflected in the physical stability of the samples below the MLC regardless of being stored below or above the T_g of the drugs. On the other hand, above the MLC and below the PFC, the confined amorphous drug is thermodynamically unstable and consequently resulted in recrystallization of during storage. Nevertheless, the confinement of the amorphous drug did prolong its physical stability compared to the pure amorphous drug, which in turn allowed the experimental determination of the MLC of the poor glass former NAP.

Acknowledgments

This work was financially supported by the Brazilian research funding agencies, *Coordenação de Aperfeiçoamento de Pessoal de Nível Superior* (CAPES), Ministry of Education, Brasília-Brazil (88887.146238/2017-00), and *Fundação de Apoio à Pesquisa do Estado de Goiás* (FAPEG), Goiânia-Brazil (88887.178498/2018-00).

References

Andersson, J., Rosenholm, J., Areva, S., Lindén, M., 2004. Influences of material characteristics on ibuprofen drug loading and release profiles from ordered micro-and mesoporous silica matrices. Chemistry of Materials. 16, 4160-4167.

Avramov, I., Zanotto, E., Prado, M., 2003. Glass-forming ability versus stability of silicate glasses. II. Theoretical demonstration. Journal of non-crystalline solids. 320, 9-20.

Azaïs, T., Tourné-Péteilh, C., Aussenac, F., Baccile, N., Coelho, C., Devoisselle, J.-M., Babonneau, F., 2006. Solid-state NMR study of ibuprofen confined in MCM-41 material. Chemistry of Materials. 18, 6382-6390.

Baird, J.A., Van Eerdenbrugh, B., Taylor, L.S., 2010. A classification system to assess the crystallization tendency of organic molecules from undercooled melts. Journal of Pharmaceutical Sciences. 99, 3787-3806.

Bavnhøj, C.G., Knopp, M.M., Madsen, C.M., Löbmann, K., 2019. The role interplay between mesoporous silica pore volume and surface area and their effect on drug loading capacity.

International Journal of Pharmaceutics: X. 100008. https://doi.org/10.1016/j.ijpx.2019.100008.

Blaabjerg, L.I., Lindenberg, E., Rades, T., Grohganz, H., Löbmann, K., 2017. Influence of preparation pathway on the glass forming ability. International Journal of Pharmaceutics. 521, 232-238.

Choudhari, Y., Hoefer, H., Libanati, C., Monsuur, F., McCarthy, W., 2014. Mesoporous silica drug delivery systems, Amorphous Solid Dispersions. Springer, pp. 665-693.

Dovesi, R., Erba, A., Orlando, R., Zicovich-Wilson, C.M., Civalleri, B., Maschio, L., Rérat, M., Casassa, S., Baima, J., Salustro, S., 2018. Quantum-mechanical condensed matter simulations with CRYSTAL. WIREs Comput Mol Sci. 8:e1360, e1360. https://doi.org/10.1002/wcms.1360.

Genina, N., Hadi, B., Löbmann, K., 2018. Hot Melt Extrusion as Solvent-Free Technique for a Continuous Manufacturing of Drug-Loaded Mesoporous Silica. Journal of Pharmaceutical Sciences. 107, 149-155.

Grimme, S., Antony, J., Ehrlich, S., Krieg, H., 2010. A consistent and accurate ab initio parametrization of density functional dispersion correction (DFT-D) for the 94 elements H-Pu. The Journal of Chemical Physics. 132, 154104. https://doi.org/10.1063/1.3382344.

Grimme, S., Ehrlich, S., Goerigk, L., 2011. Effect of the damping function in dispersion corrected density functional theory. Journal of computational chemistry. 32, 1456-1465.

Hempel, N.-J., Brede, K., Olesen, N.E., Genina, N., Knopp, M.M., Löbmann, K., 2018. A fast and reliable DSC-based method to determine the monomolecular loading capacity of drugs with good glass-forming ability in mesoporous silica. International journal of pharmaceutics. 544, 153-157.

Hutter, J., Iannuzzi, M., Schiffmann, F., VandeVondele, J.J.W.I.R.C.M.S., 2014. cp2k: atomistic simulations of condensed matter systems. WIREs Comput Mol Sci. 4, 15-25. doi:10.1002/wcms.1159.

Kumar, D., Chirravuri, S.S., Shastri, N.R., 2014. Impact of surface area of silica particles on dissolution rate and oral bioavailability of poorly water soluble drugs: a case study with aceclofenac. International Journal of Pharmaceutics: X. 461, 459-468. https://doi.org/10.1016/j.ijpharm.2013.12.017.

Laitinen, R., Löbmann, K., Strachan, C.J., Grohganz, H., Rades, T., 2013. Emerging trends in the stabilization of amorphous drugs. Internacional Journal of Pharmaceutics. 453, 65-79. https://doi.org/10.1016/j.ijpharm.2012.04.066.

Martyna, G.J., Klein, M.L., Tuckerman, M., 1992. Nosé–Hoover chains: The canonical ensemble via continuous dynamics. The Journal of Chemical Physics. 97, 2635-2643. https://doi.org/10.1063/1.463940.

Nosé, S., 1984. A unified formulation of the constant temperature molecular dynamics methods. The Journal of Chemical Physics. 81, 511-519. https://doi.org/10.1063/1.447334.

Nosé, S., 2002. A molecular dynamics method for simulations in the canonical ensemble. Molecular Physics. 100, 191-198. DOI: 10.1080/00268978400101201.

Perdew, J.P., Burke, K., Ernzerhof, M., 1996. Generalized gradient approximation made simple. Physical Review Letters. 77, 3865. https://doi.org/10.1103/PhysRevLett.77.3865.

Qian, K.K., Bogner, R.H., 2011. Spontaneous crystalline-to-amorphous phase transformation of organic or medicinal compounds in the presence of porous media, part 1: thermodynamics of spontaneous amorphization. Journal of Pharmaceutical Sciences. 100, 2801-2815. 10.1002/jps.22519.

Qian, K.K., Bogner, R.H., 2012. Application of mesoporous silicon dioxide and silicate in oral amorphous drug delivery systems. Journal of Pharmaceutical Sciences. 101, 444-463. 10.1002/jps.22779.

Rengarajan, G., Enke, D., Steinhart, M., Beiner, M., 2008. Stabilization of the amorphous state of pharmaceuticals in nanopores. Journal of Materials Chemistry. 18, 2537-2539.

Riikonen, J., Xu, W., Lehto, V.-P., 2018. Mesoporous systems for poorly soluble drugs–recent trends. International journal of pharmaceutics. 536, 178-186.

Rouquerol, J., Avnir, D., Fairbridge, C., Everett, D., Haynes, J., Pernicone, N., Ramsay, J., Sing, K., Unger, K., 1994. Recommendations for the characterization of porous solids (Technical Report). Pure Applied Chemistry. 66, 1739-1758. https://doi.org/10.1351/pac199466081739.

Sayed, E., Karavasili, C., Ruparelia, K., Haj-Ahmad, R., Charalambopoulou, G., Steriotis, T., Giasafaki, D., Cox, P., Singh, N., Giassafaki, L.-P.N., 2018. Electrosprayed mesoporous particles for improved aqueous solubility of a poorly water soluble anticancer agent: in vitro and ex vivo evaluation. Journal of Controlled Release. 278, 142-155.

Shen, S.C., Ng, W.K., Chia, L., Dong, Y.C., Tan, R.B., 2010. Stabilized amorphous state of ibuprofen by co-spray drying with mesoporous SBA-15 to enhance dissolution properties. Journal of Pharmaceutical Sciences. 99, 1997-2007.

VandeVondele, J., Hutter, J., 2007. Gaussian basis sets for accurate calculations on molecular systems in gas and condensed phases. The Journal of Chemical Physics. 127, 114105. https://doi.org/10.1063/1.2770708.

VandeVondele, J., Krack, M., Mohamed, F., Parrinello, M., Chassaing, T., Hutter, J., 2005. Quickstep: Fast and accurate density functional calculations using a mixed Gaussian and plane waves approach. Computer Physics Communications. 167, 103-128. https://doi.org/10.1016/j.cpc.2004.12.014.

Weigend, F., Ahlrichs, R., 2005. Balanced basis sets of split valence, triple zeta valence and quadruple zeta valence quality for H to Rn: Design and assessment of accuracy. Physical Chemistry Chemical Physics. 7, 3297-3305.

Yani, Y., Chow, P.S., Tan, R.B., 2016. Pore size effect on the stabilization of amorphous drug in a mesoporous material: Insights from molecular simulation. Microporous and Mesoporous Materials. 221, 117-122.

CONSIDERAÇÕES FINAIS

O desenvolvimento de novos sistemas de liberação torna-se fundamental para a produção de formulações mais eficazes e com melhor desempenho terapêutico.

O entendimento adequado do conceito de muco e das propriedades e mecanismos da mucoadesão foi estruturado na forma de uma revisão de literatura apresentada no capítulo 1. O estudo e a sistematização das características do muco e de mucoadesão, além dos mecanismos que estão envolvidos na mucoadesão e as formulações mucoadesivas já disponíveis, foram determinantes para a elaboração e desenvolvimento da nova formulação apresentada no segundo capítulo.

Com o conhecimento das propriedades e características adequadas dos polímeros foi possível desenvolver e obter uma nova formulação mucoadesiva e gelificante *in situ* para o tratamento de mucosas inflamadas do trato gastrointestinal. No segundo capítulo, foi descrita a eficácia de uma dispersão de Pluronic® F127 carregada com budesonida em reduzir consideravelmente a inflamação no trato gastrointestinal após mucosite induzida por um agente quimioterápico em camundongos. Este efeito foi demonstrado com base em uma discussão sólida, juntamente com uma caracterização completa da formulação, incluindo mucoadesão *in vitro* e *in vivo*, comportamento termorreversível, estrutura micelar e solubilização do fármaco. O aspecto inovador deste trabalho é baseado na completa caracterização físico - química das dispersões, bem como nas propriedades mucoadesivas *in vivo* e *ex vivo* da formulação, juntamente com a retenção prolongada da formulação na mucosa, do esôfago para o intestino delgado, como demonstrado pela resolução da mucosite induzida. A formulação proposta pode ser aplicada como uma plataforma potencial para o tratamento de diversas patologias inflamatórias do trato gastrointestinal.

A ideia aplicada no desenvolvimento da dispersão pode ser utilizada para a incorporação de fármacos pouco solúveis, devido às propriedades mucoadesivas e solubilização do fármaco dentro das micelas poliméricas. Estes resultados contribuem para o desenvolvimento de formulações mais eficazes para o tratamento de doenças causadas no trato gastrointestinal. Ainda foi apresentada a patente publicada desta formulação mucoadesiva e gelificante *in situ* como produto estabelecido da parceria indústria-universidade na aplicação de tecnologia farmacêutica para o desenvolvimento de novos sistemas de liberação de fármacos e, posteriormente novos medicamentos (anexo 2).

No terceiro capítulo foi apresentado um trabalhado no campo de partículas de sílica mesoporosas carregadas com fármacos com o objetivo geral de estabilizar a forma amorfa de um determinado fármaco pouco solúvel, a fim de aumentar sua solubilidade. Em particular, neste trabalho foi desenvolvido um método termoanalítico para determinar a carga máxima de fármaco adsorvido em partículas de sílica mesoporosas. O sistema foi aplicado a fármacos de difícil amorfização. Ressaltando-se o ineditismo da proposta aqui desenvolvida, que provou sucesso do emprego de partículas de sílica mesoporosas carregadas com fármaco. Além disso, uma característica interessante deste trabalho foi a identificação que apenas o fármaco que está em contato direto com a superfície da sílica permanece amorfo, enquanto o fármaco dentro dos poros, mas sem contato direto com a superfície da sílica, está propenso à recristalização. Este achado é especialmente importante, uma vez que sugere que apenas o fármaco em contato com a superfície da sílica, ou seja, formando a monocamada permanece fisicamente estável durante a vida de prateleira de uma forma farmacêutica.

ANEXOS

Anexo 1 – Parecer da Comissão de Ética no Uso de Animais (CEUA) e Parecer referente ao relatório final do protocolo Nº. 001/17

Goiânia, 20 de março de 2017.

PARECER CONSUBSTANCIADO REFERENTE AO ATENDIMENTO DE PENDÊNCIA DO PROTOCOLO Nº. 001/17

I - Finalidade do projeto de pesquisa (pesquisa/aula prática): Pesquisa

II - Identificação:

- **Data de apresentação a CEUA:** 13/01/17
- **Título do projeto:** Avaliação da bioadesão de géis termorreversíveis na mucosa esofágica para o tratamento da eosinofilia esofágica.
- **Pesquisador Responsável/ Unidade:** Eliana Martins Lima/Faculdade de Farmácia
- **Pesquisadores Participantes:** Thais Leite Nascimento, Leonardo Gomes Souza, Rayane Santa Cruz Martins de Queiróz Antonino, Marcília Viana Pavam Gonçalves, Edilson Ribeiro de Oliveira Júnior
- **Médico Veterinário/CRMV:** Daniel Silva Goulart/CRMV 4632
- **Unidade onde será realizado:** Faculdade de Farmácia

III - Objetivos e justificativa do projeto:

Não há protocolos padronizados para o tratamento de esofagite eosinofílica. Uma variedade de abordagens terapêuticas, incluindo a supressão ácida, modificações dietéticas, corticosteroides tópicos e dilatação endoscópica podem ser utilizadas sozinhas ou em combinação. Por não existir um tratamento específico para EoE, este projeto busca desenvolver uma formulação para o tratamento da EoE, através de géis termoreversíveis, com atividade bioadesiva na mucosa do esôfago, ampliando assim as possibilidades farmaco-terapêuticas. O objetivo geral do projeto de pesquisa é desenvolver uma formulação com bioadesividade à mucosa esofágica para o tratamento da EoE e realizar estudos *ex vivo* e *in vivo* para avaliação das formulações.

Objetivo específicos:

a) Caracterização da mucoadesão *ex vivo*; As formulações marcadas com rodamina B serão aplicadas em segmentos do tecido esofágico de ratos. Posteriormente o tecido será lavado com solução Hartmann e realizada quantificação, sendo possível assim determinar a porcentagem de formulação aderida à mucosa.

b) Caracterização da mucoadesão *in vivo*; As formulações serão marcadas com IR-780 e administrada por via oral em camundongos. As imagens da mucoadesão em todo trato gastrointestinal serão captadas por um tomógrafo de fluorescência.

IV - Sumário do projeto:

- **Discussão sobre a possibilidade de métodos alternativos e necessidade do número de animais:** Não existe nenhum método alternativo que possibilite mensurar a bioadesão de géis na mucosa esofágica, sendo necessário o uso de animais nesta etapa do projeto. A pesquisa bibliográfica foi realizada em artigos científicos publicados na plataforma de buscas PubMed mantida pela National Library of Medicine – National Institutes of Health – USA e pelo banco de dados Alt Tox – Non animal Methods for Toxicity Testing.
- **Prevê Projeto Piloto:** Sim

- **Espécie animal utilizada/ número total de animais/ Número de animais por tratamento ou grupo experimental:** Estão previstos para o piloto 3 ratos Wistar machos e 3 camundongos Swiss fêmeas. Para o projeto de pesquisa estão previstos 25 ratos Wistar machos e 15 camundongos Swiss fêmeas.
- **Descrição do animal utilizado (Explicitar: espécie/ linhagem/ sexo (informar número por sexo)/ peso e/ou idade etc):** Estão previstos para o piloto 3 ratos Wistar machos com peso em torno de 350-400g e 3 camundongos Swiss fêmeas com peso de 25-30g. Para o projeto de pesquisa estão previstos 25 ratos Wistar machos e 15 camundongos Swiss fêmeas, com as mesmas especificações de peso do projeto piloto.
- **Fonte de obtenção do animal:** Biotério Central ICB/UFG
- **Descrição das instalações utilizadas e número de animais/área/qualidade do ambiente (ar, temperatura, umidade), alimentação/hidratação**: Os animais serão alojados no biotério da Faculdade de Farmácia, sendo mantidos em condições controladas de temperatura e iluminação (ciclo claro/escuro de 12 h), em sala climatizada sob temperatura constante de 23 ± 2ºC e umidade relativa de 50%. Além disso, ratos serão distribuídos 3 a 3 ou 4 a 4 em gaiolas plásticas de 50 x 60 x 22 cm, e camundongos 5 a 5 gaiolas 30x20x20cm, utilizando maravalha como cama. Os animais permanecerão em período de adaptação por 10 dias.
- **Utilização de agente infeccioso/gravidade da infecção a ser observada e análise dos riscos aos pesquisadores/alunos:** Não serão utilizados agentes infecciosos. O contato com tecidos e sangue dos camundongos e ratos podem transmitir algumas doenças. No entanto, os riscos de contaminação biológica envolvidos são considerados muito reduzidos ou nulos, uma vez que os animais provem de colônias mantidas sobre rígidas condições de controle patológico nos biotérios de origem (Biotério Central da UFG). O pessoal manipulador utilizará EPIs e estarão vacinados contra anti-hepatite B (recombinante); vacina diftérica e tétano adulto (dupla tipo adulto -dT) e vacina anti-rábica.
- **Procedimentos experimentais do projeto de pesquisa:** Estudo Ex-vivo: Ratos Wistar machos (350-400 g) (n=5, para cada formulação), serão anestesiados por injeção intraperitoneal de ketamina 50 mg/kg e xilazina 10 mg/kg e eutanasiados por punção cardíaca. Antes da remoção do esôfago. Segmentos do tecido esofágico serão cortados longitudinalmente e as seções obtidas mantidos a 4 ° C em solução de Hartmann. Para cada formulação estudada, um volume de amostra 30 µL, será aplicado a um pedaço da mucosa esofágica, em um ambiente de temperatura controlada a 37ºC, e logo seguida, lavadas 4 vezes com 1,0 ml de solução de Hartmann. As soluções obtidas serão analisadas no fluorímetro para quantificação da rodamina b.

  Estudo In-vivo: *Camundongos Swiss* fêmeas com 25-30 g (n=5 para cada formulação), serão utilizados para a avaliação *in vivo* de bioadesão das formulações. Os animais serão imobilizados e 20 µL das formulações de gel contendo IR-780 na concentração de 2,5 mg/kg serão administradas na cavidade bucal, utilizando micropipeta. A extensão e duração da bioadesão das formulações no tudo digestivo serão avaliadas através de imagens coletadas pelo equipamento FMT Fluorescence Tomography in vivo Imaging Systems (Perkin Elmer, Estados Unidos). As imagens serão feitas 5, 15, 30, 60 e 120 minutos após administração. Os animais serão anestesiados utilizando isoflurano na concentração de 3% em ar comprimido para indução e 1,5% para manutenção da anestesia. Após o experimento os animais serão eutanasiados.
- **Métodos utilizados para minimizar o sofrimento e aumentar o bem-estar dos animais antes, durante e após a pesquisa. Pontos Finais Humanitários:** Além do uso de anestésico geral durante os procedimentos, determinamos alguns endpoints em nossos experimentos para minimizar e/ou evitar a dor e sofrimento dos animais durante o estudo. Os animais serão monitorados diariamente e serão avaliados em relação à aparência,

peso, comportamento e ingesta de água/ração. Qualquer alteração, como as descritas abaixo, o animal será retirado da pesquisa e será eutanasiado.

- O animal não é mais capaz de comer ou beber,
- O animal apresenta sinais de dor,
- O animal perdeu mais de 15% de peso corporal num relativamente curto espaço de tempo (1-2 dias), ou a sua diminuição de peso em mais de 20% em relação ao seu peso no início do experimento,
- O animal tem um sangramento significante,
- O comportamento e locomoção do animal são totalmente anormais.

Os pesquisadores se comprometeram a consultar o médico veterinário responsável pela pesquisa em caso de reações adversas nos animais, afim de promover tratamento suporte se necessário.

- ❑ **Grau de invasividade:** GI1
- ❑ **Material utilizado em outros projetos:** Não menciona
- ❑ **Método de eutanásia:** Os ratos serão eutanasiados por punção cardíaca após anestesia com quetamina e xilazina. Camundongos serão eutanasiados por deslocamento cervical após anestesia inalatória com isoflurano.
- ❑ **Destino do animal:** Os animais serão eutanasiados e todo o resíduo biológico será congelado a -20 °C e levado à Faculdade de Medicina Veterinária/UFG para incineração.

V – Comentários do relator frente às orientações da CEUA:

- ❑ **Quanto aos documentos exigidos pela CEUA/UFG:** O pesquisador apresentou toda a documentação necessária
- ❑ **Quanto aos cuidados e manejo dos animais e riscos aos pesquisadores:** Pesquisadores indicam que farão o correto manejo dos animais e tomarão os devidos cuidados para tentar minimizar os riscos.

VI - Parecer da CEUA:

De acordo com a documentação apresentada à CEUA, consideramos o projeto **APROVADO**.

Informação aos pesquisadores:

Reiteramos a importância deste Parecer Consubstanciado, e lembramos que a pesquisadora responsável deverá encaminhar à CEUA-PRPI-UFG o Relatório Final baseado na conclusão do estudo e na incidência de publicações decorrentes deste, de acordo com o disposto na Lei nº. 11.794 de 08/10/2008, e Resolução Normativa nº. 01, de 09/07/2010 do Conselho Nacional de Controle de Experimentação Animal-CONCEA. O prazo para entrega do Relatório é de até 30 dias após o encerramento da pesquisa, a qual está prevista para finalizar suas ações até **10 de novembro de 2017**.

VII - Data da reunião: 20/03/17.

Dra. Marina Pacheco Miguel
Coordenadora da CEUA/PRPI/UFG

Goiânia, 14 de outubro de 2019.

PARECER CONSUBSTANCIADO REFERENTE AO RELATÓRIO FINAL DO PROTOCOLO Nº. 001/17

I. IDENTIFICAÇÃO:

1. **Título do projeto**: Avaliação da bioadesão de géis termorreversíveis na mucosa esofágica para o tratamento da eosinofilia esofágica
2. **Pesquisador Responsável:** Eliana Martins Lima
3. **Unidade/Órgão:** Faculdade de Farmácia/FARMATEC/UFG
4. **Pesquisadores Participantes:** Thais Leite Nascimento/FF, Leonardo Gomes Souza/FF, Rayane Santa Cruz Martins de Queiróz Antonino/FF, Marcília Viana Pavam Gonçalves/FF, Edilson Ribeiro de Oliveira Júnior/FF.
5. **Unidade onde será realizado:** Biotério da Faculdade de Farmácia – UFG
6. **Data de apresentação do protocolo ao CEUA:** 13/01/2017
7. **Data de Apresentação do Relatório Final:** 09/09/2019

II - Parecer da CEUA:

Não houve emendas no projeto. O autor apresentou o resumo dos resultados encontrados na pesquisa.

Produtos resultantes deste projeto de pesquisa:

1. Thermoreversible mucoadhesive polymer-drug dispersion for sustained local delivery of budesonide to treat inflammatory disorders of the GI tract Author links open overlay panel. Rayane S.C.M.Q et al. Journal of Controlled Release, v.303, 2019, p.12-23.

Os pesquisadores apresentaram um produto resultante da pesquisa, com comprovante em anexo.

Informamos que a *Comissão de Ética no Uso de Animais/CEUA* da Universidade Federal de Goiás, **APROVOU** o Relatório Final do projeto acima referido, por estar de acordo com a Resolução Normativa nº1 da Lei 11.794/08 e estar em consonância com os princípios éticos vigentes.

Desta forma, o emprego de animais deste protocolo encontra-se concluído. É permitido ao pesquisador o processamento posterior de dados e de amostras biológicas obtidas dos animais aprovados durante a vigência do projeto, portanto, torna-se importante manter a documentação referente à aprovação arquivada.

III - Data da reunião: 14/10/2019.

Dra. Marina Pacheco Miguel
Coordenadora da CEUA/PRPI/UFG

Anexo 2 – Oral Pharmaceutical Compositions of Corticosteroids - Patente

(12) INTERNATIONAL APPLICATION PUBLISHED UNDER THE PATENT COOPERATION TREATY (PCT)

(19) World Intellectual Property Organization
International Bureau

(43) International Publication Date
25 October 2018 (25.10.2018)

WIPO | PCT

(10) International Publication Number
WO 2018/193423 A1

(51) International Patent Classification:
A61K 9/08 (2006.01) *A61K 31/58* (2006.01)
A61K 47/10 (2017.01) *A61P 1/04* (2006.01)
A61K 9/06 (2006.01)

(21) International Application Number:
PCT/IB2018/052771

(22) International Filing Date:
20 April 2018 (20.04.2018)

(25) Filing Language: English

(26) Publication Language: English

(30) Priority Data:
62/488,462 21 April 2017 (21.04.2017) US

(71) Applicant: **FERRING B.V.** [NL/NL]; Polaris Avenue 144, 2132 JX Hoofddorp (NL).

(72) Inventors: **WOOLLEY, Robert F.**; c/o Ferring Pharmaceuticals SA, Praca Sao Marcos, 624, 05455-505 Sao Paulo (BR). **LIMA, Eliana Martins**; Universidade Federal de Goias, Praca Univeritaria - 5a, Avenida esq/Rua 240 s/n, 74605-170 Goiania (BR). **NASCIMENTO, Thais Leite**; Universidade Federal de Goias, Praca Univeritaria - 5a, Avenida esq/Rua 240 s/n, 74605-170 Goiania (BR). **ANTONINO, Rayane Santa Cruz**; Universidade Federal de Goias, Praca Univeritaria - 5a, Avenida esq/Rua 240 s/n, 74605-170 Goiania (BR). **RIBEIRO, Edilson**; Universidade Federal de Goias, Praca Univeritaria - 5a, Avenida esq/Rua 240 s/n, 74605-170 Goiania (BR).

(81) Designated States *(unless otherwise indicated, for every kind of national protection available)*: AE, AG, AL, AM, AO, AT, AU, AZ, BA, BB, BG, BH, BN, BR, BW, BY, BZ, CA, CH, CL, CN, CO, CR, CU, CZ, DE, DJ, DK, DM, DO, DZ, EC, EE, EG, ES, FI, GB, GD, GE, GH, GM, GT, HN, HR, HU, ID, IL, IN, IR, IS, JO, JP, KE, KG, KH, KN, KP, KR, KW, KZ, LA, LC, LK, LR, LS, LU, LY, MA, MD, ME, MG, MK, MN, MW, MX, MY, MZ, NA, NG, NI, NO, NZ, OM, PA, PE, PG, PH, PL, PT, QA, RO, RS, RU, RW, SA, SC, SD, SE, SG, SK, SL, SM, ST, SV, SY, TH, TJ, TM, TN, TR, TT, TZ, UA, UG, US, UZ, VC, VN, ZA, ZM, ZW.

(84) Designated States *(unless otherwise indicated, for every kind of regional protection available)*: ARIPO (BW, GH,

(54) Title: ORAL PHARMACEUTICAL COMPOSITIONS OF CORTICOSTEROIDS

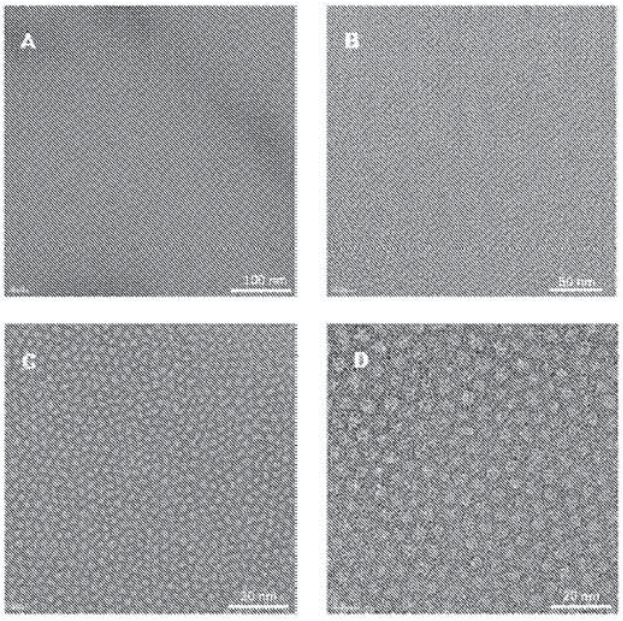

FIGS. 1A-1D

(57) Abstract: Described herein are oral pharmaceutical compositions of corticosteroids that undergo a sol- gel transition, as well as methods of making such oral pharmaceutical compositions, and therapeutic methods using them. The compositions typically comprise a corticosteroid, a solvent for the corticosteroid and a thermoreversible polymer. The compositions are particularly useful for treating inflammatory conditions of the esophagus, such as eosinophilic esophagitis.

WO 2018/193423 A1

[Continued on next page]

GM, KE, LR, LS, MW, MZ, NA, RW, SD, SL, ST, SZ, TZ, UG, ZM, ZW), Eurasian (AM, AZ, BY, KG, KZ, RU, TJ, TM), European (AL, AT, BE, BG, CH, CY, CZ, DE, DK, EE, ES, FI, FR, GB, GR, HR, HU, IE, IS, IT, LT, LU, LV, MC, MK, MT, NL, NO, PL, PT, RO, RS, SE, SI, SK, SM, TR), OAPI (BF, BJ, CF, CG, CI, CM, GA, GN, GQ, GW, KM, ML, MR, NE, SN, TD, TG).

Published:

— *with international search report (Art. 21(3))*
— *in black and white; the international application as filed contained color or greyscale and is available for download from PATENTSCOPE*

ORAL PHARMACEUTICAL COMPOSITIONS OF CORTICOSTEROIDS CROSS-REFERENCE TO RELATED PATENT APPLICATIONS

[0001] This application claims the priority benefits under 35 USC § l 19(e) to U.S. provisional application 62/488,462, filed April 21, 2017, the entire contents of which are incorporated herein by reference in their entirety.

FIELD

[0002] Described herein are oral pharmaceutical compositions of corticosteroids that undergo a sol-gel transition, as well as methods of making such oral pharmaceutical compositions, and therapeutic methods using them.

BACKGROUND

[0003] Eosinophilic esophagitis (EoE) is a clinicopathologic disease characterized by upper intestinal symptoms and the finding of more than 15 or 20 eosinophils in the esophageal epithelium, unresponsive to proton pump inhibitor treatment. The pathogenesis of EoE is still not clear, but a growing body of evidence has established that this condition represents a T cell-mediated immune response involving several pro-inflammatory mediators and chemo- attractants known to regulate eosinophilic accumulation in the esophagus, such as IL-4, IL-5, IL-3, eotaxin-1, eotaxin-2, and eotaxin-3.

[0004] EoE prevalence seems to be worldwide (prevalence estimated at 43/100,000 inhabitants; incidence estimated at 7.4/100,000 inhabitants) but the patient population diagnosed with eosinophilic esophagitis appears to be increasing. Food impaction and dysphagia are the most common presenting symptoms in older children and adults. EoE pathogenesis is likely to be associated with allergen sensitization in predisposed individuals. EoE has a strong familial pattem based on the growing clinical literature. Approximately 8% of pediatric patients with EoE have at least one sibling or parent with EoE as well. ln addition, it has been recently reported that three adult brothers with dysphagia were found to have EoE. Taken together, EoE appears to demonstrate a strong familial pattem with a much higher prevalence in siblings.

[0005] There is no specific treatment available for EoE, but some physicians prescribe budesonide and fluticasone pumps and/or dry powder to be swallowed. Several issues exist for finding a proper treatment for EoE. For example, a lack of dosage standardization compromises treatment efficacy. Additionally, patients have a difficult time adhering to treatment (such as budesonide and fluticasone pumps and/or dry powder) due to poor product taste and stomach pain and gas resulting from air ingestion. Furthermore, budesonide and fluticasone pumps and/or dry powder can also lead to cavities and oral moniliasis.

[0006] Thus, there remains a need for oral pharmaceutical compositions of corticosteroids suitable for use in treating EoE.

SUMMARY

[0007] Provided herein are oral pharmaceutical compositions comprising (a) a corticosteroid, (b) a solvent for the corticosteroid, and (e) a thermoreversible polymer, wherein the composition is a liquid at room temperature and a gel at body temperature.

[0008] Also provided are oral pharmaceutical compositions comprising: (a) a corticosteroid, (b) a solvent selected from one or more of propylene glycol, ethylene glycol, sorbitol, and cyclodextrin, and (e) a polymer selected from one or more of Poloxamer 407; Poloxamer 338; Poloxamer 188; Pluronic F68; Pluronic F127; and Pluronic F98. ln some embodiments, the polymer comprises Poloxamer 407.

[0009] ln any embodiments of the compositions described herein, the composition may comprise micelles that comprise the polymer, corticosteroid, and solvent.

[0010] ln any embodiments of the compositions described herein, the composition may be a liquid at 25ºC and a gel at 37ºC.

[0011] ln any embodiments of the compositions described herein, the composition may have a sol-gel transition temperature of from 25 to 32ºC, or from 27 to 32ºC, or from 29 to 32ºC.

[0012] ln any embodiments of the compositions described herein, the corticosteroid may be selected from one or more of budesonide, fluticasone, and ciclesonide. ln some embodiments, the corticosteroid is budesonide. ln some embodiments, the corticosteroid is fluticasone. In some embodiments, the corticosteroid is ciclesonide.

[0013] ln any embodiments of the compositions described herein, the corticosteroid may be present in an amount of 0.001 to 10% w/w or 0.01 to 10% w/w of the composition. ln some embodiments, the polymer is present in an amount of 15-30% w/w of the composition.

[0014] ln any embodiments of the compositions described herein, the solvent may be present in an amount of 0.2 to 10% w/w of the composition.

[0015] ln some embodiments of any of the compositions described herein, the polymer is Poloxamer 407 and is present in an amount of 15-30% w/w of the composition. ln some embodiments, the polymer is Poloxamer 407 and is present in an amount of from 15 to 17% w/w, or from I5.5 to I6.5% w/w, of the composition.

[0016] ln some embodiments of any of the compositions described herein, the solvent is propylene glycol and is present in an amount of 0.2 to 10% w/w, or 3 to 7% w/w, or 4 to 6% w/w of the composition.

[0017] ln some embodiments of any of the compositions described herein, the corticosteroid is budesonide and is present in an amount of 0.001 to 10% w/w, the polymer is Poloxamer 407 and is present in an amount of 15-30% w/w, and the solvent is propylene glycol and is present in an amount of 0.2 to 10% w/w of the composition. ln some embodiments, the corticosteroid is budesonide and is present in an amount of 0.001 to 10% w/w, the polymer is Poloxamer 407 and is present in an amount of 15-30% w/w, and the solvent is propylene glycol and is present in an amount of 4 to 6% w/w of the composition.

[0018] ln some embodiments of any of the compositions described herein, the corticosteroid is fluticasone and is present in an amount of 0.001 to 10% w/w, the polymer is Poloxamer 407 and is present in an amount of 15-30% w/w, and the solvent is propylene glycol and is present in an amount of 0.2 to 10% w/w of the composition. ln some embodiments, the corticosteroid is fluticasone and is present in an amount of 0.01 to 10% w/w, the polymer is Poloxamer 407 and is present in an amount of 15-30% w/w, and the solvent is propylene glycol and is present in an amount of 4 to 6% w/w of the composition.

[0019] ln some embodiments of any of the compositions described herein, the corticosteroid is ciclesonide and is present in an amount of 0.001 to 10% w/w, the polymer is Poloxamer 407 and is present in an amount of 15-30% w/w, and the solvent is propylene glycol and is present in an amount of 0.2 to 10% w/w of the composition. ln some embodiments, the corticosteroid is ciclesonide and is present in an amount of 0.01 to 10% w/w, the polymer is Poloxamer 407 and is present in an amount of 15-30% w/w, and the solvent is propylene glycol and is present in an amount of 4 to 6% w/w of the composition.

[0020] ln any embodiments of any of the compositions described herein, the composition further comprises water and, optionally, one or more additional pharmaceutically acceptable excipients. ln some embodiments, the composition comprises one or more additional pharmaceutically acceptable excipients in an amount of 0.01-10% w/w of the composition. ln some embodiments, the composition comprises one or more additional pharmaceutically acceptable excipients selected from preservatives, such as methyl-p-hydroxybenzoate.
Additionally, or alternatively, in some embodiments, the composition comprises one or more additional pharmaceutically acceptable excipients selected sweeteners, such as acesulfame potassium.

[0021] ln any embodiments of any of the compositions described herein, the composition may adhere to the esophagus. ln some embodiments, the compositions adhere to the esophagus for at least 30 minutes, or for at least 45 minutes, or for at least 60 minutes.

[0022] Also provided are methods of treating an inflammatory condition of the esophagus, such as eosinophilic esophagitis, comprising orally administering any oral pharmaceutical composition as described herein.

[0023] Also provided are uses of a corticosteroid in the manufacture of a medicament for treating an inflammatory condition of the esophagus, such as eosinophilic esophagitis, wherein the medicament comprises any oral pharmaceutical composition as described herein.

[0024] Also provided are methods of preparing any oral pharmaceutical composition as described herein, comprising (a) dissolving the corticosteroid in the solvent; (b) mixing the corticosteroid solution with the polymer; and (e) optionally, adding water and, optionally, one or more additional pharmaceutically acceptable excipients.

[0025] Also provided are methods of preparing any oral pharmaceutical composition as described herein, comprising (a) dispersing the polymer in water and chilling the polymer dispersion; (b) dissolving the corticosteroid in the solvent; (e) mixing the corticosteroid solution with the polymer dispersion; (d) increasing the temperature of the mixture until the mixture becomes a gel; (e) cooling

the gel until the gel becomes a liquid; and (f) optionally, adding water and, optionally, one or more additional pharmaceutically acceptable excipients.

BRIEF DESCRIPTION OF THE DRAWINGS

[0026] FIGS. 1A-1D are transmission electron microscope (TEM) images of a composition as described herein at 25ºC. FIG. 1A is a magnification of 29000x; FIG. 1B is a magnification of 62000x; FIG. 1C is a magnification of 1OOOOOx; FIG. 1D is a magnification of 200000x.

[0027] FIGS. 2A-2B are TEM images of a composition as described herein at 37ºC. FIG. 2A is a magnification of 62000x; FIG. 2B is a magnification of 1OOOOOx.

[0028] FIGS. 3A-B are *ex vivo* images of the gastrointestinal tract of animals four hours after treatment with 20 µl of a composition as described herein (FIG. 3A) and 20 µl l of a control composition (with IR780 dye) (FIG. 3B).

[0029] FIGS. 4A-D are *ex vivo* images of the esophagus of animals four hours after treatment with 20 µl of a composition as described herein (FIGS. 4A-B) and 20 µl of a control composition (with IR780 dye) (FIGS. 4C-D).

DETAILED DESCRIPTION

[0030] Described herein are oral pharmaceutical compositions comprising a corticosteroid, methods of making such oral pharmaceutical compositions, and therapeutic methods using them. The compositions undergo a sol-gel transition as described herein, and typically comprise a corticosteroid, a solvent, and a thermoreversible polymer capable of undergoing a sol-gel transition. ln particular embodiments, the compositions are liquids at room temperature and gels at body temperature. ln accordance with these embodiments, the compositions can be readily ingested as liquids, after which they transition to a gel state in which they may exhibit increased adhesion to mucosal surfaces, such as mucosal surfaces of the esophagus. Thus, in some embodiments, the compositions provide local delivery of corticosteroid to the esophagus. Further, in embodiments where the compositions adhere to mucosal surfaces, such as mucosal surfaces of the esophagus, they provide prolonged delivery of corticosteroid to the esophagus. These embodiments may offer particular advantages in the context of treating EoE, by providing local and prolonged delivery of corticosteroid to the site of pathology.

Definitions

[0031] Technical and scientific terms used herein have the meanings commonly understood by one of ordinary skill in the art of pharmaceutical compositions to which the present disclosure pertains, unless otherwise defined. Reference is made herein to various methodologies known to those of ordinary skill in the art. Suitable materials and/or methods known to those of ordinary skill in the art can be utilized in carrying out the present disclosure. However, specific materials and methods are described. Materials, reagents and the like to which reference is made in the following description and examples are obtainable from commercial sources, unless otherwise noted.

[0032] As used herein, the singular forms "a," "an," and "the" designate both the singular and the plural, unless expressly stated to designate the singular only.

[0033] As used herein, the term "about" means that the number or range is not limited to the exact number or range set forth, but encompass values around the recited number or range as will be understood by persons of ordinary skill in the art depending on the context in which the number or range is used. Unless otherwise apparent from the context or convention in the art, "about" means up to plus or minus 10% of the particular term.

[0034] As used herein, "subject" denotes any mammal, including humans. For example, a subject may be suffering from or at risk of developing a condition that can be diagnosed, treated or prevented with a corticosteroid, or may be taking a corticosteroid for other purposes.

[0035] The terms "administer," "administration," or "administering" as used herein refer to (1) providing, giving, dosing and/or prescribing, such as by either a health professional or his or her authorized agent or under his direction, and (2) putting into, taking or consuming, such as by a health professional or the subject.

[0036] The terms "treat", "treating" or "treatment", as used herein, include alleviating, abating or ameliorating a disease or condition or one or more symptoms thereof, whether or not the disease or condition is considered to be "cured" or "healed" and whether or not all symptoms are resolved. The terms also include reducing or preventing progression of a disease or condition or one or more symptoms thereof, impeding or preventing an underlying mechanism of a disease or condition or one or more symptoms thereof, and achieving any therapeutic and/or prophylactic benefit.

[0037] As used herein, the phrase "therapeutically effective amount" refers to a dose that provides the specific pharmacological effect for which the drug is administered in a subject in need of such treatment. It is emphasized that a therapeutically effective amount will not always be effective in treating the conditions described herein, even though such dose is deemed to be a

therapeutically effective amount by those of skill in the art. For convenience only, exemplary doses and therapeutically effective amounts are provided below with reference to human subjects. Those skilled in the art can adjust such amounts in accordance with standard practices as needed to treat a specific subject and/or condition/disease.

COMPOSITIONS

[0038] Described herein are oral pharmaceutical compositions comprising a corticosteroid, methods of making such oral pharmaceutical compositions, and therapeutic methods using them. The compositions typically undergo a sol-gel transition as described herein, and comprise a corticosteroid, a solvent, and a thermoreversible polymer capable of undergoing a sol-gel transition.

[0039] As noted above, in particular embodiments the compositions described herein undergo a sol-gel transition. For example, in particular embodiments, the compositions are liquids at room temperature and gels at body temperature. ln some embodiments, the compositions are liquids at temperatures of about 20-25ºC (typical room temperatures) or lower and gels at temperatures of about 36.5-37.5ºC (typical body temperatures) or greater. ln some embodiments, the compositions are liquids at temperatures of about 23ºC or lower and gels at temperatures of about 37ºC or greater. ln some embodiments, the compositions are liquids at 20ºC and gels at 37ºC. ln some embodiments, the compositions undergo a sol- gel transition at a temperature of about 25-32ºC or 27-32ºC or 29-32ºC.

[0040] As noted above, the compositions typically comprise corticosteroid, thermoreversible polymer, and solvent. While not wanting to be bound by theory or mechanism of action, it is believed that thermoreversible polymer molecules present in the composition form micelles which comprise solubilized (dissolved) corticosteroid. Thus, in some embodiments, the compositions comprise micelles that comprise thermoreversible polymer, corticosteroid, and solvent. The micelles may be present well-below the sol-gel temperature. For example, micelles may be observed at temperatures of about 10-20ºC.

[0041] ln some embodiments the gel form of the compositions described herein exhibit a viscosity or mucoadhesive strength such that they adhere to mucosal surfaces, such as the esophagus. ln some embodiments, the composition adheres to the esophagus for at least 15 minutes, or at least 20 minutes, or at least 25 minutes, or at least 30 minutes, or at least 35 minutes, or at least 40 minutes, or at least 45 minutes, or at least 50 minutes, or at least 55 minutes, or at least 60 minutes, or at least 65 minutes, or at least 75 minutes, or at least 75 minutes, after administration. ln some embodiments, the

composition adheres to the esophagus for at least 30 minutes after administration. ln some embodiments, the composition adheres to the esophagus for at least 45 minutes after administration. ln some embodiments, the composition adheres to the esophagus for at least 60 minutes after administration. ln some embodiments, the composition adheres to the esophagus for at least 75 minutes after administration.

[0042] As used herein, the term "mucoadhesive strength" refers to the force required to remove the oral pharmaceutical composition from a mucin disc using a texturometer TA.XT Plus equipment (Stable Micro Systems) as illustrated in the examples. ln some embodiments, the gel form of the compositions described herein exhibit a mucoadhesive strength of from about 5 g to about 15 g. ln some embodiments, the mucoadhesive strength is from about 7 g to about 14 g, about 8 g to about 12 g, about 9 g to about 11 g, or from about 10 g to about 11g. ln some embodiments, the mucoadhesive strength is about 5, 6, 7, 8, 9, 10, 11, 12, 13, 14, or 15 g. ln some embodiments, the mucoadhesive strength is about 11 g.

[0043] While not wanting to be bound by theory, it is believed that these mucoadhesive properties enhance the therapeutic effect of the compositions, such as by providing improved and/or prolonged contact between the corticosteroid-composition and target treatment site, such as esophageal tissue, for improved drug delivery and/or prolonged effect.

Thermoreversible Polymer

[0044] As noted above, the compositions described herein include a polymer capable of undergoing a sol-gel transition, i.e., a thermoreversible polymer. Thermoreversible polymers are polymers that exhibit a temperature-dependent transition from a "sol" state (e.g., a liquid or primarily liquid-like state) to a "gel" stated (e.g., to a state exhibiting gel properties such as elasticity). The temperature at which a polymer (or composition) undergoes a transition from a sol state to a gel state is referred to as the sol-gel temperature. ln general, the sol-gel temperature of a polymer is inversely proportional to its molecular weight, with lower molecular weight polymers exhibiting higher sol-gel temperatures. The sol-gel temperature
of a composition will depend on the components of the composition as a whole, including the relative amount of thermoreversible polymer, and the identity and amounts of other components. Moreover, different components may have different effects on a compositions ability to exhibit a sol-gel transition, such as if one or more components interferes with ability of the polymer molecules to organize and form cross-linkages.

[0045] One class of pharmaceutically acceptable thermoreversible polymers that exhibit this property are poloxamers, which are block copolymers of polyoxyethylene (also referred to as poly(ethylene oxide) or poly(ethylene glycol) blocks) and polyoxypropylene (also referred to as poly(propylene oxide) or poly(propylene glycol) blocks). Poloxamers typically have a central polyoxypropylene block flanked on each side by polyoxyethylene blocks.
Pharmaceutically acceptable poloxamers are known in the art and commercially available.

[0046] Thus, in some embodiments, the thermoreversible polymer comprises a poloxamer, *e.g.,* a polymer having a central polyoxypropylene block flanked on each side by polyoxyethylene blocks. ln some embodiments, the thermoreversible polymer is one or more selected from Poloxamer 407 (also known as Pluronic F 127), Poloxamer 338, Poloxamer 188, Pluronic F68, and Pluronic F98. ln accordance with conventional nomenclature for "Poloxamers," the first two and Pluronic numbers x l00 correspond to the approximate molecular mass of the polyoxypropylene block, while the last number x 10 corresponds to the relatíve content of polyoxyethylene. Thus, for example, Poloxamer 407 is a polyoxyethylene-polyoxypropylene- polyoxyethylene tri-block polymer with an approximate polyoxypropylene molecular mass of 4,000 g/rnol and a 70% polyoxyethylene content; Poloxamer 338 is a polyoxyethylene- polyoxypropylene-polyoxyethylene tri-block polymer with an approximate polyoxypropylene molecular mass of 3300 g/mol and a 80% polyoxyethylene content, and Poloxamer 188 is a polyoxyethylene-polyoxypropylene- polyoxyethylene tri-block polymer with an approximate polyoxypropylene molecular mass of 1800 g/mol and a 80% polyoxyethylene content. Thus, in some embodiments, the thermoreversible polymer is selected from polyoxyethylene-polyoxypropylene-polyoxyethylene tri-block polymers with an approximate poly oxypropylene mol ecular mass of 4,000 gímol and a 70% polyoxyethylene contem; polyoxyethylene-polyoxypropylene-polyoxyethylene tri-block polymers with an approximate polyoxypropylene molecular mass of 3300 g/mol and a 80% polyoxyethylene content, and polyoxyethylene-polyoxypropylene- polyoxyethylene tri-block polymers wi th an approxi rn ate polyoxypropylene molecular mass of 1800 g/mol and a 80% polyoxyethylene content.

[0047] The amount of thermoreversible polymer present in the composition can be selected and controlled to achieve the target sol-gel temperature and/or other desired properties of the composition, such as adhesion to mucosal surfaces. Exemplary amounts are discussed in more detail below.

[0048] For example, in some embodiments, the thermoreversible polymer is present in an amount from about 10% to about 30% w/w of the composition. **ln** some embodiments, the thermoreversible polymer is present in an amount from about 10% to about 25%, or about 15% to about 25%, or about 15% to about 20%, or about 10% to about 20%, or about 10% to about 18%, or about 10% to about

17%, or about 10% to about 16%, or about 10% to about 15% w/w of the composition. **In** some embodiments, the sol-gel polymer is present in an amount of about 10%, 11%, 12%, 13%, 14%, 15%, 16%, 17%, 18%, 19%, 20%, 21%, 22%, 23%, 24%, or 25% w/w of the composition.

[0049] For example, in some embodiments, the thermoreversible polymer comprises a poloxamer, which is present in an amount from about 10% to about 30% w/w of the composition. **In** some embodiments, the poloxamer is present in an amount from about 10% to about 25%, or about 15% to about 25%, or about 15% to about 20%, or about 10% to about 20%, or about 10% to about 18%, or about 10% to about 17%, or about 10% to about 16%, or about 10% to about 15% w/w of the composition. **In** some embodiments, the poloxamer is present in an amount of about 10%, 11%, 12%, 13%, 14%, 15%, 16%, 17%, 18%, 19%, 20%, 21%, 22%, 23%, 24%, or 25% w/w of the composition.

[0050] In some embodiments, the thermoreversible polymer comprises Poloxamer 407. In some embodiments, Poloxamer 407 is present in in amount from about 10% to about 30%, or about 15% to about 25%, or about 15% to about 20%, or about 10% to about 18%, or about 10% to about 17%, or about 10% to about 16%, or about 10% to about 15% w/w of the composition. In some embodiments, Poloxamer 407 is present in an amount of about 10% to about 30% w/w of the composition. **In** some embodiments, Poloxamer 407 is present in an amount of about 15% to about 30% w/w of the composition. **In** some embodiments, Poloxamer 407 is present in an amount of about 15%, 15.5%, 16%, 16.5%, or 17% w/w of the composition. **In** some embodiments, Poloxamer 407 is present in an amount of from 15 to 17% w/w of the composition. **In** some embodiments, Poloxamer 407 is present in an amount of from 15.5 to 16.5% w/w of the composition. **In** some embodiments, Poloxamer 407 is present in an amount of about 16% w/w of the composition.

Corticosteroids

[0051] The compositions described herein may comprise any one or more pharmaceutically acceptable corticosteroids, such as any one or more corticosteroids pharmaceutically acceptable for oral administration, such as topically active steroids. Non-limiting examples of suitable corticosteroids include one or more selected from budesonide, fluticasone, cicelsonide, cortisone, hydrocortisone, methylprednisolone, prednisolone, prednisone, triamcinolone, amcinonide, desonide, fluocinolone acetonide, fluocinonide, halcinonide, triamcinolone acetonide, beclometasone, betamethasone, dexamethasone, fluocortolone, halometasone, mometasone, flunisolide, ciclesonide, and fludrocortisone, and pharmaceutically acceptable salts and esters of each thereof.

[0052] In some embodiments, a composition as described herein comprises budesonide. Budesonide has the molecular formula $C_{25}H_{34}0_6$, a molecular weight of 430.53, and the chemical

name 16,l 7-butylidenebis(oxy)-11,21-dihydroxy-, (11β, 16α)-pregna-l,4-diene-3,20-dione. It is registered under CAS Registry Number 51333-22-3 and Einecs 257-139-7.

[0053] ln some embodiments, a composition as described herein comprises fluticasone. Fluticasone has the molecular formula $C_{22}H_{27}F_30_4S$, a molecular weight of 444.51, and the chemical name 6α,9α-difluoro-l1β, l 7α-dihydroxy-16a-methyl-21-thia-21-fluoromethylpregna-l,4-dien-3,20-dione. Fluticasone is registered under CAS Registry Number 90566-53-3.

[0054] ln some embodiments, a composition as described herein comprises ciclesonide. Ciclesonide has the molecular formula $C_{32}H_{44}0_7$, a molecular weight of 540.69 g/mol, and the chemical name (11β, 16α)-16, 17-[[(R)-cyclohexylmethylene]bis(oxy)]-11-hydroxy-21-(2-methyl-l -oxopropoxy)- pregna-1, 4-diene-3, 20-dione. Ciclesonide is registered under CAS Registry Number 126544-47-6.

[0055] ln some embodiments, a composition as described herein comprises budesonide. ln some embodiments, a composition as described herein comprises fluticasone. ln some embodiments, a composition as described herein comprises ciclesonide.

[0056] Pharmaceutically acceptable salts and esters of corticosteroids are known in the art. Exemplary pharmaceutically acceptable salts include acid addition salts, such as hydrochloride salts. Any pharmaceutically acceptable salt can be used, such as sodium and calcium salts. Other non-limiting exemplary salts include salts formed with a carboxylic acid group, alkali metal salts, and alkaline earth metal salts. Non-limiting examples of pharmaceutically acceptable esters include straight chain or branched C1-C18 alkyl esters, including methyl, ethyl, propyl, isopropyl, butyl, isobutyl, amyl, hexyl, heptyl, octyl, nonyl, decyl, lauryl, myristyl, cetyl, and stearyl, and the like; straight chain or branched C2-C18 alkenyl esters, including vinyl, allyl, undecenyl, oleyl, linolenyl, and the like; C3-C8 cycloalkyl esters, including cyclopropyl, cyclobutyl, cyclopentyl, cyclohexyl, cycloheptyl and cyclooctyl, and the like; aryl esters, including phenyl, toluoyl, xylyl, naphthyl, and the like; alicyclic esters, including menthyl and the like; or aralkyl esters, including benzyl, phenethyl, and the like.

[0057] The compositions described herein may include a therapeutically effective amount of corticosteroid. The therapeutically effective amount may depend on the specific corticosteroid being used, the subject being treated, the condition being treated, the desired effect, and the intended duration of therapeutic effect of the compositions. Compositions comprising more than one corticosteroid may include a therapeutically effective amount of each corticosteroid, or an amount of one or more of the corticosteroids that is not therapeutically effective on its own, but the amount of all corticosteroids present is therapeutically effective.

[0058] ln some embodiments, the corticosteroid is present in an amount of from about 0.001% to about 10% w/w of the composition. ln some embodiments, the corticosteroid is present in an amount of from about 0.01% to about 0.5%, or about 1.0%, or about 1.5%, or about 2.0%, or about 2.5% or about 3.0%, or about 3.5%, or about 4.0%, or about 4.5%, or about 5.0%, or about 6.0%, or about 7.0%, or about 8.0%, or about 9.0%, or about 10% w/w of the composition. ln some embodiments, the corticosteroid is present in an amount of from about 0.01% to about 0.03%, or about 0.04%, or about 0.05%, or about 0.06%, or about 0.07%, or about 0.08%, or about 0.09%, or about 0.1%, or about 0.2%, or about 0.3%, or about 0.4%, w/w of the composition. ln some embodiments, the corticosteroid is present in an amount of from about 0.01 to about 0.1% w/w of the composition. ln some embodiments, the corticosteroid is present in an amount of about 0.05% w/w the composition.

[0059] ln some embodiments of compositions comprising more than one corticosteroid, the amount of each is selected independently of the other. ln some such embodiments, the composition may include one of these amounts of each corticosteroid. ln other embodiments of compositions comprising more than one corticosteroid, the amount of each is selected to complement the other. **ln** some such embodiments, the compositions may have a total corticosteroid content corresponding to one of these amounts. Other embodiments of compositions comprising more than one corticosteroid also are contemplated.

[0060] ln some embodiments, the corticosteroid comprises budesonide. ln some embodiments, the budesonide is present in an amount of from about 0.001% to about 10% w/w of the composition, or from about 0.01% to about 0.5%, or about 1.0%, or about 1.5%, or about 2.0% w/w of the composition. ln some embodiments, the budesonide is present in amount of from about 0.01% to about 0.03%, or about 0.04%, or about 0.05%, or about 0.06%, or about 0.07%, or about 0.08%, or about 0.09%, or about 0.1% w/w of the composition. ln some embodiments, the budesonide is present in an amount of from about 0.001% to about 10% w/w of the composition. ln some embodiments, the budesonide is present in an amount of from about 0.01 to 0.1% w/w of the composition.

[0061] ln some embodiments, the corticosteroid comprises fluticasone. ln some embodiments, the fluticasone is present in an amount of from about 0.001% to about 10% w/w of the composition, or from about 0.01% to about 0.5%, or about 1.0%, or about 1.5%, or about 2.0% w/w of the composition. ln some embodiments, the fluticasone is present in amount of from about 0.01% to about 0.03%, or about 0.04%, or about 0.05%, or about 0.06%, or about 0.07%, or about 0.08%, or about 0.09%, or about 0.1% w/w of the composition. ln some embodiments, the fluticasone is present in an amount of from about 0.001% to about 10% w/w of the composition. ln some embodiments, the fluticasone is present in an amount of from about 0.01 to 0.1% w/w of the composition.

[0062] ln some embodiments, the corticosteroid comprises ciclesonide. ln some embodiments, the ciclesonide is present in an amount of from about 0.001% to about I0% w/w of the composition, or from about 0.01% to about 0.5%, or about 1.0%, or about 1.5%, or about 2.0% w/w of the composition. **ln** some embodiments, the ciclesonide is present in amount of from about 0.01% to about 0.03%, or about 0.04%, or about 0.05%, or about 0.06%, or about 0.07%, or about 0.08%, or about 0.09%, or about O. I% w/w of the composition. **ln** some embodiments, the ciclesonide is present in an amount of from about 0.001% to about 10% w/w of the composition. ln some embodiments, the ciclesonide is present in an amount of from about 0.01 to 0.1% w/w of the composition.

[0063] ln some embodiments, the corticosteroid is present at a concentration of from about 0.1 mg/ml to about 1.0 mg/ml. ln some embodiments, the corticosteroid is present at a concentration of from about 0.1 to about 0.2 mg/ml, or about 0.3 mg/ml, or about 0.4 mg/ml, or about 0.5 mg/ml, or about 0.6 mg/ml, or about 0.7 mg/ml, or about 0.8 mg/ml, or about 0.9 mg/ml. ln some embodiments, the corticosteroid is present at a concentration of from about 0.2 mg/ml to about 0.8 mg/ml; or from about 0.3 mg/ml to about 0.7 mg/ml; or from about 0.4 mg/ml to about 0.5 mg/ml. ln some embodiments, the corticosteroid is present at a concentration of about 0.5 mg/ml. ln some embodiments of compositions comprising more than one corticosteroid, the amount of each is selected independently of the other. ln some such embodiments, the composition may include one of these amounts of each corticosteroid. ln other embodiments of compositions comprising more than one corticosteroid, the amount of each is selected to complement the other. ln some such embodiments, the compositions may have a total corticosteroid content corresponding to one of these amounts. Other embodiments of compositions comprising more than one corticosteroid also are contemplated.

[0064] ln some embodiments, the corticosteroid comprises budesonide. ln some embodiments, the budesonide is present at a concentration of from about 0.1 mg/ml to about 1.0 mg/ml. ln some embodiments, the budesonide is present at a concentration of from about 0.1 to about 0.2 mg/ml, or about 0.3 mg/ml, or about 0.4 mg/ml, or about 0.5 mg/ml, or about 0.6 mg/ml, or about 0.7 mg/ml, or about 0.8 mg/ml, or about 0.9 mg/ml. ln some embodiments, the budesonide is present at a concentration of from about 0.2 mg/ml to about 0.8 mg/ml; or from about 0.3 mg/ml to about 0.7 mg/ml; or from about 0.4 mg/ml to about 0.5 mg/ml. ln some embodiments, the budesonide is present at a concentration of about 0.5 mg/ml.

[0065] ln some embodiments, the corticosteroid comprises fluticasone. ln some embodiments, the fluticasone is present at a concentration of from about 0.1 mg/ml to about 1.0 mg/ml. ln some embodiments, the fluticasone is present at a concentration of from about 0.1 to about 0.2 mg/ml, or about 0.3 mg/ml, or about 0.4 mg/ml, or about 0.5 mg/ml, or about 0.6 mg/ml, or about 0.7 mg/ml, or

about 0.8 mg/ml, or about 0.9 mg/ml. ln some embodiments, the fluticasone is present at a concentration of from about 0.2 mg/ml to about 0.8 mg/ml; or from about 0.3 mg/ml to about 0.7 mg/ml; or from about 0.4 mg/ml to about 0.5 mg/ml. ln some embodiments, the fluticasone is present at a concentration of about 0.5 mg/ml.

[0066] ln some embodiments, the corticosteroid comprises ciclesonide. ln some embodiments, the ciclesonide is present at a concentration of from about 0.1 mg/ml to about 1.0 mg/ml. ln some embodiments, the ciclesonide is present at a concentration of from about 0.1 to about 0.2 mg/ml, or about 0.3 mg/ml, or about 0.4 mg/ml, or about 0.5 mg/ml, or about 0.6 mg/ml, or about 0.7 mg/ml, or about 0.8 mg/ml, or about 0.9 mg/ml. ln some embodiments, the ciclesonide is present at a concentration of from about 0.2 mg/ml to about 0.8 mg/ml; or from about 0.3 mg/ml to about 0.7 mg/ml; or from about 0.4 mg/ml to about 0.5 mg/ml. ln some embodiments, the ciclesonide is present at a concentration of about 0.5 mg/ml.

Solvent

[0067] As noted above, the compositions described herein also include a solvent. **ln** some embodiments, the solvent is compatible with both the corticosteroid(s) and the thermoreversible polymer(s). ln some embodiments, the solvent is a solvent for the corticosteroid(s). Examples of suitable solvents include but are not limited to propylene glycol, ethylene glycol, sorbitol, cyclodextrin, glycerin, and mygliol, and mixtures of any two or more thereof. ln some embodiments, the solvent is propylene glycol.

[0068] The amount of solvent present in the composition can be selected and controlled to provide solubilization of the corticosteroid (and other components that may be present), and achieve the target sol-gel temperature and/or other desired properties of the composition, such as adhesion to mucosal surfaces. Exemplary amounts are discussed in more detail below.

[0069] For example, the solvent may be present in an amount from about 0.2 to about 10% w/w of the composition. ln some embodiments, the solvent is present in an amount from about 0.5% to about 9%, or about 1% to about 8%, or about 3% to about 7%, or about 4% to about 6% w/w of the composition.

[0070] ln some embodiments, the solvent comprises propylene glycol. ln some embodiments the propylene glycol is present in an amount of from about 0.2 to about 10%, or about 0.5% to about 9%, or about 1% to about 8%, or about 3% to about 7%, or about 4% to about 6% w/w of the composition. ln some embodiments, the propylene glycol is present in an amount of about 0.2% to about 10%

w/w of the composition. ln some embodiments, the propylene glycol is present in an amount from about 3% to about 7% w/w of the composition. ln some embodiments, the propylene glycol is present in an amount from about 4% to about 6% w/w of the composition. ln some embodiments, the propylene glycol is present in an amount of about 5% w/w of the composition.

Other Components

[0071] The compositions described herein typically further comprise water and, optionally, one or more optional pharmaceutically acceptable excipients.

[0072] Examples of optional pharmaceutically acceptable excipients include but are not limited to preservatives, sweeteners, antioxidants, chelating agents, colorants, flavoring agents, and/or pH adjusting agents.

[0073] Non-limiting examples of preservatives include methyl-p-hydroxybenzoate, potassium sorbate, C12 to C15 alkyl benzoates, alkyl p-hydroxybenzoates, propyl and butyl p-hydroxybenzoates, aloe vera extract, ascorbic acid, benzalkonium chloride, benzoic acid, benzoic acid esters of C9 to C15 alcohols, butylated hydroxytoluene, castor oil, cetyl alcohols, chlorocresol, citric acid, cocoa butter, coconut oil, diazolidinyl urea, diisopropyl adipate, dimethyl polysiloxane, DMDM hydantoin, ethanol, fatty acids, fatty alcohols, hexadecyl alcohol, hydroxybenzoate esters, iodopropynyl butylcarbamate, isononyl iso-nonanoate, jojoba oil, lanolin oil, methylparaben, mineral oil, oleie acid, olive oil, polyethers, polyoxypropylene butyl ether, polyoxypropylene cetyl ether, silicone oils, sodium propionate, sodium benzoate, sodium bisulfite, disodium metabisulfite, sorbic acid, stearic fatty acid, vitamin E, vitamin E acetate and derivatives, esters, salts and mixtures thereof. ln some embodiments, the preservative is or includes methyl-p-hydroxybenzoate.

[0074] Non-limiting examples of sweeteners include acesulfame potassium, sorbitol, rebaudioside A, rebaudioside B, rebaudioside C, rebaudioside D, rebaudioside E, rebaudioside F, dulcoside A, dulcoside B, rubusoside, stevia, stevioside, mogroside IV, mogroside V, sorbitol, Luo Han Guo sweetener, siamenoside, monatin and its salts (monatin SS, RR, RS, SR), curculin, glycyrrhizic acid and its salts, thaumatin, monellin, mabinlin, brazzein, hernandulcin, phyllodulcin, glycyphyllin, phloridzin, trilobatin, baiyunoside, osladin, polypodoside A, pterocaryoside A, pterocaryoside **B,** mukuroziosíde, phlomisoside **1,** periandrin **1,** abrsoside A, cyclocarioside **1,** sucralose, acesulfame potassium and other salts, aspartame, alitame, saccharin, neohesperidin dihydrochalcone, cyclamate, neotame, N-[N- [3-(3-hydroxy-4-methoxyphenyl)propyl]-L-a-aspartyl]-L-phenylalanine 1-methyl ester, N- [N-[3-(3-hydroxy-4-methoxyphenyl)-3-methylbutyl]-L-

a-aspartyl]-L-phenylalanine 1-methyl ester, N-[N-[3-(3-methoxy-4-hydroxyphenyl)propyl]-L-a-aspartyl]-L-phenylalanine 1- methyl ester, and salts and combinations thereof. ln some embodiments, the sweetener is or includes acesulfame potassium.

[0075] Non-limiting examples of antioxidants include glutathione, quinolines, polyphenols, carotenoids, sodium metabisulphite, tocopherol succinate, propyl galate, butylated hydroxy toluene, butyl hydroxy anisol, flavanoids, and a vitamin C source. Non-limiting examples of vitamin C sources may include ascorbic acid; ascorbyl palmitate; dipalmitate L-ascorbate; sodium L-ascorbate-2-sulfate; an ascorbic salt, such as sodium, potassium, or calcium ascorbate; and mixtures thereof.

[0076] Non-limiting examples of chelating agents include ethylenediaminetetraacetic acid (EDTA) and citric acid, hydrates thereof, salts thereof, and hydrates of the salts thereof. Examples of such chelating agents include ethylenediaminetetraacetic acid disodium salt, ethylenediaminetetraacetic acid disodium salt dihydrate, and citric acid monohydrate. Various combinations of chelating agents can be used if desired.

[0077] Non-limiting examples of colorants include commercially available pigments such as FD&C Blue #1 Aluminum Lake, FD&C Blue #2, other FD&C Blue colors, titanium dioxide, iron oxide, and/or combinations thereof.

[0078] Non-limiting examples of flavoring agents include berry flavor, root beer flavor, cream flavor, chocolate flavor, peppermint flavor, spearmint flavor, butterscotch flavor, and wintergreen flavor and combinations thereof. Suitable berry flavoring agents include black cherry, strawberry, cherry, blueberry, raspberry and the like.

[0079] Non-limiting examples of pH-adjusting agents include acetate buffers, aminomethylamine buffers, ammonium hydroxide, benzoate buffers, borate buffers, carbonate buffers, citrate buffers, diethylamine buffers, diisopropylamine buffers, hydrochloric acid, lactic acid buffers, perchloric acid, aphosphate buffers, tartric acid, triethylamine buffers, proprioate buffers, sodium hydroxide, tetrahydroxypropylethylendiamine buffers, citric acid, and mixtures thereof.

[0080] The identities and amounts of the excipients can be selected and adjusted to achieve the desired effect while retaining the desired properties of the composition as a whole. ln some embodiments, the oral pharmaceutical composition comprises about 0.01% to about 10%, or about 0.03% to about 9%, or about 0.05% to about 7%, or about 0.01% to about 3%, or about 0.02% to about 2.5%, or about 0.03% to about 2.5%, or about 0.05% to about 2.5%, or about 0.1% to about 2%, or about O. I %

to about I .5%, or about I % to about I .5% w/w of excipients. ln some embodiments, the oral pharmaceutical composition may comprise about 0.01% to about 10% w/w of excipients.

[0081] ln some embodiments, the compositions include one or more preservatives. Additionally or altematively, in some embodiments, the compositions include one or more sweeteners and/or flavoring agents. ln some embodiments, the compositions include one or more preservatives and one or more sweeteners and/or flavoring agents. ln some embodiments, the composition includes potassium sorbate as a preservative and acesulfame potassium and sorbitol as sweeteners. ln some embodiments, the composition includes methyl-p-hydroxybenzoate as a preservative and acesulfame potassium as a sweetener.

Methods of Manufacture

[0082] Also provided herein are processes for making the compositions described herein. ln general, the compositions can be made by methods known in the art, in view of the following guidance.

[0083] ln general, the compositions are made by combining the corticosteroid, solvent, and thermoreversible polymer, and water, and any other optional excipients being used.

[0084] ln some embodiments, the corticosteroid is dissolved in the solvent before being mixed with the thermoreversible polymer. ln such embodiments, the amount and identity of solvent used is such that the corticosteroid remains in solution when added to the thermoreversible polymer, and does not precipitate. Thus, in some embodiments, a method of making a composition as described herein comprises (a) dissolving a corticosteroid in a solvent and (b) mixing the corticosteroid solution with a thermoreversible polymer. ln some embodiments, the methods further comprise adding water and, optionally, one or more optional excipients to the composition.

[0085] ln some embodiments, a method of making a composition as described herein comprises dissolving budesonide in propylene glycol, mixing the budesonide solution with Poloxamer 407, and adding water acesulfame potassium, and methyl-p-hydroxybenzoate.

[0086] **ln** some embodiments, the thermoreversible polymer is at a temperature below room temperature when mixed with the corticosteroid. For example, the thermoreversible polymer may be prepared and held in an ice bath prior to use. **ln** accordance with such embodiments, the polymer and corticosteroid solution can be mixed in a liquid state, and then the temperature can be increased to induce micellization, which is believed to solubilize the corticosteroid in the polymeric formulation.

[0087] For example, a composition may be prepared as follows:

dispersing a thermoreversible polymer in water and chilling the polymer dispersion to below room temperature;

dissolving the corticosteroid in a solvent;

mixing the corticosteroid solution with the polymer dispersion;

increasing the temperature of the mixture until the mixture becomes a gel;

cooling the gelled mixture until the mixture becomes a liquid; and

optionally, adding water and, optionally, adding one or more additional pharmaceutically acceptable excipients.

[0088] For example, in specific embodiments, a composition may be prepared as follows:

- The thermoreversible polymer is prepared by dispersing in water and chilling. **ln** some embodiments, the chilling is to 4 ºC. ln some embodiments, the chilling is ovemight.

- The corticosteroid solution is prepared by dissolving the corticosteroid in the solvent, such as in an ultrasound bath. ln some embodiments, the ultrasound bath accelerates the dissolution of the corticosteroid in the solvent.

- The corticosteroid solution is added to the thermoreversible polymer dispersion under stirring. ln some embodiments, the stirring is conducted at 700 rpm.

- The temperature is then increased to induce micellization and gel formation. ln some embodiments, the corticosteroid solution may be heated with a heating plate. ln some embodiments, the corticosteroid solution in an industrial scale may be heated with a heated water circulation in a processing reactor jacket. For example, in some embodiments, the temperature is increased to 40 ºC to induce micellization.

- Then, the composition is cooled to achieve a liquid state. For example, in some embodiments, the gel is cooled to below 20 ºC, whereby a liquid state is achieved.

- Then, when the composition is in a liquid state, water and any optional excipients are optionally added under stirring. ln some embodiments, the stirring is conducted at 500 rpm. ln some embodiments, water is added to achieve the desired concentration of the thermoreversible polymer.

Therapeutic Methods

[0089] Also provided herein are methods of administering a corticosteroid to a subject in need thereof, comprising orally administering to the subject a composition as described herein. **ln** some embodiments, the method is effective to deliver the corticosteroid to the esophagus of the subject.

[0090] **ln** some embodiments, the method is effective to provide prolonged delivery of corticosteroid to the esophagus of the subject, such as delivery for at least 15 minutes, or at least 20 minutes, or at least 25 minutes, or at least 30 minutes, or at least 35 minutes, or at least 40 minutes, or at least 45 minutes, or at least 50 minutes, or at least 55 minutes, or at least 60 minutes, or at least 65 minutes, or at least 75 minutes, or at least 75 minutes.

[0091] ln any embodiments, the subject may be suffering from or at risk of developing an inflammatory condition of the upper gastrointestinal tract, particularly the esophagus. ln some embodiments, the subject may be suffering from or at risk of developing eosinophilic esophagitis (EoE). ln some embodiments, the subject may be a child (e.g., up to 18 years, including up to 10 years) or an adult.

[0092] ln embodiments related to the treatment of EoE, suitable doses of budesonide may be up to 1 mg/day for children younger than 10 years and up to 2 mg daily for older patients, suitable doses of fluticasone may be 440 µg to 880 µg twice daily for adults and 88 µg to 440 µg two to four times a day for children (up to the maximum adult dose), and suitable doses of ciclesonide may be about to 320 µg twice a day for children. Treatment may comprise repeated doses one to four times a day, and may be continued for **1** day or longer, 3 days or longer, 7 days or longer, one week or longer, two weeks or longer, three weeks or longer, four weeks or longer, five weeks or longer, six weeks or longer, seven weeks or longer, or eight weeks or longer.

[0093] Also provided herein are methods of treating an inflammatory condition of the esophagus, including eosinophilic esophagitis, comprising orally administering to a subject in need thereof a composition as described herein. As noted above, a suitable subject may be suffering from one or more inflammatory conditions of the esophagus, including eosinophilic esophagitis.

[0094] The methods may comprise administering the composition as described herein one or more times per day, such as one, two, three, four, five, or more, times per day.

[0095] Also provided are uses of a corticosteroid in the preparation of a medicament for orally administering the corticosteroid to an esophagus of a subject in need thereof, wherein the medicament comprises an oral pharmaceutical composition as described herein. Also provided are uses of a corticosteroid in the preparation of a medicament for treating an inflammatory condition of the esophagus, such as eosinophilic esophagitis, wherein the medicament comprises an oral pharmaceutical composition as described herein.

[0096] Also provided are oral pharmaceutical compositions as described herein for orally administering a corticosteroid to an esophagus of a subject in need thereof. Also provided are oral pharmaceutical compositions as described herein for treating an inflammatory condition of the esophagus, such as eosinophilic esophagitis.

EXAMPLES

[0097] The following specific examples are included as illustrative of the compositions described herein. These examples are in no way intended to limit the scope of the disclosure. Other aspects of the disclosure will be apparent to those skilled in the art to which the disclosure pertains.

Example 1: Preparation of Sol-Gel Budesonide Composition

[0098] The solubility of budesonide in propylene glycol was determined to be 11 mg/ml at room temperature. Based on this information and other experimentation, it was determined that a propylene glycol content of 5% w/w should be sufficient to solubilize budesonide in the composition.

[0099] To prepare a budesonide composition as described herein, Poloxamer 407 was dispersed in water and chilled at 4 ºC overnight. Budesonide was then dissolved in propylene glycol in an ultrasound bath at room temperature. The budesonide solution was then added to the Poloxamer 407 dispersion under stirring at 700 rpm. The temperature of the mixture was then raised to 40 ºC to induce micellization and sol-gel transition. The gel was then chilled to below 20 ºC so that the gel transitioned back into a liquid. To the liquid composition, water and excipients such as acesulfame potassium and methyl-p- hydroxybenzoate were added under stirring. The composition obtained was liquid at room temperature.

Example 2: Physicochemical Characterization of Sol-Gel Budesonide Compositions

[0100] A composition having the following components was prepared by methodology described above:

Component	w/w %
Methyl-p-hydroxybenzoate	0.2%
Acessulfame potassium	0.3%
Propylene Glycol	5%
Budesonide	0.5 mg/mL
Poloxamer 407	16%
Water	q.s.

[0101] Similar compositions having 15% or 17% Poloxamer 407 also were prepared.

[0102] The sol-gel transition temperature of the compositions was determined by methodology known in the art using by microrheology and RHEOLASER® LAB (Formulaction) equipment. For example, 20 mL of test composition was subjected to heating for evaluation of viscoelastic parameters, G'(elastic modulus) and G"(viscous modulus). The sol-gel temperature was defined as the temperature at which the values of the viscoelastic modules are between the solution and gel values. Sol-gel temperature determination was performed in triplicate for each formulation.

[0103] The compositions prepared with 16% Poloxamer 407 exhibited a sol-gel transition temperature of about 32ºC. ln contrast, compositions prepared with 15% Poloxamer 407 exhibited a sol-gel transition at about 39ºC, while compositions prepared with 17% Poloxamer 407 exhibited a sol-gel transition at about 29ºC.

[0104] The mucoadhesive force of the compositions was determined by methodology known in the art, by measuring the force required to remove the composition from a mucin disc using a texturometeter (TA.XT *plus,* Stable Micro Systems, Surrey, UK). For example, to prepare a mucin disc, 250 mg of mucin was weighed and compressed with 140-150 kg force. The mucin disc was fixed on a O.SR cylindrical probe and hydrated with 5% mucin solution for 2 minutes. Then, 10 mL of test composition was placed in a Petri dish and maintained at 37ºC ± 0.5 to begin the test. The probe containing the mucin disc was lowered to the test composition at a constant speed (0.1 mm/s) and a force of 5 g was applied. The mucin disc and test composition were kept in contact for 60 seconds, after which the probe was lifted 15 mm. The force required to remove the probe from being in contact with the test composition was used as a measure of the mucoadehsive force.

[0105] The compositions prepared with 16% Poloxamer 407 exhibited a mucoadhesive force of 10.88 g. ln contrast, compositions prepared with 15% Poloxamer 407 exhibited a mucoadhesive force of 5.27 g, while compositions prepared with 17% Poloxamer 407 exhibited a mucoadhesive force of 14.58 g.

Example 3: Morphological Characterization of Sol-Gel Budesonide Compositions

[0106] A composition having the following components was prepared by methodology described above:

Component	w/w %
Methyl-p-hydroxybenzoate	0.2%
Acessulfame potassium	0.3%
Propylene Glycol	5%

Budesonide	0.5 mg/mL
Poloxamer 407	16%
Water	q.s.

[0107] Morphological characterization was performed at 25 ºC by transmission election microscopy (TEM), and showed micellization. See FIGS. 1A-1D. Morphological characterization was performed at 37 ºC revealed dehydration of the micelles and the gelation process. See FIGS. 2A-2B.

[0108] These figures confirm that budesonide was completely solubilized and molecularly dispersed in the composition, since no budesonide crystals are visible. This indicates that all the budesonide is fully available for contact with and delivery to the esophageal tissue.

Example 4: Dynamic Gelling

[0109] A dynamic gelling experiment was conducted to mimic *in vivo* conditions. Aliquots of 1 ml of the compositions described above were applied by a syringe to a heated 40 cm glass tube (37ºC) positioned at 90º, and displacement of each composition was assessed.

[0110] The composition with 15% Poloxamer 407 did not form a gel, traveled the entire length of the tube, and drained out of the tube. The composition with 16% Poloxamer 407 traveled about 25 cm along the tube over a period of about 3 seconds, during which time gelation was occurring. The composition with 17% Poloxamer 407 traveled about 15 cm along the tube over a period of about 2 seconds.

[0111] These results indicate that compositions with different sol-gel temperatures below 37ºC will form a gel more or less quickly at 37ºC, indicating that compositions having a target gelation time at a given temperature (e.g., body temperature) can be prepared by controlling the sol-gel temperature of the composition. These results also indicate that a Poloxamer 407 content of about 16% w/w is suitable for delivering budesonide to the esophagus, based on typical travel time to the esophagus after oral administration.

Example 5: *In Vivo* Mucoadhesion

[0112] A composition having the following components was prepared by methodology described above:

Component	w/w %
Acessulfame potassium	0.3%
Propylene Glycol	5%
Budesonide	0.5 mg/mL
Poloxamer 407	16%
Water	q.s.

[0113] An *in vivo* study was carried out to verify the mucoadhesion of a 16% Poloxamer 407 composition as described above. The composition was fluorescently labeled using 3 mg/ml IR-780, and a volume of 100 µL was orally administered to Swiss mice (25 g ±). The extent and duration of adhesion in the gastrointestinal tract were evaluated using fluorescence images acquired by tomography.

[0114] It was not possible to observe the presence of the composition in the gastrointestinal tract, possibly due to an insufficient concentration of the fluorescent marker to emit a signal detectable through the animal body. However, ex vivo imaging evidenced mucoadhesion along the gastrointestinal tract, particularly in the esophagus (see FIGS. 3A-B and FIGS. 4A- D). FIGS. 3A-B show ex vivo images of the gastrointestinal tract of animals four hours after treatment with 20 µ1 of the above formulation (FIG. 3A) or a control composition prepared without budesonide but with the fluorescent dye IR-780 (FIG. 3B). FIGS. 4A-D show ex vivo images of the esophagus of animals four hours after treatment with 20 µ1 of the above formulation (FIGS. 4A-B) or control composition (FIGS. 4C-D).

WHAT IS CLAIMED IS:

1. An oral pharmaceutical composition comprising:

a) a corticosteroid,

b) a solvent for the corticosteroid, and

c) a thermoreversible polymer that undergoes a sol-gel transition, wherein the composition is a liquid at room temperature and a gel at body temperature.

2. An oral pharmaceutical composition comprising:

a) a corticosteroid,

b) a solvent selected from one or more of propylene glycol, ethylene glycol, sorbitol, and cyclodextrin, and

c) a polymer selected from one or more of Poloxamer 407; Poloxamer 338; Poloxamer 188; Pluronic F68; Pluronic F127; and Pluronic F98.

3. The composition of claim 1 or 2, wherein the composition comprises micelles that comprise the polymer, corticosteroid, and solvent.

4. The composition of any one of claims 1-3, wherein the composition is a liquid at 25ºC and a gel at 37º.

5. The composition of any one of claims 1-4, wherein the composition has a sol- gel transition temperature of from 25 to 32ºC.

6. The composition of any one of claims 1-4, wherein the composition has a sol- gel transition temperature of from 29 to 32ºC.

7. The composition of any one of claims 1-6, wherein the polymer comprises Poloxamer 407.

8. The composition of any one of claims 1-7, wherein the corticosteroid is selected from

one or more of budesonide, fluticasone, and ciclesonide.

9. The composition of any one of claims 1-7, wherein the corticosteroid is budesonide.

10. The composition of any one of claims 1-7, wherein the corticosteroid is fluticasone.

11. The composition of any one of claims 1-10, wherein the corticosteroid is present in an amount of 0.001 to 10% w/w of the composition.

12. The composition of any one of claims 1-10, wherein the corticosteroid is present in an amount of 0.01 to 10% w/w of the composition.

13. The composition of any one of claims 1-12, wherein the polymer is present in an amount of 15-30% w/w of the composition.

14. The composition of any one of claims 1-13, wherein the solvent is present in an amount of 0.2 to 10% w/w of the composition.

15. The composition of any one of claims 1-14, wherein the polymer is Poloxamer 407 and is present in an amount of 15-30% w/w of the composition.

16. The composition of any one of claims 1-15, wherein the solvent is propylene glycol and is present in an amount of 0.2 to 10% w/w of the composition.

17. The composition of any one of claims 1-15, wherein the solvent is propylene glycol and is present in an amount of 3 to 7% w/w of the composition.

18. The composition of any one of claims 1-15, wherein the solvent is propylene glycol and is present in an amount of 4 to 6% w/w of the composition.

19. The composition of any one of claims 1-7, wherein the corticosteroid is budesonide and is present in an amount of 0.001 to 10% w/w, the polymer is Poloxamer 407 and is present in an amount of 15-30% w/w, and the solvent is propylene glycol and is present in an amount of 0.2 to 10% w/w of the composition.

20. The composition of any one of claims I-7, wherein the corticosteroid is budesonide and is present in an amount of 0.01 to 10% w/w, the polymer is Poloxamer 407 and is present in an

amount of 15-30% w/w, and the solvent is propylene glycol and is present in an amount of 4 to 6% w/w of the composition.

21. The composition of any one of claims 1-7, wherein the corticosteroid is fluticasone and is present in an amount of 0.001 to 10% w/w, the polymer is Poloxamer 407 and is present in an amount of 15-30% w/w, and the solvent is propylene glycol and is present in an amount of 0.2 to 10% w/w of the composition.

22. The composition of any one of claims 1-7, wherein the corticosteroid is fluticasone and is present in an amount of 0.01 to 10% w/w, the polymer is Poloxamer 407 and is present in an amount of 15-30% w/w, and the solvent is propylene glycol and is present in an amount of 4 to 6% w/w of the composition.

23. The composition of any one of claims 1-22, wherein the polymer is Poloxamer 407 and is present in an amount of 15 to 17% w/w of the composition.

24. The composition of any one of claims 1-22, wherein the polymer is Poloxamer 407 and is present in an amount of 15.5 to 16.5% w/w of the composition.

25. The composition of any one of claims 1-24, further comprising water and, optionally, one or more additional pharmaceutically acceptable excipients.

26. The composition of claim 25, comprising one or more additional pharmaceutically acceptable excipients in an amount of 0.01 -10% w/w of the composition.

27. The composition of claim 25 or 26, comprising one or more additional pharmaceutically acceptable excipients selected from preservatives.

28. The composition of claim 26, wherein the preservative is or comprises methyl-p-hydroxybenzoate.

29. The composition of any one of claims 25-28, comprising one or more additional pharmaceutically acceptable excipients selected from sweeteners.

30. The composition of claim 29, wherein the sweetener is or comprises acesulfame potassium.

31. The composition of any one of the preceding claims, wherein the composition adheres to the esophagus.

32. The composition of claim 31, wherein the compositions adheres to the esophagus for at least 30 minutes.

33. The composition of claim 31, wherein the compositions adheres to the esophagus for at least 45 minutes.

34. The composition of claim 31, wherein the compositions adheres to the esophagus for at least 60 minutes.

35. The composition of any one of claims 1-34, for treating an inflammatory condition of the esophagus.

36. The composition of any one of claims 1-34, for treating eosinophilic esophagitis.

37. A method of treating an inflammatory condition of the esophagus, comprising orally administering a composition of any one of claims 1-34 to a subject in need thereof.

38. A method of treating eosinophilic esophagitis, comprising orally administering a composition of any one of claims 1-34 to a subject in need thereof.

39. Use of a corticosteroid in the manufacture of a medicament for treating an inflammatory condition of the esophagus, wherein the medicament comprises a composition of any one of claims 1-34.

40. Use of a corticosteroid in the manufacture of a medicament for treating eosinophilic esophagitis, wherein the medicament comprises a composition of any one of claims 1-34.

41. A method of preparing a composition of any one of claims 1-34, comprising:

(a) dissolving the corticosteroid in the solvent;

(b) mixing the corticosteroid solution with the polymer; and

(c) optionally, adding water and, optionally, one or more additional pharmaceutically acceptable excipients.

42. A method of preparing a composition of any one of claims 1-34, comprising:

(a) dispersing the polymer in water and chilling the polymer dispersion to below room temperature;

(b) dissolving the corticosteroid in the solvent;

(c) mixing the corticosteroid solution with the polymer dispersion;

(d) increasing the temperature of the mixture until the mixture becomes a gel;

(e) cooling the gelled mixture until the mixture becomes a liquid; and

(f) optionally, adding water and, optionally, one or more additional pharmaceutically acceptable excipients.

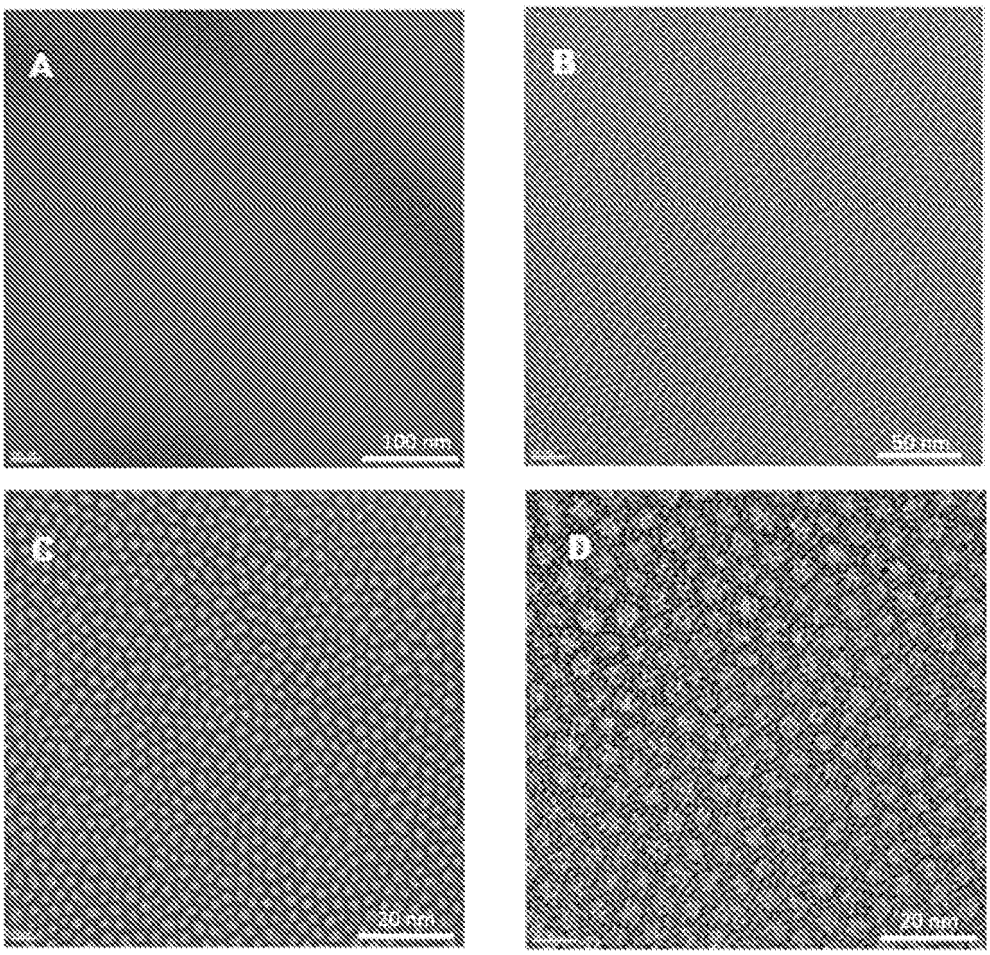

FIGS. lA-lD

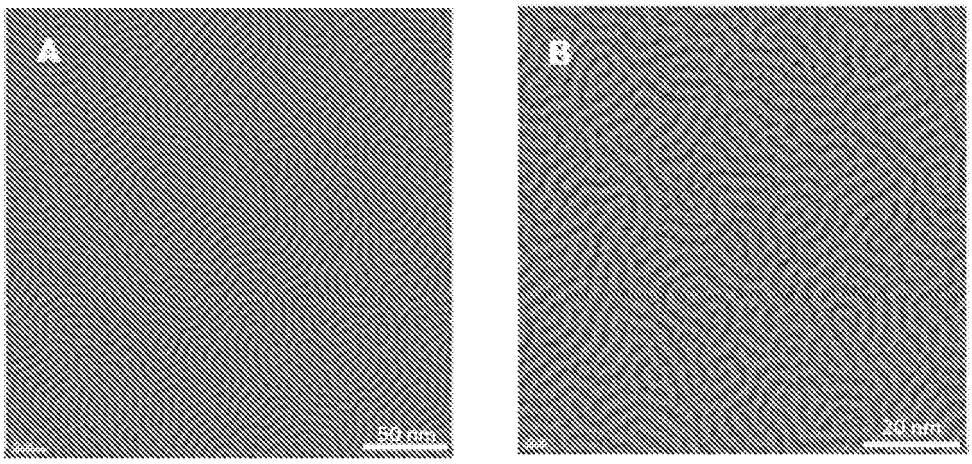

FIGS. 2A-2B

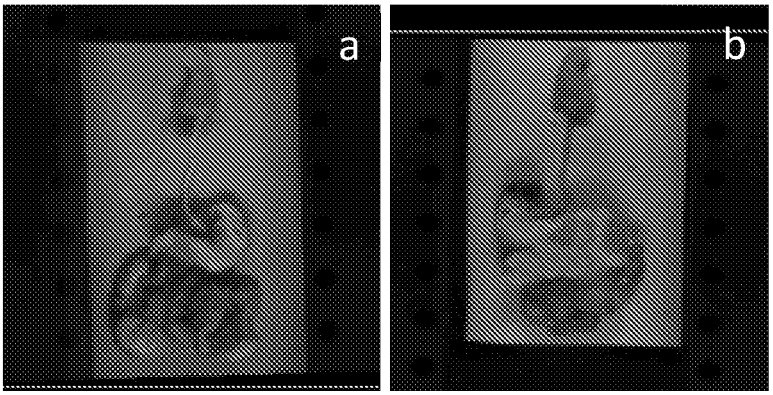

FIGS. 3A-B

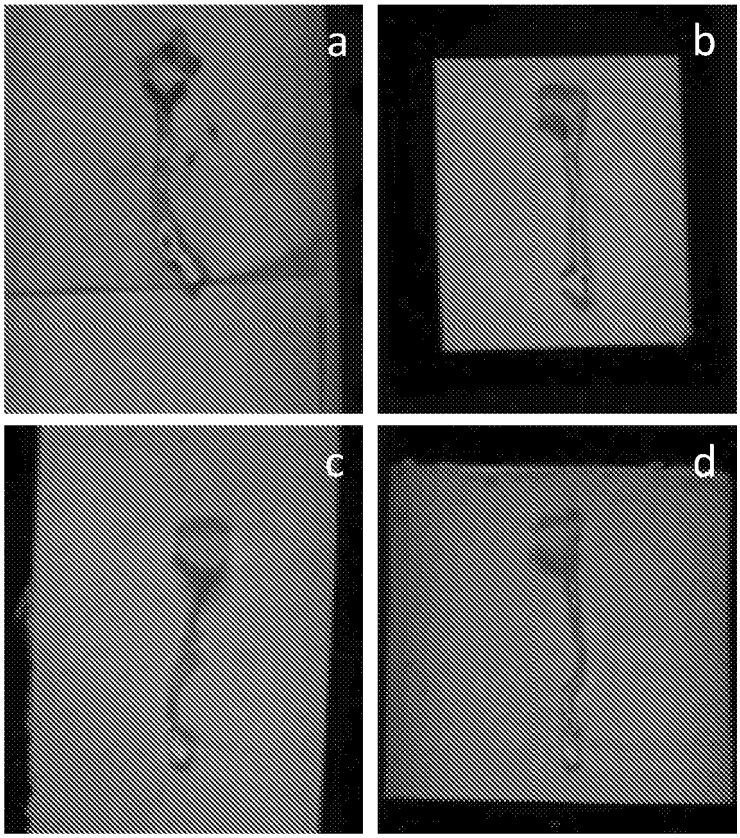

FIGS. 4A-D

Anexo 3 – Versão publicada referente ao capítulo 01

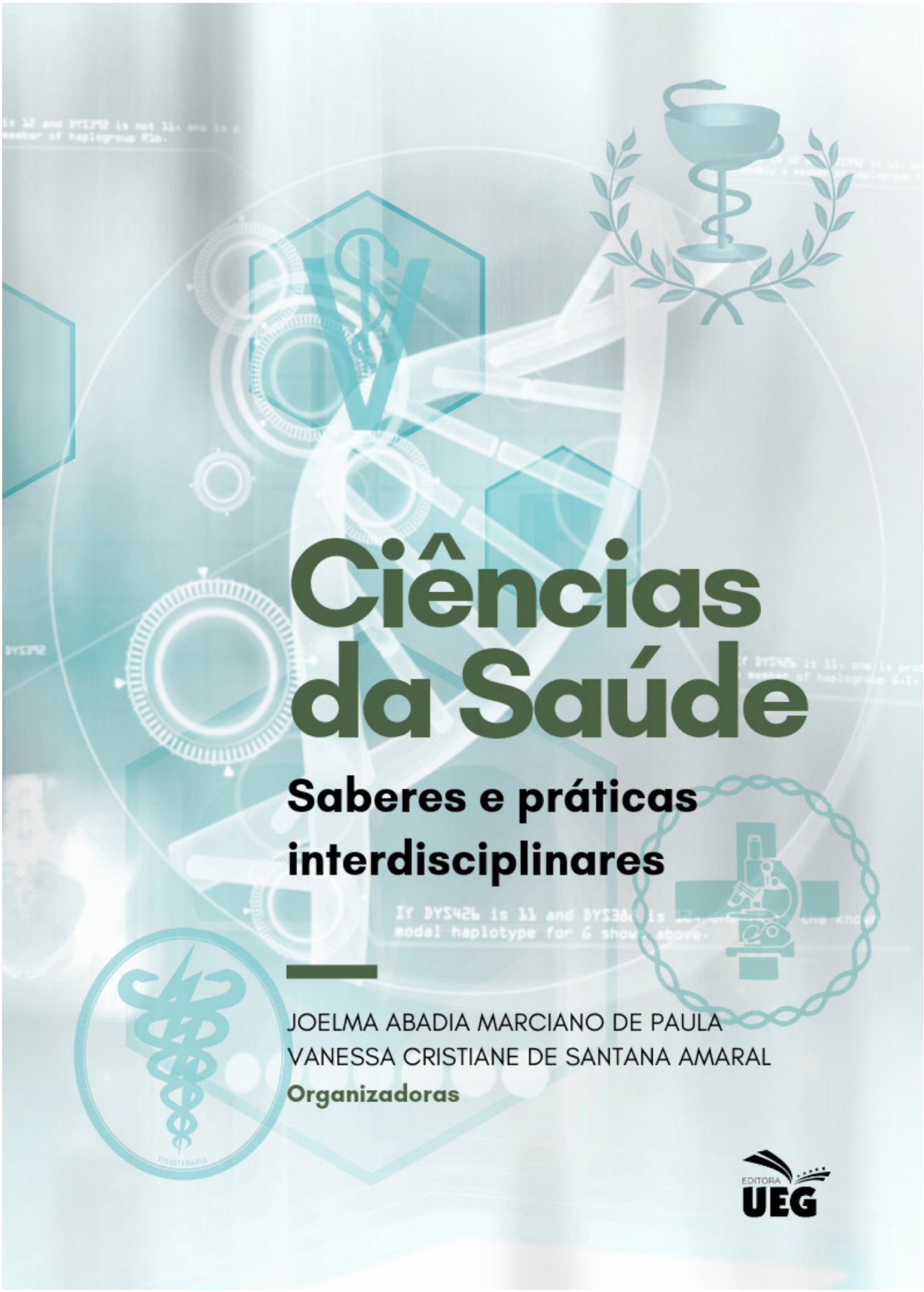
Ciências da Saúde
Saberes e práticas interdisciplinares
JOELMA ABADIA MARCIANO DE PAULA
VANESSA CRISTIANE DE SANTANA AMARAL
Organizadoras
EDITORA UEG

14.

ESTRATÉGIAS PARA FORMULAÇÃO DE PRODUTOS FARMACÊUTICOS MUCOADESIVOS

RAYANE SANTA CRUZ MARTINS DE QUEIROZ ANTONINO
ELIANA MARTINS LIMA
THAIS LEITE NASCIMENTO

O avanço em tecnologias que buscam melhorias e inovações na área da saúde inclui o desenvolvimento de novos produtos e materiais. Os frutos dessas pesquisas visam atender as necessidades de terapias com objetivos cada vez mais específicos e refinados (CAMBLIN et al., 2016; LATHEESHJAL et al., 2011).

Na área de tecnologia farmacêutica, a pesquisa em medicamentos busca maior eficácia, segurança e melhoria do bem-estar do paciente em tratamento (PATIL et al., 2016). Essa busca movimenta três setores importantes da sociedade: pesquisa, indústria e clínica. Dentro das inúmeras estratégias de desenvolvimento de novas formas farmacêuticas, estão as formulações mucoadesivas, que têm como objetivo aumentar o tempo de contato do fármaco com a superfície mucosa, aumentando sua absorção e eficiência terapêutica (LAFFLEUR, 2016; RAJARAM; LAXMAN, 2017).

Neste capítulo, o leitor será introduzido às definições sobre muco e o processo de interação de formulações com as mucosas. As formas farmacêuticas mucoadesivas e os materiais que as compõem, assim como as técnicas e ensaios utilizados para quantificarem a mucoadesão de formulações, serão abordados.

Anexo 4 – Versão publicada referente ao capítulo 02

Journal of Controlled Release 303 (2019) 12–23

Contents lists available at ScienceDirect

Journal of Controlled Release

journal homepage: www.elsevier.com/locate/jconrel

Thermoreversible mucoadhesive polymer-drug dispersion for sustained local delivery of budesonide to treat inflammatory disorders of the GI tract

Rayane S.C.M.Q. Antonino[a], Thais L. Nascimento[a], Edilson R. de Oliveira Junior[a], Leonardo G. Souza[a], Aline C. Batista[b], Eliana M. Lima[a,*]

[a] Laboratório de Nanotecnologia Farmacêutica e Sistemas de Liberação de Fármacos, FarmaTec, Faculdade de Farmácia, Universidade Federal de Goiás – UFG, Goiânia, Goiás, Brazil

[b] Laboratório de Patologia Bucal, Faculdade de Odontologia, Universidade Federal de Goiás – UFG, Goiânia, Goiás, Brazil

ARTICLE INFO

Keywords:
TGI
Inflammatory diseases
Mucoadhesion
Microrheology
Oscillatory rheometry
Micelles

ABSTRACT

Mucoadhesive drug formulations have been studied and used as alternatives to conventional formulations in order to achieve prolonged retention at the intended site. In addition to providing a controlled drug release, several drugs and disease conditions might benefit from mucoadhesive formulations, contributing to better therapeutic outcomes. Here, we describe the development and the *in vitro/in vivo* characterization of a mucoadhesive *in situ* gellifying formulation using PF127, a thermo reversible polymer, entrapping budesonide (BUD), a potent corticosteroid used for the treatment of a wide range of inflammatory diseases, including those affecting mucosas, such as in the GI tract. PF127 formulations (15–17%) were successfully prepared by a cold method as a thermo reversible *in situ* gelling dispersion for mucosal drug delivery, as confirmed by DSC. Sol-gel temperatures of PF127 formulations (25–39 °C) were observed by dynamic gelation and determined by microrheology and oscillatory rheometry. X-ray diffractograms and TEM images showed that BUD was completely solubilized within the polymeric micelles. *In vitro*, the gels showed 5–14 g force of mucoadhesion, and the *ex vivo* studies confirmed that the formulation efficiently adhered to the mucosa. Histopathological analysis combined with fluorescence images and *ex vivo* intestinal permeation confirmed that the formulation remained on the TGI mucosa for at least 4 h after administration. *In vivo* studies conducted in a murine model of intestinal mucositis demonstrated that the 16% PF127 BUD formulation was able to resolve the inflammatory injury in the intestinal mucosa. Results demonstrate that fine-tuning of PF127 formulations along with adequate selection of the drug agent, thorough characterization of the dispersions and their interactions with biological interfaces leads to the development of effective controlled drug delivery systems targeted to GI inflammatory diseases.

1. Introduction

Budesonide (BUD) is a glucocorticoid with high local anti-inflammatory activity and low systemic absorption [54]. Its limited bioavailability is also due to the rapid conversion of the molecule in the liver into metabolites with little or no steroid activity [23]. This reduces the adverse effects inherent to systemic corticosteroids, such as suppression of the hypothalamic-pituitary adrenal axis, making BUD a favorable therapeutic option for the treatment of inflammatory diseases of the gastrointestinal tract (GI) such as Crohn's disease, ulcerative colitis, mucositis of the upper and lower intestinal tract and esophageal eosinophilia [3,39,72]. Despite widespread clinical use, BUD has low aqueous solubility [79] and extensive first pass biotransformation [80]. It exhibits a high ratio of topical-to-systemic activity, which is attributed to its strong local anti-inflammatory effect and extensive first-pass elimination (up to 90%), which considerably limits its systemic bioavailability and effects [65]. Inflammatory disorders of the TGI mucosa affect an increasingly large number of patients ([56]; [28]). The treatment of these conditions still lack therapeutic efficacy, and is limited to the administration of oral medications in the form of anti-inflammatory solutions and/or suspensions [27,39].

The possibility of enabling mucus retention and site-specific drug release, achieved by formulations with distinctive physical and chemical properties [73], has directed the use of mucoadhesive formulations to achieving therapeutic effect directly on the affected mucosa [37]. We explored this approach, focusing on providing local and

* Corresponding author at: Universidade Federal de Goiás - UFG, Faculdade de Farmácia, FarmaTec – 5ª Avenida c/Rua 240 s/n, Praça Universitária, Goiânia, GO 74605-170, Brazil.
E-mail address: emlima@ufg.br (E.M. Lima).

https://doi.org/10.1016/j.jconrel.2019.04.011
Received 12 February 2019; Received in revised form 5 April 2019; Accepted 9 April 2019
Available online 11 April 2019
0168-3659/

Anexo 5 – Versão publicada referente ao capítulo 03

International Journal of Pharmaceutics: X 1 (2019) 100026

Contents lists available at ScienceDirect

International Journal of Pharmaceutics: X

journal homepage: www.journals.elsevier.com/international-journal-of-pharmaceutics-x

Impact of drug loading in mesoporous silica-amorphous formulations on the physical stability of drugs with high recrystallization tendency

Rayane S.C.M.Q. Antonino[a,b], Michael Ruggiero[c], Zihui Song[c], Thais Leite Nascimento[b], Eliana Martins Lima[b], Adam Bohr[a], Matthias Manne Knopp[d], Korbinian Löbmann[a,*]

[a] Department of Pharmacy, University of Copenhagen, Copenhagen, Denmark
[b] Laboratório de Nanotecnologia Farmacêutica e Sistemas de Liberação de Fármacos, Faculdade de Farmácia, Universidade Federal de Goiás – UFG, Goiânia, Goiás, Brazil
[c] Department of Chemistry, University of Vermont, Burlington, VT, USA
[d] Bioneer:FARMA, Department of Pharmacy, University of Copenhagen, Copenhagen, Denmark

ARTICLE INFO

Keywords:
Mesoporous silica
Loading capacity
Differential scanning calorimetry (DSC)
Amorphous

ABSTRACT

In this study, a method is described to determine the monolayer loading capacity (MLC) of the drugs naproxen and ibuprofen, both having high recrystallization tendencies, in mesoporous silica (MS), a well known carrier that is able to stabilize the amorphous form of a drug. The stabilization has been suggested to be due to direct absorption of the drug molecules onto the MS surface, i.e. the drug monolayer. In addition, drug that is not in direct contact with MS surface can fill the pores up to its pore filling capacity (PFC) and is potentially stabilized by confinement due to the pore size being smaller than a crystal nuclei. For drugs with high recrystallization tendencies, any drug outside the pores crystallizes due to its poor physical stability. The drug monolayer does not contribute to the glass transition temperature (T_g) in the DSC, however, the confined amorphous drug above MLC has a T_g and the heat capacity (ΔC_p) over the T_g increases with an increasing fraction of confined amorphous drug. Hence, several drug loading values above the MLC were investigated towards the presence of a T_g and ΔC_p using differential scanning calorimetry (DSC). A linear correlation between the amount of confined amorphous drug and its ΔC_p was identified for the mixtures between the MLC and PFC. By subsequent extrapolation to zero ΔC_p the experimental MLC could be determined. Using theoretical density functional theory (DFT) and *ab initio* Molecular Dynamics (AIMD), the binding energies for the monolayer suggested that the monolayer in fact is thermodynamically more favorable than the crystalline form, whereas the confined amorphous form is thermodynamically less favorable. Consequently, a physical stability study showed that the confined amorphous drugs above the MLC were thermodynamically unstable and consequently flowing out of the pores in order to crystallize, whereas the monolayer remained physically stable.

1. Introduction

Amorphous formulations are one of the most efficient ways of improving bioavailability in an era of drug discovery where a large percentage of new molecules have solubility-limited dissolution rates (Riikonen et al., 2018; Sayed et al., 2018). In this context, mesoporous silica (MS), having small pores (e.g., pore diameter between 2 and 50 nm) and large specific surface areas (e.g., often greater than 300 m^2/g) (Andersson et al., 2004), have received quite some attention, due to their ability to stabilize the amorphous form of a drug within their mesopores (Kumar et al., 2014; Laitinen et al., 2013; Rouquerol et al., 1994).

Inhibition of drug crystallization through adsorption to a MS has generally been explained by two responsible mechanisms: i) molecular interactions (e.g., hydrogen bonding) between functional groups of the drug molecules and the surface of the MS, and ii) confinement and spatial separation of the drug in the pores of MS, since the diameter of the mesopores is smaller than a critical crystalline nuclei of the drug (Azaïs et al., 2006; Rengarajan et al., 2008). With respect to i), the large MS surface area provides additional surface free energy, and it has been suggested that the adsorption of the drug in the amorphous form is actually thermodynamically favorable because of the lower free energy state than the crystalline drug (Andersson et al., 2004; Qian and Bogner, 2011, 2012). When all binding sites on the MS surface are occupied by drug molecules and an excess amount of drug is present in the system, it cannot be in direct contact with the MS surface anymore,

* Corresponding author.
E-mail address: korbinian.lobmann@sund.ku.dk (K. Löbmann).

https://doi.org/10.1016/j.ijpx.2019.100026
Received 4 June 2019; Received in revised form 19 July 2019; Accepted 19 July 2019
Available online 22 July 2019

Anexo 6 – Estrutura da budesonida

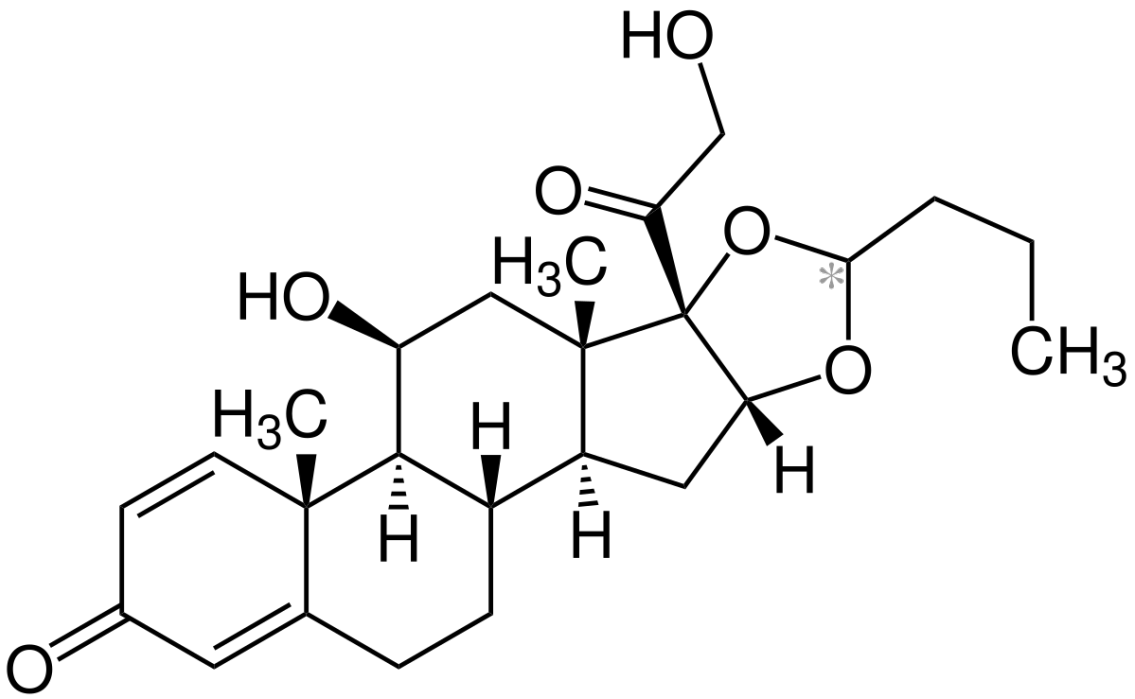

Figura 1. Estrutura da budesonida. Fonte: wikipedia.org/wiki/Budesonida

Anexo 7 – Difratograma do naproxeno puro

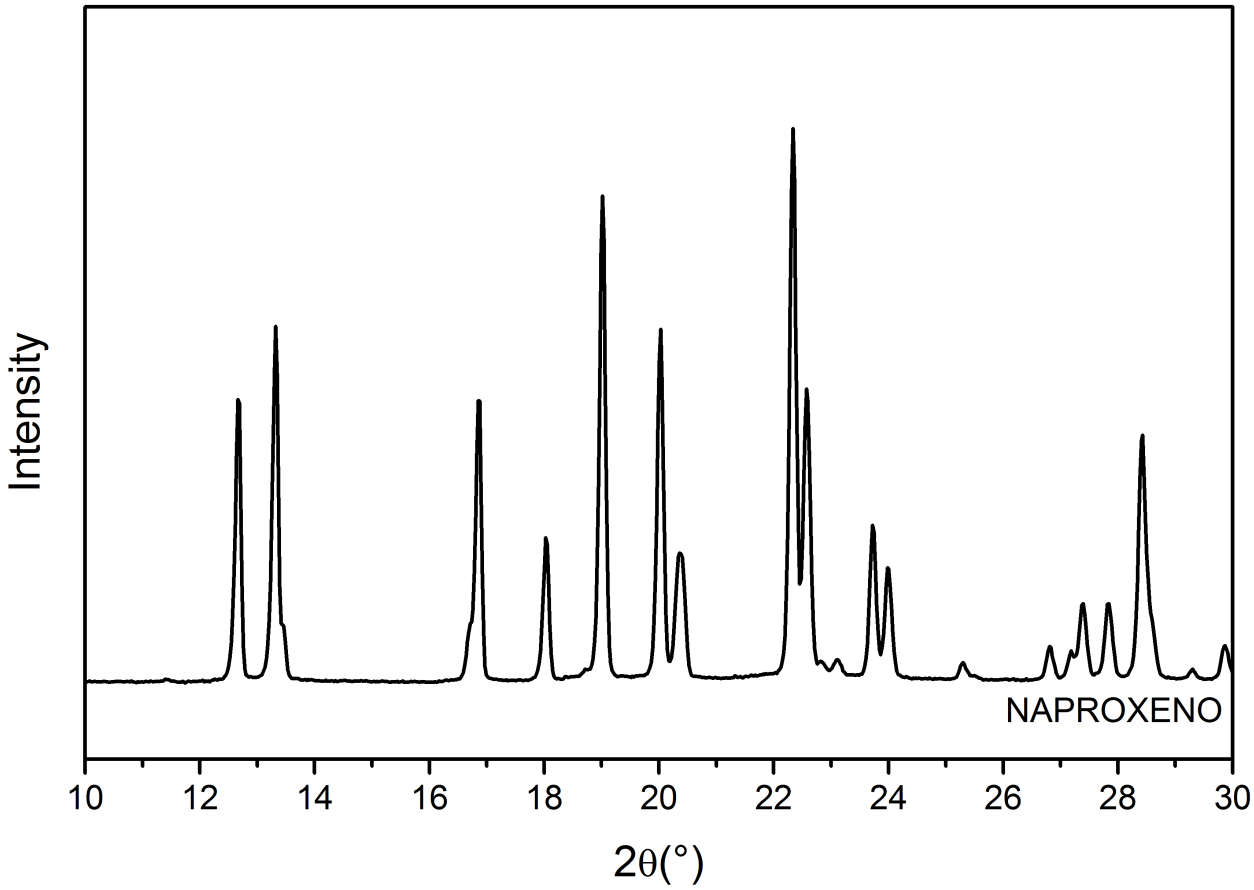

Figura 1. Difratograma do naproxeno puro obtido por difração de raios X.

Anexo 8 – Difratograma do ibuprofeno puro

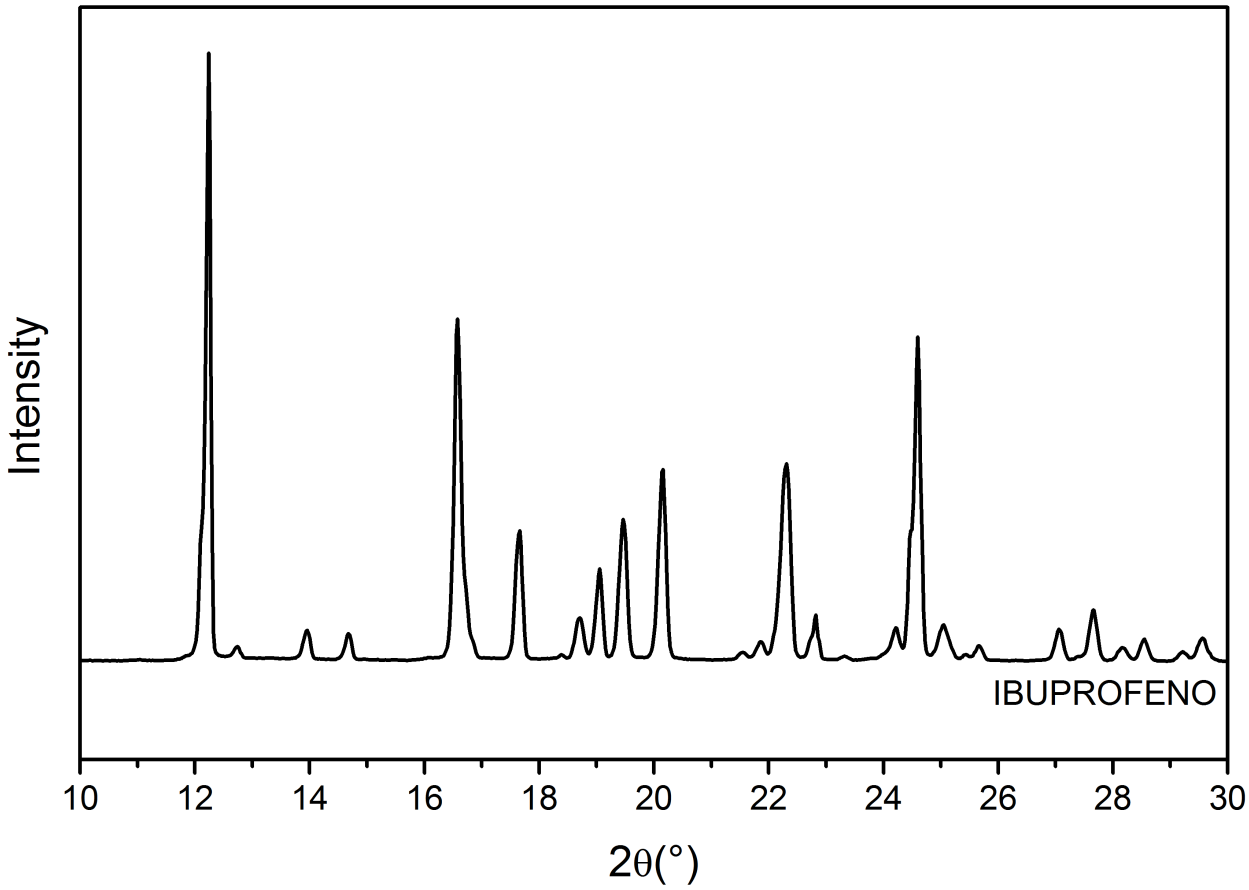

Figura 1. Difratograma do ibuprofeno puro obtido por difração de raios X.

REFERÊNCIAS

AALTONEN, J.; RADES, T. J. D. T. Commentary: Towards physicorelevant dissolution testing: The importance of solid-state analysis in dissolution. v. 16, p. 47-54, 2009.

AHUJA, N. et al. Studies on dissolution enhancement and mathematical modeling of drug release of a poorly water-soluble drug using water-soluble carriers. v. 65, n. 1, p. 26-38, 2007. ISSN 0939-6411.

AKASH, M. S. H.; REHMAN, K. Recent progress in biomedical applications of Pluronic (PF127): pharmaceutical perspectives. **Journal of Controlled Release,** v. 209, p. 120-138, 2015. ISSN 0168-3659.

AKKARI, A. C. et al. Poloxamer 407/188 binary thermosensitive hydrogels as delivery systems for infiltrative local anesthesia: Physico-chemical characterization and pharmacological evaluation. **Materials Science and Engineering: C,** v. 68, p. 299-307, 2016. ISSN 0928-4931.

ALLEN JR, L. V.; POPOVICH, N. G.; ANSEL, H. C. **Formas Farmacêuticas e Sistemas de Liberação de Fármacos-9**. Artmed Editora, 2013. ISBN 8565852857.

ANDERSSON, J. et al. Influences of material characteristics on ibuprofen drug loading and release profiles from ordered micro-and mesoporous silica matrices. **Chemistry of Materials,** v. 16, n. 21, p. 4160-4167, 2004. ISSN 0897-4756.

ATTWOOD, D.; COLLETT, J.; TAIT, C. The micellar properties of the poly (oxyethylene)-poly (oxypropylene) copolymer Pluronic F127 in water and electrolyte solution. **International journal of pharmaceutics,** v. 26, n. 1-2, p. 25-33, 1985. ISSN 0378-5173.

BAN, E. et al. Poloxamer-Based Thermoreversible Gel for Topical Delivery of Emodin: Influence of P407 and P188 on Solubility of Emodin and Its Application in Cellular Activity Screening. **Molecules,** v. 22, n. 2, p. 246, 2017.

BASHIR, R. et al. Floating Oral In-Situ Gel: A Review. v. 9, n. 2, p. 442-448, 2019. ISSN 2250-1177.

BHOWMIK, M. et al. Effect of xanthan gum and guar gum on in situ gelling ophthalmic drug delivery system based on poloxamer-407. **International journal of biological macromolecules,** v. 62, p. 117-123, 2013. ISSN 0141-8130.

BOATENG, J.; OKEKE, O.; KHAN, S. Polysaccharide based formulations for mucosal drug delivery: A review. **Current pharmaceutical design,** v. 21, n. 33, p. 4798-4821, 2015. ISSN 1381-6128.

BREMMELL, K. E.; PRESTIDGE, C. A. Enhancing oral bioavailability of poorly soluble drugs with mesoporous silica based systems: opportunities and challenges. **Drug Development and Industrial Pharmacy,** v. 45, n. 3, p. 349-358, 2019. ISSN 0363-9045.

BRUSCHI, M. L. et al. Semisolid systems containing propolis for the treatment of periodontal disease: in vitro release kinetics, syringeability, rheological, textural, and mucoadhesive properties. **Journal of pharmaceutical sciences,** v. 96, n. 8, p. 2074-2089, 2007. ISSN 1520-6017.

CARAMELLA, C. M. et al. Mucoadhesive and thermogelling systems for vaginal drug delivery. **Advanced drug delivery reviews,** v. 92, p. 39-52, 2015. ISSN 0169-409X.

CHUNG, B. L. et al. Delivery of Cancer Nanotherapeutics. In: (Ed.). **Nanotheranostics for Cancer Applications**: Springer, 2019. p.163-205.

CORRIGAN, O.; HOLOHAN, E.; SABRA, K. J. I. J. O. P. Amorphous forms of thiazide diuretics prepared by spray-drying. v. 18, n. 1-2, p. 195-200, 1984. ISSN 0378-5173.

DUDOGNON, E. et al. Formation of budesonide/α-lactose glass solutions by ball-milling. v. 138, n. 2, p. 68-71, 2006. ISSN 0038-1098.

ENGERS, D. et al. A solid-state approach to enable early development compounds: Selection and animal bioavailability studies of an itraconazole amorphous solid dispersion. v. 99, n. 9, p. 3901-3922, 2010. ISSN 1520-6017.

ESCOBAR-CHÁVEZ, J. J. et al. Applications of thermo-reversible pluronic F-127 gels in pharmaceutical formulations. **Journal of Pharmacy & Pharmaceutical Sciences,** v. 9, n. 3, p. 339-58, 2006. ISSN 1482-1826.

ESHEL-GREEN, T.; BIANCO-PELED, H. Mucoadhesive acrylated block copolymers micelles for the delivery of hydrophobic drugs. **Colloids and Surfaces B: Biointerfaces,** v. 139, p. 42-51, 2016. ISSN 0927-7765.

HANCOCK, B. C.; ZOGRAFI, G. J. J. O. P. S. Characteristics and significance of the amorphous state in pharmaceutical systems. v. 86, n. 1, p. 1-12, 1997. ISSN 0022-3549.

HEMPEL, N.-J. et al. A fast and reliable DSC-based method to determine the monomolecular loading capacity of drugs with good glass-forming ability in mesoporous silica. **International journal of pharmaceutics,** v. 544, n. 1, p. 153-157, 2018. ISSN 0378-5173.

JANSSENS, S.; VAN DEN MOOTER, G. J. J. O. P.; PHARMACOLOGY. Physical chemistry of solid dispersions. v. 61, n. 12, p. 1571-1586, 2009. ISSN 0022-3573.

JENKINS, R.; SNYDER, R. L. **Introduction to X-ray powder diffractometry**. Wiley New York, 1996.

KAWABATA, Y. et al. Formulation design for poorly water-soluble drugs based on biopharmaceutics classification system: basic approaches and practical applications. v. 420, n. 1, p. 1-10, 2011. ISSN 0378-5173.

LAITINEN, R. et al. Emerging trends in the stabilization of amorphous drugs. v. 453, n. 1, p. 65-79, 2013. ISSN 0378-5173.

LÉBER, A. et al. Combination of Zinc Hyaluronate and Metronidazole in a Lipid-Based Drug Delivery System for the Treatment of Periodontitis. v. 11, n. 3, p. 142, 2019.

LENAERTS, V. et al. Temperature-dependent rheological behavior of Pluronic F-127 aqueous solutions. **International journal of pharmaceutics,** v. 39, n. 1-2, p. 121-127, 1987. ISSN 0378-5173.

MASUDA, T. et al. Cocrystallization and amorphization induced by drug–excipient interaction improves the physical properties of acyclovir. v. 422, n. 1-2, p. 160-169, 2012. ISSN 0378-5173.

PRESTIDGE, C. A. et al. Mesoporous silicon: a platform for the delivery of therapeutics. v. 4, n. 2, p. 101-110, 2007. ISSN 1742-5247.

QIAN, K. K.; BOGNER, R. H. Spontaneous crystalline-to-amorphous phase transformation of organic or medicinal compounds in the presence of porous media, part 1: thermodynamics of spontaneous amorphization. **Journal of Pharmaceutical Sciences,** v. 100, n. 7, p. 2801-15, Jul 2011. ISSN 1520-6017 (Electronic)
0022-3549 (Linking). Disponível em: < https://www.ncbi.nlm.nih.gov/pubmed/21337545 >.

_____. Application of mesoporous silicon dioxide and silicate in oral amorphous drug delivery systems. **Journal of Pharmaceutical Sciences,** v. 101, n. 2, p. 444-463, Feb 2012. ISSN 1520-6017 (Electronic)
0022-3549 (Linking). Disponível em: < https://www.ncbi.nlm.nih.gov/pubmed/21976048 >.

QURESHI, M. et al. Formulation and Evaluation of Neuroactive Drug Loaded Chitosan Nanoparticle for Nose to Brain Delivery: In-vitro Characterization and In-vivo Behavior Study. v. 16, n. 2, p. 123-135, 2019. ISSN 1567-2018.

SAUNDERS, M. et al. The potential of high speed DSC (Hyper-DSC) for the detection and quantification of small amounts of amorphous content in predominantly crystalline samples. **International journal of pharmaceutics,** v. 274, n. 1-2, p. 35-40, 2004. ISSN 0378-5173.

SEKIGUCHI, K.; OBI, N. J. C.; BULLETIN, P. Studies on Absorption of Eutectic Mixture. I. A Comparison of the Behavior of Eutectic Mixture of Sulfathiazole and that of Ordinary Sulfathiazole in Man. v. 9, n. 11, p. 866-872, 1961. ISSN 0009-2363.

SERAJUDDIN, A. T. J. A. D. D. R. Salt formation to improve drug solubility. v. 59, n. 7, p. 603-616, 2007. ISSN 0169-409X.

STORPIRTIS, S. et al. **Biofarmacotécnica, Ciências Farmacêuticas**: Guanabara Koogan 2009.

VASCONCELOS, T.; SARMENTO, B.; COSTA, P. Solid dispersions as strategy to improve oral bioavailability of poor water soluble drugs. **Drug discovery today,** v. 12, n. 23-24, p. 1068-1075, 2007. ISSN 1359-6446.

ZŮZA, D. et al. Silica particles with three levels of porosity for efficient melt amorphisation of drugs. v. 274, p. 61-69, 2019. ISSN 1387-1811.